Two-Step Nonlinear ARDL Estimation: Theory and Application*

JIN SEO CHO

School of Economics, Yonsei University, Seoul, Korea
jinseocho@yonsei.ac.kr

MATTHEW GREENWOOD-NIMMO

Faculty of Business and Economics, University of Melbourne, Carlton, Australia
Centre for Applied Macroeconomic Analysis, Australian National University, Canberra, Australia
matthew.greenwood@unimelb.edu.au

YONGCHEOL SHIN

Department of Economics and Related Studies, University of York, York, U.K.
yongcheol.shin@york.ac.uk

November 2024

Abstract

The nonlinear autoregressive distributed lag (NARDL) model is a single-equation error correction model that has been widely applied to accommodate asymmetry in the long-run equilibrium relationship and the short-run dynamic coefficients with respect to positive and negative changes in the explanatory variable(s). The NARDL model exhibits an asymptotic singularity issue that frustrates efforts to derive the asymptotic properties of the single-step estimator. We propose a two-step estimation in which the parameters of the long-run relationship are estimated by the fully-modified least squares estimator before the short-run dynamic parameters are estimated by OLS. We establish that the two-step NARDL estimators follow a limiting normal distribution, the validity of which is confirmed by Monte Carlo simulations. We demonstrate the utility of our approach with an application to the asymmetric relationship between R&D intensity and investment in the U.S.

Key Words: Two-step Estimation of NARDL Model, Asymptotic Singularity, Fully-Modified Estimator, Asymmetric relationship between R&D intensity and investment.

JEL Classifications: C22, E22, O32.

---

*We are grateful for the insightful comments of In Choi, Tae-Hwan Kim, Rui Lin, Viet Nguyen, Barbara Rossi, Michael Thornton, Ting Xie as well as seminar participants at the Universities of Melbourne, Yonsei, and York. Cho is grateful for financial support from the Ministry of Education of the Republic of Korea and the National Research Foundation of Korea (Grant number NRF-2019S1A5A2A01035568). Greenwood-Nimmo and Shin acknowledge financial support from the Economic and Social Research Council (Grant number ES/T01573X/1). The usual disclaimer applies.

Disclosure statement: The authors declare no conflicts of interest.

1 Introduction

The nonlinear autoregressive distributed lag (NARDL) model proposed by Shin, Yu, and Greenwood-Nimmo (2014, hereafter SYG) is an asymmetric generalization of the ARDL model of Pesaran and Shin (1998) and Pesaran et al. (2001). It is a single-equation error-correction model that has been widely applied to accommodate asymmetry in the long-run equilibrium relationship and/or the short-run dynamic coefficients via the use of partial sum decomposition of the explanatory variable(s). The NARDL approach has grown in popularity, with applications in fields including criminology (Box et al., 2019), economic growth (Eberhardt and Presbitero, 2015), energy economics (Hammoudeh et al., 2015), exchange rates and trade (Brun-Aguerre et al., 2017), financial economics (He and Zhou, 2018), health economics (Barati and Farid-itavana, 2020), and political science (Ferris et al., 2020), to list only a few.See Cho et al. (2023b) for an extensive survey. Despite its popularity, the theoretical foundations for estimation of and inference on the NARDL model have yet to be fully developed. It is this issue that we address.

SYG show that the parameters of the NARDL model can be estimated in a single step by ordinary least squares (OLS), though the positive and negative partial sums of the regressors are dominated by deterministic trends that are asymptotically perfectly collinear. But, these collinear trends introduce an asymptotic singularity that represents a barrier to the development of asymptotic theory for the single- step estimator, frustrating efforts to derive its limit distribution. Consequently, SYG only conduct Monte Carlo simulations to validate the properties of the single-step OLS estimator in finite samples.

To address this important issue, we first consider a bivariate model with a scalar dependent variable, y_t, and a scalar explanatory variable, x_t. In this case, the asymmetric long-run relationship is expressed among the level of the dependent variable and the positive and negative cumulative partial sums of the regressor, denoted x_t^+ and x_t^-, respectively, the latter of which share asymptotically collinear trends. But, the long-run relationship can be expressed equivalently via a one-to-one transformation as a relationship between y_t, x_t and x_t^+. By excluding one partial sum process, the asymptotic singularity in the long-run relationship is resolved. It is important to realize, however, that this reparameterization is insufficient to resolve the singularity problem associated with the single-step NARDL estimator; in fact, we show that it introduces a further asymptotic singularity problem, once again frustrating efforts to obtain the necessary limit theory.

In this regard, our solution is to adopt a two-step estimation framework. In the first step, the parameters of the transformed long-run relationship are estimated using any consistent estimator with a convergence rate faster than the square root of the sample size, $\sqrt{T}$. We advocate the use of the fully-modified (FM) estimator of Phillips and Hansen (1990) in the first step, which we show to follow an asymptotic mixed normal distribution that facilitates standard inference on the long-run parameters. Moreover, FM is robust to potential endogeneity of the regressors and to residual serial correlation. Given the super-consistency of the FM estimator, the error correction term can be treated as known in the second step, where OLS provides a consistent and asymptotically normal estimator for the short-run dynamic parameters.

Notwithstanding its simplicity, the two-step estimator described above cannot be directly applied to estimating the NARDL model with multiple explanatory variables, where a further singular matrix problem arises when estimating the reparameterized long-run equation due to the collinearity of the trends in $\boldsymbol{x}_t^+$ and/or $\boldsymbol{x}_t$. To resolve this issue, we propose to first detrend $\boldsymbol{x}_t^+$ by OLS and then to use the OLS residuals as a regressor together with a time trend and $\boldsymbol{x}_t$. This modified two-step procedure allows for estimation of the long-run relationship without any singularity problem in models with multiple regressors. The short-run parameters can be estimated by OLS in a final step.

Because the NARDL model allows for asymmetry in both the long-run equilibrium relationship and the short-run dynamic parameters, we develop Wald tests for symmetry in the long run and in the short run. We establish that the null distribution of the Wald statistics weakly converges to a chi-squared distribution. A suite of Monte Carlo simulations confirm that the Wald tests of both the short- and long-run symmetry are well-sized with high power even in small samples.

We demonstrate the utility of our approach with an application to the asymmetric relationship between R&D intensity and physical investment using quarterly data in the U.S. covering the period from 1960q1 to 2019q4. The potentially asymmetric relationship between research and development (R&D) expenditure and investment has received little attention, despite the growing literature on innovation and growth (e.g., Romer, 1990; Agarwal and Audretsch, 2001; Aghion et al., 2009; Chung and Shin, 2020). In the Online Supplement we develop a theory relating early-stage *innovative* and later-stage *managerial* R&D expenditures to physical investment. We derive a theoretical prediction that innovative R&D is a complement to investment while managerial R&D is a substitute and develop the testable hypothesis that innovative R&D expenditure is positively related with investment by virtue of complementarity while the relationship between managerial R&D expenditure and investment may be negative due to their nature as substitutes. Overall, we find that investment responds positively to R&D expenditures in the long run when their growth rate exceeds the growth rate of GDP, but negatively when they grow more slowly than GDP. This supports our theoretical predictions regarding the nature of innovative (managerial) R&D expenditure as a complement to (substitute for) physical investment. Furthermore, we find that investment is more sensitive to changes in R&D intensity when managerial R&D activity prevails.

This paper proceeds in 7 sections. In Section 2, we introduce the NARDL model and analyze the asymptotic singularity problem. Sections 3 and 4 introduce the two-step estimation framework and develop Wald tests for the null hypotheses of the short-run and long-run symmetry. In Section 5, we scrutinize the finite sample properties of the tests by simulation. Section 6 is devoted to our empirical application, and Section 7 concludes. Proofs of the main claims, further singularity issues associated with the one-step NARDL estimator, the theory relating early-stage innovative and later-stage managerial R&D expenditures to investment, and additional simulation/empirical results are relegated to the Online Supplement.

2 The NARDL Model

Consider the NARDL(p, q) process: $y_t = \gamma_* + \sum_{j=1}^{p} \phi_{j*} y_{t-j} + \sum_{j=0}^{q} (\boldsymbol{\theta}_{j*}^{+\prime} \boldsymbol{x}_{t-j}^{+} + \boldsymbol{\theta}_{j*}^{-\prime} \boldsymbol{x}_{t-j}^{-}) + e_t$, where $\boldsymbol{x}_t \in \mathbb{R}^k$, $\boldsymbol{x}_t^{+} := \sum_{j=1}^{t} \Delta \boldsymbol{x}_j^{+}$, $\boldsymbol{x}_t^{-} := \sum_{j=1}^{t} \Delta \boldsymbol{x}_j^{-}$, $\Delta \boldsymbol{x}_t^{+} := \max[\mathbf{0}, \Delta \boldsymbol{x}_t]$, and $\Delta \boldsymbol{x}_t^{-} := \min[\mathbf{0}, \Delta \boldsymbol{x}_t]$, such that $\Delta \boldsymbol{x}_t$ is a stationary process. The corresponding error-correction model is given by

$$\Delta y_t = \gamma_* + \rho_* y_{t-1} + \boldsymbol{\theta}_*^{+\prime} \boldsymbol{x}_{t-1}^{+} + \boldsymbol{\theta}_*^{-\prime} \boldsymbol{x}_{t-1}^{-} + \sum_{j=1}^{p-1} \varphi_{j*} \Delta y_{t-j} + \sum_{j=0}^{q-1} \left(\boldsymbol{\pi}_{j*}^{+\prime} \Delta \boldsymbol{x}_{t-j}^{+} + \boldsymbol{\pi}_{j*}^{-\prime} \Delta \boldsymbol{x}_{t-j}^{-} \right) + e_t, \quad (1)$$

for some ρ_*, $\boldsymbol{\theta}_*^{+}$, $\boldsymbol{\theta}_*^{-1}$, γ_*, φ_{j*} $(j = 1, 2, \ldots, p-1)$, $\boldsymbol{\pi}_{j*}^{+}$, and $\boldsymbol{\pi}_{j*}^{-}$ $(j = 0, 1, \ldots, q-1)$, where $\{e_t, \mathcal{F}_t\}$ is a martingale difference sequence and $\mathcal{F}_t$ is the smallest σ-algebra driven by $\{y_{t-1}, \boldsymbol{x}_t^{+}, \boldsymbol{x}_t^{-}, y_{t-2}, \boldsymbol{x}_{t-1}^{+}, \boldsymbol{x}_{t-1}^{-}, \ldots\}$. If y_t is cointegrated with $(\boldsymbol{x}_t^{+\prime}, \boldsymbol{x}_t^{-\prime})'$, then we may rewrite it as

$$\Delta y_t = \gamma_* + \rho_* u_{t-1} + \sum_{j=1}^{p-1} \varphi_{j*} \Delta y_{t-j} + \sum_{j=0}^{q-1} \left(\boldsymbol{\pi}_{j*}^{+\prime} \Delta \boldsymbol{x}_{t-j}^{+} + \boldsymbol{\pi}_{j*}^{-\prime} \Delta \boldsymbol{x}_{t-j}^{-} \right) + e_t, \quad (2)$$

where $u_{t-1} := y_{t-1} - \boldsymbol{\beta}_*^{+\prime} \boldsymbol{x}_{t-1}^{+} - \boldsymbol{\beta}_*^{-\prime} \boldsymbol{x}_{t-1}^{-}$ is the cointegrating error, $\boldsymbol{\beta}_*^{+} := -(\boldsymbol{\theta}_*^{+}/\rho_*)$ and $\boldsymbol{\beta}_*^{-} := -(\boldsymbol{\theta}_*^{-}/\rho_*)$. Here, u_t is a stationary process that may be correlated with $\Delta \boldsymbol{x}_t$.

The NARDL process can capture a cointegrating relationship between a deterministic time trend process driven by a unit-root process and other unit-root processes, possibly associated with a time trend. Suppose that $\mathbb{E}[\Delta \boldsymbol{x}_t] \equiv \mathbf{0}$ and that $\boldsymbol{\mu}_*^{+} := \mathbb{E}[\Delta \boldsymbol{x}_t^{+}]$ and $\boldsymbol{\mu}_*^{-} := \mathbb{E}[\Delta \boldsymbol{x}_t^{-}]$. It follows that $\boldsymbol{\mu}_*^{+} + \boldsymbol{\mu}_*^{-} \equiv \mathbf{0}$ by construction. Therefore, if we further let $\boldsymbol{s}_t^{+} := \Delta \boldsymbol{x}_t^{+} - \boldsymbol{\mu}_*^{+}$ and $\boldsymbol{s}_t^{-} := \Delta \boldsymbol{x}_t^{-} - \boldsymbol{\mu}_*^{-}$, then $\boldsymbol{x}_t^{+} = \boldsymbol{\mu}_*^{+} t + \sum_{j=1}^{t} \boldsymbol{s}_j^{+}$ and $\boldsymbol{x}_t^{-} = \boldsymbol{\mu}_*^{-} t + \sum_{j=1}^{t} \boldsymbol{s}_j^{-}$. It is clear that $\boldsymbol{x}_t^{+}$ and $\boldsymbol{x}_t^{-}$ are deterministic time-trend processes driven by unit-root processes. It follows that Δy_t is not necessarily distributed around zero even if $\boldsymbol{x}_t$ is a unit-root process without a deterministic trend. Note that $\rho_* := 1 - \sum_{j=1}^{p} \phi_{j*}$. From the NARDL($p$, q) process, we find that

$$\delta_* := \mathbb{E}[\Delta y_t] = -\frac{1}{\rho_*}\left[\sum_{j=0}^{q}(\boldsymbol{\theta}_{j*}^{+})'\boldsymbol{\mu}_*^{+} + \sum_{j=0}^{q}(\boldsymbol{\theta}_{j*}^{-})'\boldsymbol{\mu}_*^{-}\right].$$

Therefore, if we define $d_t := \Delta y_t - \delta_*$, then $y_t = \delta_* t + \sum_{j=1}^{t} d_j$, which shows that y_t is a deterministic time-trend process driven by a unit-root process if $\delta_* \neq 0$. This has the important implication that the NARDL model can analyze an asymmetric cointegrating relationship between two integrated variables even with the mismatched drifts without the need to include a deterministic time trend in the model.

SYG propose to estimate the parameters of the NARDL model, (1) in a single step by OLS. As shown in Lemma 1, the OLS estimation suffers from the asymptotic singularity of the inverse matrix associated with the one-step NARDL estimator.

We make the following assumptions:

Assumption 1. *(i)* $\{(\Delta \boldsymbol{x}_t', u_t)'\}$ *is the* $(k+1)\times 1$ *vector of globally covariance stationary mixing processes with* ϕ *of size* $-r/(2(r-1))$ *or* α *of size* $-r/(r-2)$ *and* $r > 2$*; (ii)* $\mathbb{E}[\Delta \boldsymbol{x}_t] = \mathbf{0}$, $\mathbb{E}[|\Delta \boldsymbol{x}_{ti}|^r] < \infty$ $(i = 1, 2, \ldots, k)$, $\mathbb{E}[|u_t|^r] < \infty$*, and* $\mathbb{E}[|e_t|^2] < \infty$*; (iii)* $\lim_{T\to\infty}$ *var*$[T^{-1/2}\sum_{t=1}^{T}(\Delta \boldsymbol{x}_t', u_t)']$ *exists and is positive definite (PD); and (iv) for some* $(\rho_*, \boldsymbol{\theta}_*^{+\prime}, \boldsymbol{\theta}_*^{-\prime}, \gamma_*, \varphi_{1*}, \ldots, \varphi_{p-1*}, \boldsymbol{\pi}_{0*}^{+\prime}, \ldots, \boldsymbol{\pi}_{q-1*}^{+\prime}, \boldsymbol{\pi}_{0*}^{-\prime}, \ldots, \boldsymbol{\pi}_{q-1*}^{-\prime})'$, Δy_t *is generated by* (1) *such that* $\{e_t, \mathcal{F}_t\}$ *is a martingale difference sequence and* $\mathcal{F}_t$ *is the smallest* σ*-algebra driven by* $\{y_{t-1}, \boldsymbol{x}_t^{+}, \boldsymbol{x}_t^{-}, y_{t-2}, \boldsymbol{x}_{t-1}^{+}, \boldsymbol{x}_{t-1}^{-}, \ldots\}$. □

Let $\boldsymbol{z}_t := [\boldsymbol{z}_{1t}' \vdots \boldsymbol{z}_{2t}']' := [y_{t-1}, \boldsymbol{x}_{t-1}^{+\prime}, \boldsymbol{x}_{t-1}^{-\prime} \vdots 1, \Delta \boldsymbol{y}_{t-1}', \Delta \boldsymbol{x}_t^{+\prime}, \ldots, \Delta \boldsymbol{x}_{t-q+1}^{+\prime}, \Delta \boldsymbol{x}_t^{-\prime}, \ldots, \Delta \boldsymbol{x}_{t-q+1}^{-\prime}]'$, where $\Delta \boldsymbol{y}_{t-1} := [\Delta y_{t-1}, \Delta y_{t-2}, \ldots, \Delta y_{t-p+1}]'$. Note that $\boldsymbol{z}_t$ is partitioned into nonstationary and stationary variables. $\boldsymbol{z}_{2t}$ is further partitioned as $\boldsymbol{z}_{2t} := [1 \vdots \boldsymbol{w}_t']' := [1 \vdots \boldsymbol{w}_{1t}' \vdots \boldsymbol{w}_{2t}' \vdots \boldsymbol{w}_{3t}']' := [1 \vdots \Delta \boldsymbol{y}_{t-1}' \vdots \Delta \boldsymbol{x}_t^{+\prime}, \ldots, \Delta \boldsymbol{x}_{t-q+1}^{+\prime} \vdots \Delta \boldsymbol{x}_t^{-\prime}, \ldots, \Delta \boldsymbol{x}_{t-q+1}^{-\prime}]'$. Next, we define $\boldsymbol{\alpha}_* := [\boldsymbol{\alpha}_{1*}' \vdots \boldsymbol{\alpha}_{2*}']' := [\rho_*, \boldsymbol{\theta}_*^{+\prime}, \boldsymbol{\theta}_*^{-\prime} \vdots \gamma_*, \boldsymbol{\varphi}_*', \boldsymbol{\pi}_{0*}^{+\prime}, \ldots, \boldsymbol{\pi}_{q-1*}^{+\prime}, \boldsymbol{\pi}_{0*}^{-\prime}, \ldots, \boldsymbol{\pi}_{q-1*}^{-\prime}]'$, where $\boldsymbol{\varphi}_* := [\varphi_{1*}, \varphi_{2*}, \ldots, \varphi_{p-1*}]'$. Then, the OLS estimator is:

$$\widehat{\boldsymbol{\alpha}}_T := \left(\sum_{t=1}^{T}\boldsymbol{z}_t\boldsymbol{z}_t'\right)^{-1}\sum_{t=1}^{T}\boldsymbol{z}_t\Delta y_t = \boldsymbol{\alpha}_* + \left(\sum_{t=1}^{T}\boldsymbol{z}_t\boldsymbol{z}_t'\right)^{-1}\sum_{t=1}^{T}\boldsymbol{z}_t e_t.$$

Inference using $\widehat{\boldsymbol{\alpha}}_T$ is challenging because $\sum_{t=1}^{T}\boldsymbol{z}_t\boldsymbol{z}_t'$ is asymptotically singular as shown in Lemma 1.

Lemma 1. *Under Assumption 1, (i)* $T^{-3}\sum_{t=1}^{T}\boldsymbol{z}_{t1}\boldsymbol{z}_{t1}' \overset{\mathbb{P}}{\to} \mathbf{M}_{11} := \frac{1}{3}\boldsymbol{n}_1\boldsymbol{n}_1'$*; (ii)* $T^{-2}\sum_{t=1}^{T}\boldsymbol{z}_{1t}\ \boldsymbol{z}_{2t}' \overset{\mathbb{P}}{\to}$

$\mathbf{M}_{12} := \frac{1}{2}\boldsymbol{n}_1\boldsymbol{n}_2'$; *and (iii)* $T^{-1}\sum_{t=1}^{T}\boldsymbol{z}_{2t}\boldsymbol{z}_{2t}' \xrightarrow{\mathbb{P}} \mathbf{M}_{22}$, *where*

$$\mathbf{M}_{22} := \begin{bmatrix} 1 & \boldsymbol{n}_2^{(1)\prime} \\ \boldsymbol{n}_2^{(1)} & \mathbb{E}[\boldsymbol{w}_t\boldsymbol{w}_t'] \end{bmatrix},$$

$\boldsymbol{n}_1 := [\delta_*, \boldsymbol{\mu}_*^{+\prime}, \boldsymbol{\mu}_*^{-\prime}]'$, $\boldsymbol{n}_2 := [1, \boldsymbol{n}_2^{(1)}]$ *and* $\boldsymbol{n}_2^{(1)} := [\delta_*\boldsymbol{\iota}_{p-1}', \boldsymbol{\iota}_q' \otimes \boldsymbol{\mu}_*^{+\prime}, \boldsymbol{\iota}_q' \otimes \boldsymbol{\mu}_*^{-\prime}]'$ *with* $\boldsymbol{\iota}_a$ *being an* $a \times 1$ *vector of ones.* □

Lemma 1 implies that, if we let $\mathbf{D}_T := \text{diag}[T^{3/2}\mathbf{I}_{2+2k}, T^{1/2}\mathbf{I}_{p+2qk}]$, then $\mathbf{D}_T^{-1}(\sum_{t=1}^{T}\boldsymbol{z}_t\boldsymbol{z}_t')\,\mathbf{D}_T^{-1} \xrightarrow{\mathbb{P}} \mathbf{M}_*$, where $\mathbf{M}_*$ is 2×2 block matrix, whose i-th row and j-th column block is $\mathbf{M}_{ij}$ and $\mathbf{M}_{21} = \mathbf{M}_{12}'$. As $\mathbf{M}_*$ is singular, it is difficult to derive the limit distribution of $\widehat{\boldsymbol{\alpha}}_T$ directly, unless we can derive the limit distribution of the determinant of $\sum_{t=1}^{T}\boldsymbol{z}_t\boldsymbol{z}_t'$, which is analytically challenging.

3 Asymptotic Theory for the Two-step NARDL Estimator

We propose an analytically tractable two-step estimation procedure that draws on the work of Engle and Granger (1987) and Phillips and Hansen (1990) and derive the relevant limit distributions. For clarity of exposition, we treat the cases with $k = 1$ and $k > 1$, separately.

3.1 The Two-step NARDL Estimation with $k = 1$

3.1.1 Estimation of the Long-Run Parameters

First Step Estimation by OLS. Recall that the long-run relationship is written as $y_t = \alpha_* + \beta_*^+ x_t^+ + \beta_*^- x_t^- + u_t$. In line with the two-step estimation framework of Engle and Granger (1987), we may estimate the long-run parameters by OLS. Define $\bar{\mathbf{D}}_T := \text{diag}[T^{1/2}, T^{3/2}\mathbf{I}_2]$ and $\boldsymbol{v}_t := (1, x_t^+, x_t^-)'$ such that $\bar{\mathbf{D}}_T^{-1}\left(\sum_{t=1}^{T}\boldsymbol{v}_t\boldsymbol{v}_t'\right)\bar{\mathbf{D}}_T^{-1} \xrightarrow{\mathbb{P}} \mathbf{M}_{11}$. By Lemma 1(*i*), this is a singular matrix due to the collinear trends in x_t^+ and x_t^-.

We propose to reparameterize the long-run relationship as $y_t = \alpha_* + \lambda_* x_t^+ + \eta_* x_t + u_t$, where $x_t \equiv x_t^+ + x_t^-$, $\lambda_* = \beta_*^+ - \beta_*^-$ and $\eta_* = \beta_*^-$. It follows that $\beta_*^+ = \lambda_* + \eta_*$ and $\beta_*^- = \eta_*$. Then, the OLS estimator of $\boldsymbol{\varrho}_* := (\alpha_*, \lambda_*, \eta_*)'$ is given by $\widehat{\boldsymbol{\varrho}}_T := (\widehat{\alpha}_T, \widehat{\lambda}_T, \widehat{\eta}_T)' := \arg\min_{\alpha,\,\lambda,\,\eta}\sum_{t=1}^{T}(y_t - \alpha - \lambda x_t^+ - \eta x_t)^2$, where we can recover $\widehat{\beta}_T^+ := \widehat{\lambda}_T + \widehat{\eta}_T$ and $\widehat{\beta}_T^- = \widehat{\eta}_T$.

Letting $\boldsymbol{q}_t := (1, x_t^+, x_t)'$, then $\widehat{\boldsymbol{\varrho}}_T = \boldsymbol{\varrho}_* + (\sum_{t=1}^T \boldsymbol{q}_t\boldsymbol{q}_t')^{-1}(\sum_{t=1}^T \boldsymbol{q}_t u_t)$. Define

$$\boldsymbol{\Sigma}_* := \lim_{T\to\infty} T^{-1}\sum_{t=1}^T\sum_{s=1}^T \mathbb{E}[\boldsymbol{g}_t\boldsymbol{g}_s] \quad \text{and} \quad [\mathcal{B}_x(\cdot), \mathcal{B}_u(\cdot)]' := \boldsymbol{\Sigma}_*^{1/2}[\mathcal{W}_x(\cdot), \mathcal{W}_u(\cdot)]',$$

where $\boldsymbol{g}_t := [\Delta x_t, u_t]'$ and $[\mathcal{W}_x(\cdot), \mathcal{W}_u(\cdot)]'$ is a 2×1 vector of independent Wiener processes. Let $\sigma_*^{(i,j)}$ be the i,t-th element of $\boldsymbol{\Sigma}_*$. If $\{u_t\}$ is serially uncorrelated and independent of $\{\Delta x_t\}$, then $\boldsymbol{\Sigma}_*$ and $[\mathcal{B}_x(\cdot), \mathcal{B}_u(\cdot)]'$ are simplified to diag $[\sigma_x^2, \sigma_u^2]$ and $[\sigma_x\mathcal{W}_x(\cdot), \sigma_u\mathcal{W}_u(\cdot)]'$, respectively, where $\sigma_x^2 := \lim_{T\to\infty} T^{-1}\sum_{t=1}^T\sum_{s=1}^T \mathbb{E}[\Delta x_t \Delta x_s]$ and $\sigma_u^2 := \mathbb{E}[u_t^2]$.

Lemma 2 provides the limit behaviors of the components of the OLS estimator.

Lemma 2. *Under Assumption 1, if $k = 1$ and $\boldsymbol{\Sigma}_*$ is PD, then*

$$(i)\ \widehat{\mathbf{Q}}_T := \widetilde{\mathbf{D}}_T^{-1}\left(\sum_{t=1}^T \boldsymbol{q}_t\boldsymbol{q}_t'\right)\widetilde{\mathbf{D}}_T^{-1} \Rightarrow \boldsymbol{\mathcal{Q}} := \begin{bmatrix} 1 & \frac{1}{2}\mu_*^+ & \int \mathcal{B}_x \\ \frac{1}{2}\mu_*^+ & \frac{1}{3}\mu_*^+\mu_*^+ & \mu_*^+\int r\mathcal{B}_x \\ \int \mathcal{B}_x & \int r\mathcal{B}_x\mu_*^+ & \int \mathcal{B}_x\mathcal{B}_x \end{bmatrix},$$

where $\widetilde{\mathbf{D}}_T :=$ diag$[T^{1/2}, T^{3/2}, T]$; and (ii) if $\upsilon_* := \lim_{T\to\infty} T^{-1}\sum_{t=1}^T\sum_{i=1}^t \mathbb{E}[\Delta x_i u_t]$ is finite, then $\widehat{\mathbf{U}}_T := \widetilde{\mathbf{D}}_T^{-1}(\sum_{t=1}^T \boldsymbol{q}_t u_t) \Rightarrow \boldsymbol{\mathcal{U}} := [\int d\mathcal{B}_u, \mu_*^+\int r d\mathcal{B}_u, \int \mathcal{B}_x d\mathcal{B}_u + \upsilon_*]$. □

All integrals are evaluated with respect to $r \in [0,1]$. For example, $\int r\mathcal{B}_x$ denotes $\int_0^1 r\mathcal{B}_x(r)dr$. As $\boldsymbol{\mathcal{Q}}$ is nonsingular with probability 1, the limit distribution of $\widehat{\boldsymbol{\varrho}}_T$ is obtained as a product of $\boldsymbol{\mathcal{Q}}^{-1}$ and $\boldsymbol{\mathcal{U}}$, as stated in Corollary 1.

Corollary 1. *Under Assumption 1, if $k = 1$ and $\boldsymbol{\Sigma}_*$ is PD, then $\widetilde{\mathbf{D}}_T(\widehat{\boldsymbol{\varrho}}_T - \boldsymbol{\varrho}_*) \Rightarrow \boldsymbol{\mathcal{Q}}^{-1}\boldsymbol{\mathcal{U}}$.*[1] □

Corollary 1 has important implications. First, by the reparameterization, the collinearity between x_t^+ and x_t^- can be avoided because $\sum_{t=1}^T x_t = O_{\mathbb{P}}(T^{3/2})$ and $\sum_{t=1}^T x_t^+ = O_{\mathbb{P}}(T^2)$ lead to different convergence

[1] Alternatively, the same limit distribution can be obtained using a rotation matrix:

$$\mathbf{A} := \begin{pmatrix} 1 & 0 & 0 \\ 0 & 1 & 0 \\ 0 & 1 & 1 \end{pmatrix}, \quad \text{so that} \quad (\mathbf{A}')^{-1}\begin{pmatrix} \widehat{\alpha}_T - \alpha_* \\ \widehat{\beta}_*^+ - \beta_*^+ \\ \widehat{\beta}_*^- - \beta_*^- \end{pmatrix} = \begin{pmatrix} \widehat{\alpha}_T - \alpha_* \\ (\widehat{\beta}_*^+ - \beta_*^+) - (\widehat{\beta}_*^- - \beta_*^-) \\ \widehat{\beta}_*^- - \beta_*^- \end{pmatrix} = \widehat{\boldsymbol{\varrho}}_T - \boldsymbol{\varrho}_*.$$

Then,

$$\widetilde{\mathbf{D}}_T(\widehat{\boldsymbol{\varrho}}_T - \boldsymbol{\varrho}_*) = \widetilde{\mathbf{D}}_T(\mathbf{A}')^{-1}\begin{pmatrix} \widehat{\alpha}_T - \alpha_* \\ \widehat{\beta}_*^+ - \beta_*^+ \\ \widehat{\beta}_*^- - \beta_*^- \end{pmatrix} = \left(\widetilde{\mathbf{D}}_T^{-1}\sum_{t=1}^T \mathbf{A}\boldsymbol{v}_t\boldsymbol{v}_t'\mathbf{A}'\widetilde{\mathbf{D}}_T^{-1}\right)^{-1}\left(\widetilde{\mathbf{D}}_T^{-1}\sum_{t=1}^T \mathbf{A}\boldsymbol{v}_t u_t\right)$$
$$= \left(\widetilde{\mathbf{D}}_T^{-1}\sum_{t=1}^T \boldsymbol{q}_t\boldsymbol{q}_t'\widetilde{\mathbf{D}}_T^{-1}\right)^{-1}\left(\widetilde{\mathbf{D}}_T^{-1}\sum_{t=1}^T \boldsymbol{q}_t u_t\right) \Rightarrow \boldsymbol{\mathcal{Q}}^{-1}\boldsymbol{\mathcal{U}},$$

where the third equality holds by noting that $\mathbf{A}\boldsymbol{v}_t = \boldsymbol{q}_t$.

rates for $\widehat{\lambda}_T$ and $\widehat{\eta}_T$, viz., $\widehat{\lambda}_T - \lambda_* = O_{\mathbb{P}}(T^{-3/2})$ and $\widehat{\eta}_T - \eta_* = O_{\mathbb{P}}(T^{-1})$. Second, to derive the limit distribution of $\widehat{\boldsymbol{\varrho}}_T$, we apply the FCLT only to $\sum_{t=1}^{T(\cdot)} \boldsymbol{g}_t$ where $\boldsymbol{g}_t := [\Delta x_t, u_t]'$, not to $\sum_{t=1}^{[T(\cdot)]}(x_t^+ - \mu_*^+)$. Third, using the definition of $\widehat{\lambda}_T$, we have: $T\{(\widehat{\beta}_T^+ - \widehat{\beta}_T^-) - (\beta_*^+ - \beta_*^-)\} = O_{\mathbb{P}}(T^{-1/2})$, implying that the limit distributions of $T(\widehat{\beta}_T^+ - \beta_*^+)$ and $T(\widehat{\beta}_T^- - \beta_*^-)$ are asymptotically equivalent. Finally, as the long-run parameter estimator is super-consistent, $\widehat{\beta}_T^+$ and $\widehat{\beta}_T^-$ can be treated as given when estimating the short-run dynamic parameters.

Theorem 1 presents the limit distribution of the OLS estimator of the long-run parameters.

Theorem 1. *For $k = 1$, under Assumption 1, $T[(\widehat{\beta}_T^+ - \beta_*^+), (\widehat{\beta}_T^- - \beta_*^-)]' \Rightarrow \boldsymbol{\iota}_2 \otimes \mathbf{S}\boldsymbol{\mathcal{Q}}^{-1}\boldsymbol{\mathcal{U}}$, where $\mathbf{S} := [\mathbf{0}_{1\times 2}, 1]$.* □

Due to its dependence on the nuisance parameters $\boldsymbol{\Sigma}_*$ and υ_*, the OLS estimator of the long-run parameters in Theorem 1 does not follow a normal distribution asymptotically. Except in the special case where $\{u_t\}$ is independent of $\{\Delta x_t\}$ and/or serially uncorrelated, the OLS estimator of the long-run parameter exhibits an asymptotic bias determined by υ_*.

First Step Estimation by FM. Phillips and Hansen (1990) propose the FM estimator, which is shown to be free from asymptotic biases even in the presence of endogenous regressors and/or serial correlation, and which follows an asymptotic mixed normal distribution. Hence, we advocate the use of FM to estimate the long-run parameters in the first step.

Suppose that $\boldsymbol{\Sigma}_*$ is consistently estimated by a heteroskedasticity and autocorrelation consistent covariance matrix estimator, $\widetilde{\boldsymbol{\Sigma}}_T$ with $\widetilde{\sigma}_T^{(i,j)}$ being (i,j)-th element. For example, following Newey and West (1987), we have

$$\widetilde{\boldsymbol{\Sigma}}_T := \frac{1}{T}\sum_{t=1}^{T}\widehat{\boldsymbol{g}}_t\widehat{\boldsymbol{g}}_t' + \frac{1}{T}\sum_{k=1}^{\ell}\omega_{\ell k}\sum_{t=k+1}^{T}\{\widehat{\boldsymbol{g}}_{t-k}\widehat{\boldsymbol{g}}_t' + \widehat{\boldsymbol{g}}_t\widehat{\boldsymbol{g}}_{t-k}'\},$$

where $\widehat{\boldsymbol{g}}_t := [\Delta x_t, \widehat{u}_t]'$, $\omega_{\ell k} := 1 - k/(1+\ell)$, $\ell = O(T^{1/4})$ and $\widehat{u}_t := y_t - \widehat{\alpha}_T - \widehat{\beta}_T^+ x_t^+ - \widehat{\beta}_T^- x_t^-$. Under mild regularity conditions, it is straightforward to show that the asymptotic bias, υ_* in $\boldsymbol{\mathcal{U}}$, can be consistently estimated by $\widetilde{\boldsymbol{\Pi}}_T := \frac{1}{T}\sum_{k=0}^{\ell}\sum_{t=k+1}^{T}\widehat{\boldsymbol{g}}_{t-k}\widehat{\boldsymbol{g}}_t'$. Let $\widetilde{\pi}_T^{(i,j)}$ be the (i,j)-th element of $\widetilde{\boldsymbol{\Pi}}_T$. Define the long-run parameter estimator by

$$\widetilde{\boldsymbol{\varrho}}_T := (\widetilde{\alpha}_T, \widetilde{\lambda}_T, \widetilde{\eta}_T)' := \left(\sum_{t=1}^{T}\boldsymbol{q}_t\boldsymbol{q}_t'\right)^{-1}\left(\sum_{t=1}^{T}\boldsymbol{q}_t\widetilde{y}_t - T\mathbf{S}'\widetilde{\upsilon}_T\right),$$

where $\widetilde{y}_t := y_t - \Delta x_t(\widetilde{\sigma}_T^{(1,1)})^{-1}\widetilde{\sigma}_T^{(1,2)}$ and $\widetilde{\upsilon}_T := \widetilde{\pi}_T^{(1,2)} - \widetilde{\pi}_T^{(1,1)}(\widetilde{\sigma}_T^{(1,1)})^{-1}\,\widetilde{\sigma}_T^{(1,2)}$. Then, the FM estimators of the long-run parameters are obtained as $\widetilde{\beta}_T^+ := \widetilde{\lambda}_T + \widetilde{\eta}_T$ and $\widetilde{\beta}_T^- := \widetilde{\eta}_T$.

To derive the limit distribution of the FM estimator, we make the following assumptions.

Assumption 2. *(i)* $\mathbf{\Sigma}_*$ *is finite and PD and* $\widetilde{\mathbf{\Sigma}}_T \overset{\mathbb{P}}{\to} \mathbf{\Sigma}_*$*; and (ii)* $\mathbf{\Pi}_*$ *is finite and* $\widetilde{\mathbf{\Pi}}_T \overset{\mathbb{P}}{\to} \mathbf{\Pi}_*$*, where* $\mathbf{\Pi}_* := \lim_{T\to\infty} \frac{1}{T}\sum_{t=1}^{T}\sum_{i=1}^{t}\mathbb{E}[\boldsymbol{g}_i\boldsymbol{g}_t']$.

Let $\pi_*^{(i,j)}$ be the (i,j)-th element of $\mathbf{\Pi}_*$ such that $\pi_*^{(1,2)}$ is identical to υ_*. Lemma 3 provides the limit behavior of the components of the FM estimator.

Lemma 3. *Under Assumptions 1 and 2 and for* $k=1$, $\widetilde{\mathbf{U}}_T := \widetilde{\mathbf{D}}_T^{-1}\{\sum_{t=1}^{T}\boldsymbol{q}_t(u_t - \Delta x_t(\widetilde{\sigma}_T^{(1,1)})^{-1}\,\widetilde{\sigma}_T^{(1,2)}) - T\mathbf{S}'\widetilde{\upsilon}_T\} \Rightarrow \widetilde{\boldsymbol{\mathcal{U}}} := \tau_*[\int d\mathcal{W}_u, \mu_*^+\int r d\mathcal{W}_u, \int \mathcal{B}_x d\mathcal{W}_u]'$*, where* $\tau_*^2 := plim_{T\to\infty}\widetilde{\tau}_T^2$ *and* $\widetilde{\tau}_T^2 := \widetilde{\sigma}_T^{(2,2)} - \widetilde{\sigma}_T^{(2,1)}(\widetilde{\sigma}_T^{(1,1)})^{-1}\widetilde{\sigma}_T^{(1,2)}$. □

By Lemma 2(*i*), $\widehat{\mathbf{Q}}_T \Rightarrow \boldsymbol{\mathcal{Q}}$, which is nonsingular with probability 1. Therefore , the limit distribution of $\widetilde{\boldsymbol{\varrho}}_T$ can be obtained as the product of $\boldsymbol{\mathcal{Q}}^{-1}$ and $\widetilde{\boldsymbol{\mathcal{U}}}$:

Corollary 2. *Under Assumption 1 and for* $k=1$, $\widetilde{\mathbf{D}}_T(\widetilde{\boldsymbol{\varrho}}_T - \boldsymbol{\varrho}_*) \Rightarrow \boldsymbol{\mathcal{Q}}^{-1}\widetilde{\boldsymbol{\mathcal{U}}}$. □

Corollary 2 has several implications. First, the limit distribution of the FM-OLS estimator is mixed normal. Conditional on $\sigma\{\mathcal{B}_x(r), r \in (0,1]\}$, the limit distribution of $\widetilde{\mathbf{D}}_T(\widetilde{\boldsymbol{\varrho}}_T - \boldsymbol{\varrho}_*)$ is $N(\mathbf{0}, \tau_*^2\boldsymbol{\mathcal{Q}}^{-1})$. Consequently, the null limit distribution of a Wald test constructed using the FM estimator will be chi-squared. Second, we have: $T(\widetilde{\beta}_T^+ - \beta_*^+) = T(\widetilde{\beta}_T^- - \beta_*^-) + o_{\mathbb{P}}(1)$, implying that the limit distribution of $\widetilde{\beta}_T^+$ is equivalent to that of $\widetilde{\beta}_T^-$, where the limit distribution of $\widetilde{\beta}_T^-$ is given by that of $\widetilde{\eta}_T$. Third, the convergence rates of $\widetilde{\beta}_T^+$ and $\widetilde{\beta}_T^-$ are T, enabling us to estimate the short-run parameters in the second stage by replacing u_{t-1} with $\widetilde{u}_{t-1} := y_{t-1} - \widetilde{\alpha}_T - \widetilde{\beta}_T^+ x_{t-1}^+ - \widetilde{\beta}_T^- x_{t-1}^-$.

Theorem 2 formally presents the limit distribution of the FM estimator:

Theorem 2. *Under Assumptions 1 and 2 and for* $k=1$, $T[(\widetilde{\beta}_T^+ - \beta_*^+), (\widetilde{\beta}_T^- - \beta_*^-)]' \Rightarrow \boldsymbol{\iota}_2 \otimes \mathbf{S}\boldsymbol{\mathcal{Q}}^{-1}\widetilde{\boldsymbol{\mathcal{U}}}$. □

3.1.2 Estimation of the Short-Run Parameters

As the long-run coefficients are super-consistent, we can treat them as known when estimating the short-run parameters in (2), which can be expressed compactly as $\Delta y_t = \boldsymbol{\zeta}_*'\boldsymbol{h}_t + e_t$, where $\boldsymbol{\zeta}_* := (\rho_*, \boldsymbol{\beta}_{2*}')'$, $\boldsymbol{\beta}_{2*} := (\gamma_*, \varphi_{1*}, \ldots, \varphi_{p-1*}, \pi_{0*}^{+\prime}, \ldots, \pi_{q-1*}^{+\prime}, \pi_{0*}^{-\prime}, \ldots, \pi_{q-1*}^{-\prime},)'$ and $\boldsymbol{h}_t := (u_{t-1}, \boldsymbol{z}_{2t}')'$. Because all variables in this equation are stationary, the short-run dynamic parameters can be estimated by the OLS estimator:

$$\widehat{\boldsymbol{\zeta}}_T := \left(\sum_{t=1}^{T}\boldsymbol{h}_t\boldsymbol{h}_t'\right)^{-1}\sum_{t=1}^{T}\boldsymbol{h}_t\Delta y_t = \boldsymbol{\zeta}_* + \left(\sum_{t=1}^{T}\boldsymbol{h}_t\boldsymbol{h}_t'\right)^{-1}\sum_{t=1}^{T}\boldsymbol{h}_t e_t.$$

Lemma 4 shows the limit behaviors of the components of $\widehat{\boldsymbol{\zeta}}_T$.

Lemma 4. *Under Assumption 1, (i)* $\widehat{\boldsymbol{\Gamma}}_T := T^{-1}\sum_{t=1}^T \boldsymbol{h}_t\boldsymbol{h}_t' \overset{\mathbb{P}}{\to} \boldsymbol{\Gamma}_* := \mathbb{E}[\boldsymbol{h}_t\boldsymbol{h}_t']$*; (ii)* $T^{-1/2}\sum_{t=1}^T \boldsymbol{h}_t e_t \overset{A}{\sim} N[\mathbf{0}, \boldsymbol{\Omega}_*]$ *where* $\boldsymbol{\Omega}_* := \mathbb{E}[e_t^2\boldsymbol{h}_t\boldsymbol{h}_t']$*; and (iii)* $\boldsymbol{\Omega}_*$ *simplifies to* $\sigma_*^2\boldsymbol{\Gamma}_*$ *in the special case where* $\mathbb{E}[e_t^2|\boldsymbol{h}_t] = \sigma_*^2$. □

Using Lemma 4, we derive the limit distribution of $\widehat{\boldsymbol{\zeta}}_T$ in Theorem 3.

Theorem 3. *Suppose that* $\boldsymbol{\Gamma}_*$ *and* $\boldsymbol{\Omega}_*$ *are PD. Under Assumption 1, (i)* $\sqrt{T}(\widehat{\boldsymbol{\zeta}}_T - \boldsymbol{\zeta}_*) \overset{A}{\sim} N(\mathbf{0}, \boldsymbol{\Gamma}_*^{-1}\boldsymbol{\Omega}_*\boldsymbol{\Gamma}_*^{-1})$ *and (ii) further if* $\mathbb{E}[e_t^2|\boldsymbol{h}_t] = \sigma_*^2$*, then* $\sqrt{T}(\widehat{\boldsymbol{\zeta}}_T - \boldsymbol{\zeta}_*) \overset{A}{\sim} N(\mathbf{0}, \sigma_*^2\boldsymbol{\Gamma}_*^{-1})$. □

3.2 The Two-step NARDL Estimation with $k > 1$

If there are multiple explanatory variables in the NARDL model, then the two-step estimation procedure described in Section 3.1 needs to be modified as follows.

Let $\boldsymbol{x}_t \equiv \boldsymbol{x}_t^+ + \boldsymbol{x}_t^-$, $\boldsymbol{\lambda}_* = \boldsymbol{\beta}_*^+ - \boldsymbol{\beta}_*^-$ and $\boldsymbol{\eta}_* = \boldsymbol{\beta}_*^-$ with $k > 1$. Then, we have: $y_t = \alpha_* + \boldsymbol{\lambda}_*'\boldsymbol{x}_t^+ + \boldsymbol{\eta}_*'\boldsymbol{x}_t + u_t$. By extending Lemma 2, we have:

$$\widehat{\mathbf{Q}}_T := \widetilde{\mathbf{D}}_T^{-1}\left(\sum_{t=1}^T \boldsymbol{q}_t\boldsymbol{q}_t'\right)\widetilde{\mathbf{D}}_T^{-1} \Rightarrow \boldsymbol{\mathcal{Q}} := \begin{bmatrix} 1 & \frac{1}{2}\boldsymbol{\mu}_*^+ & \int \boldsymbol{\mathcal{B}}_x' \\ \frac{1}{2}\boldsymbol{\mu}_*^+ & \frac{1}{3}\boldsymbol{\mu}_*^+\boldsymbol{\mu}_*^{+\prime} & \boldsymbol{\mu}_*^+\int r\boldsymbol{\mathcal{B}}_x' \\ \int \boldsymbol{\mathcal{B}}_x dr & \int r\boldsymbol{\mathcal{B}}_x\boldsymbol{\mu}_*^{+\prime} & \int \boldsymbol{\mathcal{B}}_x\boldsymbol{\mathcal{B}}_x' \end{bmatrix},$$

where $\boldsymbol{q}_t := (1, \boldsymbol{x}_t^{+\prime}, \boldsymbol{x}_t')'$, $\widetilde{\mathbf{D}}_T := \mathrm{diag}[T^{1/2}, T^{3/2}\mathbf{I}_k, T\mathbf{I}_k]$, $\boldsymbol{\mathcal{B}}_x(\cdot)$ is a $k\times 1$ vector of Brownian motions with $[\boldsymbol{\mathcal{B}}_x(\cdot)', \mathcal{B}_u(\cdot)]' := \boldsymbol{\Sigma}_*^{1/2}[\boldsymbol{\mathcal{W}}_x(\cdot)', \mathcal{W}_u(\cdot)']'$ and $[\boldsymbol{\mathcal{W}}_x(\cdot)', \mathcal{W}_u(\cdot)]'$ being a $(k+1)\times 1$ vector of independent Wiener processes, and $\boldsymbol{\Sigma}_* := \lim_{T\to\infty} T^{-1}\sum_{t=1}^T\sum_{s=1}^T \mathbb{E}[\boldsymbol{g}_t\boldsymbol{g}_s]$ with $\boldsymbol{g}_t := [\Delta\boldsymbol{x}_t, u_t]'$. The blocks on the second row of $\boldsymbol{\mathcal{Q}}$ form a sub-matrix with rank equal to unity. That is, $[\frac{1}{2}\boldsymbol{\mu}_*^+, \frac{1}{3}\boldsymbol{\mu}_*^+\boldsymbol{\mu}_*^{+\prime}, \boldsymbol{\mu}_*^+\int r\boldsymbol{\mathcal{B}}_x'] = \boldsymbol{\mu}_*^+[\frac{1}{2}, \frac{1}{3}\boldsymbol{\mu}_*^{+\prime}, \int r\boldsymbol{\mathcal{B}}_x']$, implying that $\boldsymbol{\mathcal{Q}}$ is singular with probability 1. Consequently, the two-step procedure in Section 3.1 cannot be directly applied to estimating the long-run parameters.

3.2.1 Estimation of the Long-Run Parameters

First-Step Transformed OLS Estimator. To address the above singularity issue,[2] let $\boldsymbol{m}_t := \sum_{j=1}^t \boldsymbol{s}_j^+$, which is a unit-root process with zero-mean increments. Thus, if we regress $\boldsymbol{x}_t^+$ against t, then we estimate $\boldsymbol{\mu}_*^+$ by $\widehat{\boldsymbol{\mu}}_T^+ := (\sum_{t=1}^T t^2)^{-1}\sum_{t=1}^T t\boldsymbol{x}_t^+ = \boldsymbol{\mu}_*^+ + (\sum_{t=1}^T t^2)^{-1}\sum_{t=1}^T t\boldsymbol{m}_t$, and obtain $\widehat{\boldsymbol{m}}_t := \boldsymbol{x}_t^+ - \widehat{\boldsymbol{\mu}}_T^+ t$. Consequently, $\boldsymbol{m}_t = \widehat{\boldsymbol{m}}_t + t\boldsymbol{d}_T$, where $\boldsymbol{d}_T := (\sum_{t=1}^T t^2)^{-1}\sum_{t=1}^T t\boldsymbol{m}_t$. Then, $\boldsymbol{x}_t^+ = \widehat{\boldsymbol{m}}_t + \boldsymbol{\delta}_{*T}t$, where $\boldsymbol{\delta}_{*T} := \boldsymbol{\mu}_*^+ + \boldsymbol{d}_T$. Under regularity conditions, $\boldsymbol{d}_T = O_{\mathbb{P}}(T^{-1/2})$ and thus $\boldsymbol{\delta}_{*T} = \boldsymbol{\mu}_* + O_{\mathbb{P}}(T^{-1/2})$.

[2] Cho et al. (2023a) allow $E(\Delta\boldsymbol{x}_t) \neq 0$ and propose a substantial modification to the estimation and inference procedure.

Rewriting the long-run relationship as $y_t = \alpha_* + \xi_{*T} t + \boldsymbol{\lambda}_*' \widehat{\boldsymbol{m}}_t + \boldsymbol{\eta}_*' \boldsymbol{x}_t + u_t$, where $\xi_{*T} := \boldsymbol{\lambda}_*' \boldsymbol{\delta}_{*T}$, we can estimate $\boldsymbol{\lambda}_*$ and $\boldsymbol{\eta}_*$ by regressing y_t on $\boldsymbol{r}_t := (1, t, \widehat{\boldsymbol{m}}_t', \boldsymbol{x}_t')'$. Let $\ddot{\boldsymbol{\varpi}}_T := (\ddot{\alpha}_T, \ddot{\xi}_{*T}, \ddot{\boldsymbol{\lambda}}_T', \ddot{\boldsymbol{\eta}}_T')'$ be the OLS estimator of $\varpi_{*T} := (\alpha_*, \xi_{*T}, \boldsymbol{\lambda}_*', \boldsymbol{\eta}_*')'$. The long-run estimators of $\boldsymbol{\beta}_*^+$ and $\boldsymbol{\beta}_*^-$ can be obtained as $\ddot{\boldsymbol{\beta}}_T^+ := \ddot{\boldsymbol{\lambda}}_T + \ddot{\boldsymbol{\eta}}_T$ and $\ddot{\boldsymbol{\beta}}_T^- := \ddot{\boldsymbol{\eta}}_T$. Let:

$$\ddot{\mathbf{S}} := \begin{bmatrix} \mathbf{0}_{k\times 1} & \mathbf{0}_{k\times 1} & \mathbf{I}_k & \mathbf{I}_k \\ \mathbf{0}_{k\times 1} & \mathbf{0}_{k\times 1} & \mathbf{0}_{k\times k} & \mathbf{I}_k \end{bmatrix}, \quad \text{then} \quad \begin{bmatrix} \widehat{\boldsymbol{\beta}}_T^+ \\ \widehat{\boldsymbol{\beta}}_T^- \end{bmatrix} = \ddot{\mathbf{S}} \ddot{\boldsymbol{\varpi}}_T.$$

We refer to this as the *first-step transformed OLS (TOLS) estimator*. The intuition is straightforward; as it is the collinear trend in $\boldsymbol{x}_t^+$ that results in the singularity of $\boldsymbol{\mathcal{Q}}$, which, in turn, renders the first-step estimation by OLS and FM inoperable, we detrend $\boldsymbol{x}_t^+$ prior to estimation.

The limit distribution of the first-step TOLS estimator is obtained similarly to that of the first-step OLS estimator. Note that $\ddot{\boldsymbol{\varpi}}_T = \boldsymbol{\varpi}_{*T} + (\sum_{t=1}^T \boldsymbol{r}_t \boldsymbol{r}_t')^{-1} \sum_{t=1}^T \boldsymbol{r}_t u_t$. To characterize the limit behaviors of the components, we define $\ddot{\boldsymbol{\Sigma}}_* := \lim_{T\to\infty} \frac{1}{T} \sum_{t=1}^T \sum_{s=1}^T \mathbb{E}[\ddot{\boldsymbol{g}}_t \ddot{\boldsymbol{g}}_t']$ and $[\boldsymbol{\mathcal{B}}_m(\cdot)', \boldsymbol{\mathcal{B}}_x(\cdot)', \mathcal{B}_u(\cdot)]'$ $:= \ddot{\boldsymbol{\Sigma}}_*^{1/2} [\boldsymbol{\mathcal{W}}_m(\cdot)', \boldsymbol{\mathcal{W}}_x(\cdot)', \mathcal{W}_u(\cdot)]'$, where $\ddot{\boldsymbol{g}}_t := [\Delta \boldsymbol{m}_t', \Delta \boldsymbol{x}_t, u_t]'$ and $[\boldsymbol{\mathcal{W}}_m(\cdot)', \boldsymbol{\mathcal{W}}_x(\cdot)', \mathcal{W}_u(\cdot)]'$ is a $(2k+1) \times 1$ vector of independent Wiener processes.

Lemma 5. *Suppose that $\ddot{\boldsymbol{\Sigma}}_*$ is PD. Under Assumption 1, (i) $\ddot{\mathbf{R}}_T := \ddot{\mathbf{D}}_T^{-1} (\sum_{t=1}^T \boldsymbol{r}_t \boldsymbol{r}_t') \ddot{\mathbf{D}}_T^{-1} \Rightarrow \boldsymbol{\mathcal{R}}$, where $\boldsymbol{\mathcal{R}}$ is defined as:*

$$\begin{bmatrix} 1 & \frac{1}{2} & \int (1-\frac{3}{2}r)\boldsymbol{\mathcal{B}}_m' & \int \boldsymbol{\mathcal{B}}_x' \\ \frac{1}{2} & \frac{1}{3} & \mathbf{0}_{1\times k} & \int r \boldsymbol{\mathcal{B}}_x' \\ \int (1-\frac{3}{2}r)\boldsymbol{\mathcal{B}}_m & \mathbf{0}_{k\times 1} & \int \boldsymbol{\mathcal{B}}_m \boldsymbol{\mathcal{B}}_m' - 3\int r\boldsymbol{\mathcal{B}}_m \int r \boldsymbol{\mathcal{B}}_m' & \int \boldsymbol{\mathcal{B}}_m \boldsymbol{\mathcal{B}}_x' - 3\int r\boldsymbol{\mathcal{B}}_m \int r\boldsymbol{\mathcal{B}}_x' \\ \int \boldsymbol{\mathcal{B}}_x & \int r\boldsymbol{\mathcal{B}}_x & \int \boldsymbol{\mathcal{B}}_x \boldsymbol{\mathcal{B}}_m' - 3\int r\boldsymbol{\mathcal{B}}_x \int r\boldsymbol{\mathcal{B}}_m' & \int \boldsymbol{\mathcal{B}}_x \boldsymbol{\mathcal{B}}_x' \end{bmatrix},$$

and $\ddot{\mathbf{D}}_T := diag[T^{1/2}, T^{3/2}, T\mathbf{I}_{2k}]$; and (ii) if $\boldsymbol{\upsilon}_{x*} := \lim_{T\to\infty} T^{-1} \sum_{t=1}^T \sum_{i=1}^t \mathbb{E}[\Delta \boldsymbol{x}_i u_t]$ and $\boldsymbol{\upsilon}_{m*} := \lim_{T\to\infty} T^{-1} \sum_{t=1}^T \sum_{i=1}^t \mathbb{E}[\Delta \boldsymbol{m}_i u_t]$ are finite, then $\ddot{\mathbf{U}}_T := \ddot{\mathbf{D}}_T^{-1} (\sum_{t=1}^T \boldsymbol{r}_t u_t) \Rightarrow \ddot{\boldsymbol{\mathcal{U}}} := [\int d\mathcal{B}_u, \int r d\mathcal{B}_u,$ $\int \boldsymbol{\mathcal{B}}_m' d\mathcal{B}_u - 3\int r d\mathcal{B}_u \int r \boldsymbol{\mathcal{B}}_m' + \boldsymbol{\upsilon}_{m*}', \int \boldsymbol{\mathcal{B}}_x' d\mathcal{B}_u + \boldsymbol{\upsilon}_{x*}']'$. □

$\boldsymbol{\mathcal{R}}$ is no longer singular because $\sum_{t=1}^{[T(\cdot)]} \ddot{\boldsymbol{g}}_t$ obeys the FCLT using partially correlated increments.

Corollary 3. *Under Assumption 1, $\ddot{\mathbf{D}}_T(\ddot{\boldsymbol{\varpi}}_T - \boldsymbol{\varpi}_{*T}) \Rightarrow \boldsymbol{\mathcal{R}}^{-1} \ddot{\boldsymbol{\mathcal{U}}}$ and $T^{1/2}(\widehat{\xi}_T - \boldsymbol{\lambda}_*' \boldsymbol{\mu}_*^+) \Rightarrow 3\boldsymbol{\lambda}_*' \int r \boldsymbol{\mathcal{B}}_m$.* □

The first part of Corollary 3 follows from the structure of the first-step TOLS estimator. For the second part, notice that $\widehat{\xi}_T$ is not of primary interest.While the convergence rate of $(\widehat{\xi}_T - \xi_{*T})$ is $T^{3/2}$, $\xi_{*T} := \boldsymbol{\lambda}_*' \boldsymbol{\delta}_{*T}$ converges to $\boldsymbol{\lambda}_*' \boldsymbol{\mu}_*^+$ at rate $\sqrt{T}$. This implies that $T^{1/2}(\widehat{\xi}_T - \boldsymbol{\lambda}_*' \boldsymbol{\mu}_*^+)$ is asymptotically bounded in probability.

Theorem 4 provides the limit distribution of the TOLS estimator.

Theorem 4. *Suppose that $\ddot{\boldsymbol{\Sigma}}_*$ is PD. Under Assumption 1, $T[(\ddot{\boldsymbol{\beta}}_T^+ - \boldsymbol{\beta}_*^+)', (\ddot{\boldsymbol{\beta}}_T^- - \boldsymbol{\beta}_*^-)']' \Rightarrow \ddot{\mathbf{S}}\boldsymbol{\mathcal{R}}^{-1}\ddot{\boldsymbol{\mathcal{U}}}$.* □

First-Step Transformed FM Estimator. The limit distribution of the TOLS estimator in Theorem 4 does not provide a basis for inference, as it exhibits asymptotic biases driven by $\boldsymbol{\upsilon}_{*m}$ and $\boldsymbol{\upsilon}_{*x}$. Thus, we provide the first-step transformed FM (TFM) estimator.

We make the following assumptions:

Assumption 3. *(i) For finite and PD $\ddot{\boldsymbol{\Sigma}}_*$ there exists a consistent estimator of $\ddot{\boldsymbol{\Sigma}}_*$:*

$$\bar{\boldsymbol{\Sigma}}_T := \begin{bmatrix} \bar{\boldsymbol{\Sigma}}_T^{(1,1)} & \bar{\boldsymbol{\sigma}}_T^{(1,2)} \\ \bar{\boldsymbol{\sigma}}_T^{(2,1)} & \bar{\sigma}_T^{(2,2)} \end{bmatrix} \stackrel{\mathbb{P}}{\to} \ddot{\boldsymbol{\Sigma}}_* := \begin{bmatrix} \ddot{\boldsymbol{\Sigma}}_*^{(1,1)} & \ddot{\boldsymbol{\sigma}}_*^{(1,2)} \\ \ddot{\boldsymbol{\sigma}}_*^{(2,1)} & \sigma_*^{(2,2)} \end{bmatrix};$$

and (ii) if we let $\bar{\boldsymbol{\Pi}}_T := T^{-1}\sum_{k=0}^{\ell}\sum_{t=k+1}^{T}\bar{\boldsymbol{g}}_{t-k}\bar{\boldsymbol{g}}_t'$, then

$$\begin{bmatrix} \bar{\boldsymbol{\Pi}}_T^{(1,1)} & \bar{\boldsymbol{\pi}}_T^{(1,2)} \\ \bar{\boldsymbol{\pi}}_T^{(2,1)} & \bar{\pi}_T^{(2,2)} \end{bmatrix} := \bar{\boldsymbol{\Pi}}_T \stackrel{\mathbb{P}}{\to} \ddot{\boldsymbol{\Pi}}_* := \begin{bmatrix} \ddot{\boldsymbol{\Pi}}_*^{(1,1)} & \ddot{\boldsymbol{\pi}}_*^{(1,2)} \\ \ddot{\boldsymbol{\pi}}_*^{(2,1)} & \pi_*^{(2,2)} \end{bmatrix} := \lim_{T\to\infty}\frac{1}{T}\sum_{t=1}^{T}\sum_{i=1}^{t}\mathbb{E}[\ddot{\boldsymbol{g}}_t\ddot{\boldsymbol{g}}_t'],$$

which is finite, where $\bar{\boldsymbol{g}}_t := [\Delta\widehat{\boldsymbol{m}}_t', \Delta\boldsymbol{x}_t', \ddot{u}_t]'$ and $\ddot{u}_t := y_t - \ddot{\alpha}_T - \ddot{\boldsymbol{\beta}}_T^{+\prime}\boldsymbol{x}_t^+ - \ddot{\boldsymbol{\beta}}_T^{-\prime}\boldsymbol{x}_t^-$. □

Assumption 3 corresponds to Assumption 2 for $k > 1$. The TFM estimator is defined as

$$\bar{\boldsymbol{\varpi}}_T := (\bar{\alpha}_T, \bar{\xi}_T, \bar{\boldsymbol{\beta}}_T^{+\prime}, \bar{\boldsymbol{\beta}}_T^{-\prime})' := \left(\sum_{t=1}^{T}\boldsymbol{r}_t\boldsymbol{r}_t'\right)^{-1}\left(\sum_{t=1}^{T}\boldsymbol{r}_t\bar{y}_t - T\bar{\mathbf{S}}'\bar{\boldsymbol{\upsilon}}_T\right),$$

where $\bar{y}_t := y_t - \boldsymbol{\ell}_t'(\bar{\boldsymbol{\Sigma}}_T^{(1,1)})^{-1}\bar{\boldsymbol{\sigma}}_T^{(1,2)}$, $\boldsymbol{\ell}_t := (\Delta\widehat{\boldsymbol{m}}_t', \Delta\boldsymbol{x}_t')'$, $\bar{\boldsymbol{\upsilon}}_T := \bar{\boldsymbol{\pi}}_T^{(1,2)} - \bar{\boldsymbol{\Pi}}_T^{(1,1)}(\bar{\boldsymbol{\Sigma}}_T^{(1,1)})^{-1}\bar{\boldsymbol{\sigma}}_T^{(1,2)}$ and $\bar{\mathbf{S}} := [\mathbf{0}_{2k\times 2}, \mathbf{I}_{2k}]$. The limit distribution of the TFM estimator is obtained in a similar way to that of the FM estimator.

Lemma 6. *Under Assumptions 1 and 3, $\bar{\mathbf{U}}_T := \ddot{\mathbf{D}}_T^{-1}\{\sum_{t=1}^{T}\boldsymbol{r}_t(u_t - \boldsymbol{\ell}_t'(\bar{\boldsymbol{\Sigma}}_T^{(1,1)})^{-1}\bar{\boldsymbol{\sigma}}_T^{(1,2)}) - T\bar{\mathbf{S}}'\bar{\boldsymbol{\upsilon}}_T\} \Rightarrow \bar{\boldsymbol{\mathcal{U}}} := \ddot{\tau}[\int d\mathcal{W}_u, \int r d\mathcal{W}_u, \int \boldsymbol{\mathcal{B}}_m' d\mathcal{W}_u - 3\int r d\mathcal{W}_u \int r\boldsymbol{\mathcal{B}}_m', \int \boldsymbol{\mathcal{B}}_x' d\mathcal{W}_u]'$, where $\ddot{\tau}^2 := plim_{T\to\infty}\bar{\tau}_T^2$ and $\bar{\tau}_T^2 := \bar{\sigma}_T^{(2,2)} - \bar{\boldsymbol{\sigma}}_T^{(2,1)}(\bar{\boldsymbol{\Sigma}}_T^{(1,1)})^{-1}\bar{\boldsymbol{\sigma}}_T^{(1,2)}$.* □

By Lemmas 5 and 6, the limit distribution of the TFM estimator is obtained as the product of $\boldsymbol{\mathcal{R}}^{-1}$ and $\bar{\boldsymbol{\mathcal{U}}}$. Letting $[\bar{\boldsymbol{\beta}}_T^{+\prime}, \bar{\boldsymbol{\beta}}_T^{-\prime}]' := \ddot{\mathbf{S}}\bar{\boldsymbol{\varpi}}_T$, we obtain its weak limit as follows:

Theorem 5. *Under Assumptions 1 and 3, $\ddot{\mathbf{D}}_T(\bar{\boldsymbol{\varpi}}_T - \bar{\boldsymbol{\varpi}}_{*T}) \Rightarrow \boldsymbol{\mathcal{R}}^{-1}\bar{\boldsymbol{\mathcal{U}}}$ and $T[(\bar{\boldsymbol{\beta}}_T^+ - \boldsymbol{\beta}_*^+)', (\bar{\boldsymbol{\beta}}_T^- - \boldsymbol{\beta}_*^-)']' \Rightarrow \ddot{\mathbf{S}}\boldsymbol{\mathcal{R}}^{-1}\bar{\boldsymbol{\mathcal{U}}}$.* □

The limit distribution of the TFM estimator is mixed normal. That is, conditional on $\sigma\{(\boldsymbol{\mathcal{B}}_m(r)', \boldsymbol{\mathcal{B}}_x(r)')', r \in (0,1]\}$, $\bar{\mathbf{D}}_T(\bar{\boldsymbol{\varpi}}_T - \bar{\boldsymbol{\varpi}}_{*T}) \Rightarrow N(\mathbf{0}, \ddot{\tau}^2 \boldsymbol{\mathcal{R}}^{-1})$.

3.2.2 Estimation of the Short-Run Parameters

We can treat the TFM estimator of the long-run parameters as known when estimating the short-run parameters in the second step because it has a convergence rate faster than $\sqrt{T}$. Let $u_{t-1} := y_{t-1} - \boldsymbol{\beta}_*^{+\prime}\boldsymbol{x}_{t-1}^+ - \boldsymbol{\beta}_*^{-\prime}\boldsymbol{x}_{t-1}^- = y_{t-1} - \boldsymbol{\lambda}_*'\boldsymbol{\mu}_*^+(t-1) - \boldsymbol{\lambda}_*'\boldsymbol{m}_{t-1} - \boldsymbol{\eta}_*'\boldsymbol{x}_{t-1}$, where $\boldsymbol{\lambda}_*$, $\boldsymbol{\mu}_*^+$, and $\boldsymbol{\eta}_*$ are assumed to be known. This allows us to employ (2) in Section 3.1.2, and estimate the short-run parameters by the OLS estimator. Then, Theorem 3 can be applied.

4 Hypothesis Testing

We develop the testing procedure for the presence of asymmetries.

4.1 Hypothesis Testing with $k = 1$

4.1.1 Testing for Symmetry of the Long-Run Parameters

Consider $H_0' : (\beta_*^+ - \beta_*^-) = r$ vs. $H_1' : (\beta_*^+ - \beta_*^-) \neq r$ for some $r \in \mathbb{R}$. By setting $r = 0$, we can test whether $\beta_*^+ = \beta_*^-$. As $\lambda_* := \beta_*^+ - \beta_*^-$, we can restate the hypothesis as $H_0'' : \lambda_* = r$ vs. $H_1'' : \lambda_* \neq r$, from which the long-run symmetry restriction, $\beta_*^+ = \beta_*^-$, is equivalent to the restriction, $\lambda_* = 0$. It is straightforward to test this restriction if λ_* is estimated by FM, because the FM estimator is asymptotically mixed-normal. Thus, the Wald test follows an asymptotic chi-squared distribution under the null. This is an important advantage of FM over OLS.

Corollary 2 provides the limit distribution of $\widetilde{\lambda}_T$. Letting $\mathbf{S}_\ell := [0, 1, 0]$, then $T^{3/2}(\widetilde{\lambda}_T - \lambda_*) = \mathbf{S}_\ell \widetilde{\mathbf{D}}_T(\widetilde{\boldsymbol{\varrho}}_T - \boldsymbol{\varrho}_*) \Rightarrow \mathbf{S}_\ell \boldsymbol{\mathcal{Q}}^{-1}\widetilde{\boldsymbol{\mathcal{U}}}$, implying that $T^{3/2}(\widetilde{\lambda}_T - r) \Rightarrow \mathbf{S}_\ell \boldsymbol{\mathcal{Q}}^{-1}\widetilde{\boldsymbol{\mathcal{U}}}$ under H_0''. The Wald test is constructed as

$$\mathcal{W}_T^{(\ell)} := T^3(\widetilde{\lambda}_T - r)^2(\widetilde{\tau}_T^2 \mathbf{S}_\ell \widehat{\mathbf{Q}}_T^{-1}\mathbf{S}_\ell')^{-1}.$$

Notice, however, that this Wald statistic may be inappropriate to test other forms of hypothesis. For example, consider $H_0''' : \mathbf{R}\boldsymbol{\beta}_* = \mathbf{r}$ vs. $H_1''' : \mathbf{R}\boldsymbol{\beta}_* \neq \mathbf{r}$ for some $\mathbf{R} \in \mathbb{R}^{r \times 2}$ and $\mathbf{r} \in \mathbb{R}^r$ ($r \in \{1, 2\}$), where $\boldsymbol{\beta}_* := (\beta_*^+, \beta_*^-)'$. Let

$$\widetilde{\mathbf{R}}_\ell := \begin{bmatrix} 0 & 1 & 1 \\ 0 & 0 & 1 \end{bmatrix}.$$

These hypotheses can be rewritten as $H_0''': \widetilde{\mathbf{R}}\boldsymbol{\varrho}_* = \mathbf{r}$ vs. $H_1''': \widetilde{\mathbf{R}}\boldsymbol{\varrho}_* \neq \mathbf{r}$, where $\widetilde{\mathbf{R}}\boldsymbol{\varrho}_* = \boldsymbol{\beta}_*$ and $\widetilde{\mathbf{R}} := \mathbf{R}\widetilde{\mathbf{R}}_\ell$. Then, we construct the Wald test as

$$\widetilde{\mathcal{W}}_T^{(\ell)} := (\widetilde{\mathbf{R}}\widetilde{\boldsymbol{\varrho}}_T - \mathbf{r})'(\widetilde{\tau}_T^2 \widetilde{\mathbf{R}}\mathbf{Q}_T^{-1}\widetilde{\mathbf{R}}')^{-1}(\widetilde{\mathbf{R}}\widetilde{\boldsymbol{\varrho}}_T - \mathbf{r}),$$

where $\mathbf{Q}_T := \sum_{t=1}^T \boldsymbol{q}_t \boldsymbol{q}_t'$.

Theorem 6 describes the limit behavior of $\widetilde{\mathcal{W}}_T^{(\ell)}$:

Theorem 6. *Under Assumptions 1 and 2, $\mathcal{W}_T^{(\ell)} \overset{A}{\sim} \mathcal{X}_1^2$ under H_0'' and $\widetilde{\mathcal{W}}_T^{(\ell)} \overset{A}{\sim} \mathcal{X}_2^2$ under H_0'''. For any sequence, c_T and $\widetilde{c}_T$, such that $c_T = o(T^3)$ and $\widetilde{c}_T = o(T^2)$, $\mathbb{P}(\mathcal{W}_T^{(\ell)} > c_T) \to 1$ under H_1'' and $\mathbb{P}(\widetilde{\mathcal{W}}_T^{(\ell)} > \widetilde{c}_T) \to 1$ under H_1'''.* □

4.1.2 Testing for Symmetry of the Short-Run Parameters

In the NARDL literature, it is common to test for additive symmetry of the short-run dynamic parameters.[3] Consider $H_0 : \mathbf{R}_s\boldsymbol{\zeta}_* = \mathbf{r}$ vs. $H_1 : \mathbf{R}_s\boldsymbol{\zeta}_* \neq \mathbf{r}$, where $\mathbf{R}_s \in \mathbb{R}^{r\times(1+p+2q)}$ and $\mathbf{r} \in \mathbb{R}^r$ $(r \in \mathbb{N})$ are selection matrices. The null hypothesis of additive short-run symmetry can be tested against the alternative hypothesis of asymmetry: $H_0 : \sum_{j=0}^{q-1} \pi_{j*}^+ = \sum_{j=0}^{q-1} \pi_{j*}^-$ vs. $H_1 : \sum_{j=0}^{q-1} \pi_{j*}^+ \neq \sum_{j=0}^{q-1} \pi_{j*}^-$. Letting $\mathbf{R}_s := \left[\mathbf{0}_{1+p}', \boldsymbol{\iota}_q', -\boldsymbol{\iota}_q'\right]$ and $\mathbf{r} = 0$, then the Wald test is constructed as

$$\mathcal{W}_T^{(s)} := T(\mathbf{R}_s\widehat{\boldsymbol{\zeta}}_T - \mathbf{r})'(\mathbf{R}_s\widehat{\boldsymbol{\Gamma}}_T^{-1}\widehat{\boldsymbol{\Omega}}_T\widehat{\boldsymbol{\Gamma}}_T^{-1}\mathbf{R}_s')^{-1}(\mathbf{R}_s\widehat{\boldsymbol{\zeta}}_T - \mathbf{r}),$$

where $\widehat{\boldsymbol{\Omega}}_T := T^{-1}\sum_{t=1}^T \widehat{e}_t^2 \boldsymbol{h}_t\boldsymbol{h}_t'$ is a consistent estimator of $\boldsymbol{\Omega}_*$. Further, if the condition in Lemma 4(*iii*) holds, the Wald test reduces to $\mathcal{W}_T^{(s)} := T(\mathbf{R}_s\widehat{\boldsymbol{\zeta}}_T - \mathbf{r})'(\widehat{\sigma}_{e,T}^2\mathbf{R}_s\widehat{\boldsymbol{\Gamma}}_T^{-1}\mathbf{R}_s')^{-1}(\mathbf{R}_s\widehat{\boldsymbol{\zeta}}_T - \mathbf{r})$, where $\widehat{\sigma}_{e,T}^2 := T^{-1}\sum_{t=1}^T \widehat{e}_t^2$ and $\widehat{e}_t := \Delta y_t - \widehat{\boldsymbol{\zeta}}_T'\boldsymbol{h}_t$.

Theorem 7 establishes that the null and alternative limit distributions of the Wald test are standard.

Theorem 7. *Suppose that $\boldsymbol{\Gamma}_*$ and $\boldsymbol{\Omega}_*$ are PD. Under Assumption 1, $\mathcal{W}_T^{(s)} \overset{A}{\sim} \mathcal{X}_r^2$ under H_0. For any sequence, c_T such that $c_T = o(T)$, $\mathbb{P}(\mathcal{W}_T^{(s)} > c_T) \to 1$ under H_1.* □

4.2 Hypotheses Testing with $k > 1$

[3] The literature has considered several forms of short-run symmetry restrictions, including pairwise symmetry of $\boldsymbol{\pi}_{j*}^+$ and $\boldsymbol{\pi}_{j*}^-$ for $j = 0, \ldots, q-1$ (SYG) and impact symmetry defined by $\boldsymbol{\pi}_{0*}^+$ and $\boldsymbol{\pi}_{0*}^-$ (Greenwood-Nimmo and Shin, 2013). It is straightforward to test these alternative restrictions by appropriately specifying selection matrices, $\mathbf{R}_s$ and $\mathbf{r}$.

4.2.1 Testing for Symmetry of the Long-Run Parameters

Define $\boldsymbol{\beta}_* := (\boldsymbol{\beta}_*^{+\prime}, \boldsymbol{\beta}_*^{-\prime})'$ and consider $H_0^{(4)} : \mathbf{R}\boldsymbol{\beta}_* = \boldsymbol{r}$ vs. $H_1^{(4)} : \mathbf{R}\boldsymbol{\beta}_* \neq \boldsymbol{r}$ for some $\mathbf{R} \in \mathbb{R}^{r\times 2k}$ and $\boldsymbol{r} \in \mathbb{R}^r$ ($r \leq 2k$). We then construct the Wald test as $\ddot{\mathcal{W}}_T := T^2(\mathbf{R}\bar{\boldsymbol{\beta}}_T - \boldsymbol{r})'\{\bar{\tau}_T^2\mathbf{R}\ddot{\mathbf{S}}\ddot{\mathbf{R}}_T^{-1}\ddot{\mathbf{S}}'\mathbf{R}'\}^{-1}(\mathbf{R}\bar{\boldsymbol{\beta}}_T - \boldsymbol{r})$, where $\bar{\boldsymbol{\beta}}_T := (\bar{\boldsymbol{\beta}}_T^{+\prime}, \bar{\boldsymbol{\beta}}_T^{-\prime})'$.

Theorem 8 describes the limit behavior of $\ddot{\mathcal{W}}_T$.

Theorem 8. *Under Assumptions 1 and 3, $\ddot{\mathcal{W}}_T^{(\ell)} \overset{A}{\sim} \mathcal{X}_r^2$ under $H_0^{(4)}$. For any sequence c_T such that $c_T = o(T^2)$, $\mathbb{P}(\ddot{\mathcal{W}}_T^{(\ell)} > c_T) \to 1$ under $H_1^{(4)}$.* □

4.2.2 Testing for Symmetry of the Short-Run Parameters

To test for additive symmetry of the short-run dynamic parameters, we consider $H_0 : \mathbf{R}_s\boldsymbol{\zeta}_* = \mathbf{r}$ vs. $H_1 : \mathbf{R}_s\boldsymbol{\zeta}_* \neq \mathbf{r}$, where $\mathbf{R}_s \in \mathbb{R}^{r\times(1+p+2qk)}$ and $\mathbf{r} \in \mathbb{R}^r$ are selection matrices, and $\boldsymbol{\zeta}_* := (\rho_*, \gamma_*, \varphi_{1*}, \ldots, \varphi_{p-1*}, \boldsymbol{\pi}_{0*}^{+\prime}, \ldots, \boldsymbol{\pi}_{q-1*}^{+\prime}, \boldsymbol{\pi}_{0*}^{-\prime}, \ldots, \boldsymbol{\pi}_{q-1*}^{-\prime})$, which generalizes our prior definition of $\boldsymbol{\zeta}_*$ for $k = 1$ in Section 4.1.2. Let $\mathbf{R}_s := [\mathbf{0}_{k\times(1+p)}, \boldsymbol{\iota}_q' \otimes \mathbf{I}_k, -\boldsymbol{\iota}_q \otimes \mathbf{I}_k]$ and $\mathbf{r} = \mathbf{0}$, then we can test the null hypothesis of additive short-run symmetry as $H_0 : \sum_{j=0}^{q-1}\boldsymbol{\pi}_{j*}^+ = \sum_{j=0}^{q-1}\boldsymbol{\pi}_{j*}^-$ vs. $H_1 : \sum_{j=0}^{q-1}\boldsymbol{\pi}_{j*}^+ \neq \sum_{j=0}^{q-1}\boldsymbol{\pi}_{j*}^-$. If the cointegration residuals are obtained as in Section 3.2.2, then we can employ the same Wald test described in Section 4.1.2, because both TOLS and TFM estimators are super-consistent.

5 Monte Carlo Simulations

We conduct stochastic simulations to examine the finite sample properties of the Wald tests described in Section 4.[4]

5.1 Simulations Results for $k = 1$

Consider the NARDL(1,0) data generating process (DGP): $\Delta y_t = \gamma_* + \rho_* u_{t-1} + \varphi_*\Delta y_{t-1} + \pi_*^+\Delta x_t^+ + \pi_*^-\Delta x_t^- + e_t$, where $u_{t-1} := y_{t-1} - \alpha_* - \beta_*^+ x_{t-1}^+ - \beta_*^- x_{t-1}^-$, $\Delta x_t := \kappa_*\Delta x_{t-1} + \sqrt{1-\kappa_*^2}v_t$, and $(e_t, v_t)' \sim \text{IID}N(\mathbf{0}_2, \mathbf{I}_2)$.

Testing Restrictions on the Long-Run Parameters. We focus on the case where the FM estimator is used in the first step and set $(\alpha_*, \beta_*^+, \beta_*^-, \gamma_*, \rho_*, \varphi_*, \pi_*^+, \pi_*^-, \kappa_*) = (0, 2, 1, 0, -2/3, \varphi_*, 1, 1/2, 1/2)$. We test $H_0^{(\ell)} : \beta_*^+ - \beta_*^- = 0$ vs. $H_1^{(\ell)} : \beta_*^+ - \beta_*^- \neq 0$ by allowing φ_* to vary over $-1/2$, $-1/4$, 0, $1/4$ and $1/2$.

[4] In Section D of the Online Supplement we investigate the finite sample bias and mean squared error of the two-step NARDL estimators, and show that they are consistent.

The simulation results reported in Table 1 reveal some size distortion in small samples for negative values of φ_*. Nonetheless, as T increases, the distribution of the Wald test becomes well-approximated by the $\mathcal{X}_1^2$ distribution. To examine the power of the Wald test, we generate data with $(\alpha_*, \beta_*^+, \beta_*^-, \gamma_*, \rho_*, \varphi_*, \pi_*^+, \pi_*^-, \kappa_*) = (0, 1.01, 1, 0, -2/3, \varphi_*, 1/3, 1/2, 1/2)$ and allow φ_* to vary as above. The simulation results reported in Table 2 confirm that the for $\mathcal{W}_T^{(\ell)}$ statistic is consistent under the alternative hypothesis. Furthermore, its power patterns are largely insensitive to the value of φ_*.

— Insert Tables 1 and 2 Here —

Testing Restrictions on the Short-Run Parameters. To examine the empirical levels of the Wald test, we set $(\alpha_*, \beta_*^+, \beta_*^-, \gamma_*, \rho_*, \varphi_*, \pi_*^+, \pi_*^-, \kappa_*) = (0, 2, 1, 0, -2/3, \varphi_*, 1/2, 1/2, 1/2)$ and allow φ_* to vary as above. We first estimate the long-run parameters by FM and compute $\widehat{u}_t$ before estimating the short-run parameters by OLS. We then test $H_0^{(s)} : \pi_*^+ - \pi_*^- = 0$ vs. $H_1^{(s)} : \pi_*^+ - \pi_*^- \neq 0$ using $\mathcal{W}_T^{(s)}$ with the heteroskedasticity consistent covariance estimator, $\widehat{\mathbf{\Omega}}_T$.

The simulation results reported in Table 3 reveal that the finite sample distribution of $\mathcal{W}_T^{(s)}$ is well approximated by the chi-squared distribution. Its empirical level tends to the nominal level once the number of observations reaches 500. Furthermore, the empirical sizes display little sensitivity to the value of φ_* even for small T. Next, we examine the empirical powers of the Wald test. We maintain the same hypotheses but update the parameters to $(\alpha_*, \beta_*^+, \beta_*^-, \gamma_*, \rho_*, \varphi_*, \pi_*^+, \pi_*^-, \kappa_*) = (0, 2, 1, 0, -2/3, \varphi_*, 1, 1/2, 1/2)$. Two points are noteworthy in Table 4. First, the empirical power of the Wald test rises with T, indicating that the test is consistent. Second, the power of the Wald test exhibits little sensitivity to the degree of autocorrelation captured by the value of φ_*.

— Insert Tables 3 and 4 Here —

5.2 Simulations Results for $k = 2$

We generate the following NARDL(1,0) DGP: $\Delta y_t = \gamma_* + \rho_* u_{t-1} + \varphi_* \Delta y_{t-1} + \boldsymbol{\pi}_{0*}^{+\prime} \Delta \boldsymbol{x}_t^+ + \pi_{0*}^{-\prime} \Delta \boldsymbol{x}_t^- + e_t$, where $u_{t-1} := y_{t-1} - \alpha_* - \boldsymbol{\beta}_*^{+\prime} \boldsymbol{x}_{t-1}^+ - \boldsymbol{\beta}_*^{-\prime} \boldsymbol{x}_{t-1}^-$, $\Delta \boldsymbol{x}_t := \kappa_* \Delta \boldsymbol{x}_{t-1} + \sqrt{1 - \kappa_*^2} \boldsymbol{v}_t$, and $(e_t, \boldsymbol{v}_t)' \sim$ IID$N(\mathbf{0}_3, \mathbf{I}_3)$.

Testing Restrictions on the Long-Run Parameters. We confine our attention to the case where the TFM estimator is used in the first step. We set $(\alpha_*, \gamma_*, \rho_*, \varphi_*, \kappa_*) = (0, 0, -1, \varphi_*, 0.5)$, $(\boldsymbol{\beta}_*^{+\prime}, \boldsymbol{\beta}_*^{-\prime})' = (-1, 0.5, 0.75, -1.5)'$, and $(\boldsymbol{\pi}_{0*}^{+\prime}, \boldsymbol{\pi}_{0*}^{-\prime})' = (0.5, -0.5, -1, 1)'$. We test $\dot{H}_0^{(\ell)} : \boldsymbol{\iota}_2' \boldsymbol{\beta}_*^+ = -0.50$ and $\boldsymbol{\iota}_2' \boldsymbol{\beta}_*^- = -0.75$ vs. $\dot{H}_1^{(\ell)} : \boldsymbol{\iota}_2' \boldsymbol{\beta}_*^+ \neq -0.50$ or $\boldsymbol{\iota}_2' \boldsymbol{\beta}_*^- \neq -0.75$ by allowing φ_* to vary over -0.3, -0.1, 0, 0.1 and 0.3.

The simulation results are reported in Table 5. As T rises, the distribution of the Wald test becomes well approximated by the $\mathcal{X}_2^2$ distribution. If $\varphi_* = 0.3$, then a larger sample size is required to achieve a satisfactory approximation. To examine the empirical powe, we test $\dot{H}_0^{(\ell)} : \boldsymbol{\iota}_2'\boldsymbol{\beta}_*^+ = -0.40$ and $\boldsymbol{\iota}_2'\boldsymbol{\beta}_*^- = -0.65$ vs. $\dot{H}_1^{(\ell)} : \boldsymbol{\iota}_2'\boldsymbol{\beta}_*^+ \neq -0.40$ or $\boldsymbol{\iota}_2'\boldsymbol{\beta}_*^- \neq -0.65$. Table 6 shows that the Wald test is consistent and its empirical rejection rates converge to 100% for all values of φ_*.

— Insert Tables 5 and 6 Here —

Testing Restrictions on the Short-Run Parameters. We generate the DGP with $(\alpha_*, \gamma_*, \rho_*, \varphi_*, \kappa_*) = (0, 0, -1, \varphi_*, 0.5)$, $(\boldsymbol{\beta}_*^{+\prime}, \boldsymbol{\beta}_*^{-\prime})' = (-1, 0.5, 0.75, -1.5)'$, and $(\boldsymbol{\pi}_{0*}^{+\prime}, \boldsymbol{\pi}_{0*}^{-\prime})' = (0.5, 0.2, 0.5, 0.2)'$, while allowing φ_* to vary as before. We focus on the case in which the long-run parameters are estimated by TFM and construct $\widehat{u}_t$ prior to estimating the short-run parameters by OLS. We test $\dot{H}_0^{(s)} : \boldsymbol{\pi}_{0*}^+ - \boldsymbol{\pi}_{0*}^- = \mathbf{0}$ vs. $\dot{H}_1^{(s)} : \boldsymbol{\pi}_{0*}^+ - \boldsymbol{\pi}_{0*}^- \neq \mathbf{0}$, using the Wald test with the heteroskedasticity consistent covariance estimator $\widehat{\boldsymbol{\Omega}}_T$.

The simulation results in Table 7 display that the finite sample distribution of the Wald test is well approximated by the $\mathcal{X}_2^2$ distribution. Its empirical level is approximately correct for large T while displaying little sensitivity to φ_* even for small T. Next, to examine the empirical power of the Wald test, we work with the same DGP and test $\ddot{H}_0^{(s)} : \boldsymbol{\pi}_{0*}^+ - \boldsymbol{\pi}_{0*}^- = 0.3\boldsymbol{\iota}$ vs. $\ddot{H}_1^{(s)} : \boldsymbol{\pi}_{0*}^+ - \boldsymbol{\pi}_{0*}^- \neq 0.3\boldsymbol{\iota}$. From the simulation results in Table 8 we find that the Wald test becomes consistent with T, and exhibits little sensitivity to the degree of autocorrelation measured by φ_*.

— Insert Tables 7 and 8 Here —

6 Empirical Application: Asymmetric Relationship between R&D Intensity and Investment

Following Schumpeter's seminal 1942 work on creative destruction, a large literature on R&D activities has been developed, though the potentially asymmetric relationship between R&D expenditure and physical investment has received little attention. The product life cycle literature distinguishes between early-stage R&D (referred to as innovative R&D) that is often associated with new product development, and later-stage R&D (referred to as managerial R&D) that tends to focus on scaling production and achieving efficiency (e.g., Gort and Wall, 1986; Audretsch, 1987).[5] Early-stage (innovative) R&D focuses on the development

[5]A number of studies differentiate between innovative and managerial R&D activities and their effects on other economic variables (e.g., Klepper, 1996; Zif and McCarthy, 1997; Agarwal and Audretsch, 2001; Comin and Philippon, 2005; Aghion et al., 2009; Chung and Shin, 2020).

of a new product/technology, leading to a large-scale investment. By contrast, later-stage (managerial) R&D focuses on production efficiency such that it does not exceed the expected increase in output, resulting in a smaller-scale investment. Overall, R&D expenditure rises sharply in the early stage before leveling off or decreasing at the later stage.

Our empirical specification is grounded in two stylized features of innovative and managerial R&D expenditures highlighted in the theory developed in Section E.2 of the Online Supplement. First, as innovative R&D expenditures tend to focus on product innovation, their scale is often large relative to output, suggesting that R&D expenditure is expected to grow faster than output in the early stage, where start-up costs are large and the scale of production typically small. Next, managerial R&D expenditures focus on enhancing production efficiency such that their scale is typically smaller than output.

Let r_t denote aggregate R&D intensity in the t-th period, defined as a ratio of aggregate R&D expenditure to GDP. As aggregate R&D expenditure incorporates the spectrum of R&D activities conducted throughout the economy, the sign of Δr_t may determine the relative prevalence of innovative and managerial R&D activities. If $\Delta r_t \geq 0$, then R&D expenditure grows as fast as output, indicating a prevalence of innovative R&D activity. By contrast, if $\Delta r_t < 0$, then output grows faster than R&D expenditure, representing a prevalence of managerial R&D activity. Given the different characteristics of innovative and managerial R&D, we derive a theoretical prediction that innovative R&D expenditure is a complement to physical investment while managerial R&D expenditure is a substitute. We then develop a testable hypothesis that innovative R&D expenditure is positively related with investment by virtue of complementarity while the relationship between managerial R&D expenditure and investment may be negative due to their nature as substitutes (see Section E.2 of the Online Supplement for details).

We examine the asymmetric relationship between R&D intensity and physical investment using quarterly U.S. data covering the period from 1960q1 to 2019q4, collected from the Federal Reserve Economic Data service at the Federal Reserve Bank of St. Louis. R&D intensity (r_t) is measured as 100 times the ratio of seasonally adjusted nominal R&D expenditure to seasonally adjusted nominal GDP. Investment (i_t) is the log of seasonally adjusted real gross private domestic investment in 2012 prices (GPDI). The National Income and Product Accounts (NIPAs) separately aggregate R&D expenditure and GPDI, so there is no double-counting of R&D expenditure.[6]

The Phillips and Perron (1988) unit root test results indicate that both r_t and i_t are nonstationary, and we thus report descriptive statistics for the first differences of both series (see Section F in the Online Sup-

[6]The Bureau of Economic Analysis constructs a partial R&D satellite account and revises the NIPAs by treating R&D expenditure as part of investment (see Fraumeni and Okubo, 2005).

plement). While the growth rate of R&D intensity is well approximated by a normal distribution centered at zero, the GPDI growth rate exhibits a non-zero mean with negative skewness and excess kurtosis. This implies that i_t is a unit-root process with a time drift, but r_t is a driftless unit-root process.[7] As described in Section E.3 in the Online Supplement, the NARDL model can capture an asymmetric cointegrating relationship between two integrated variables with different drifts without the need to include a deterministic time trend in the model, (3) below.

We estimate the NARDL model using the two-step procedure described in Section 3, using the FM estimator in the first step. By selecting the lag order by the Akaike Information Criterion (AIC), we consider the following NARDL(2,2) error-correction model:

$$\Delta i_t = \gamma_* + \rho_* u_{t-1} + \varphi_* \Delta i_{t-1} + \pi_{0*}^+ \Delta r_t^+ + \pi_{0*}^- \Delta r_t^- + \pi_{1*}^+ \Delta r_{t-1}^+ + \pi_{1*}^- \Delta r_{t-1}^- + e_t, \tag{3}$$

where $i_t = \beta_*^+ r_t^+ + \beta_*^- r_t^- + u_t$. When applying the Phillips and Perron (1988) unit root test to the residuals, we reject the null hypothesis of no cointegration with a p-value of 0.01, concluding that there exists an asymmetric long-run relationship between i_t, r_t^+ and r_t^-.

The long-run parameter estimates reported in Table 9 are not only different in magnitude, but they also display opposite signs: $\widetilde{\beta}_*^+$ is positive and $\widetilde{\beta}_*^-$ is negative with both being highly significant. Furthermore, the null hypothesis of long-run symmetry is strongly rejected.[8] Our results indicate that an increase in R&D spending equivalent to 1% of GDP is associated with an increase of 2.7% in real investment in the long run when R&D growth exceeds GDP growth (i.e. innovative R&D is prevalent). On the other hand, when R&D growth is slower than GDP growth (i.e. managerial R&D is prevalent), an increase in R&D spending of 1% of GDP reduces real investment by 6.4%.[9] This is consistent with our theoretical prediction that $\beta_*^+ > 0$ due to the complementarity of innovative R&D expenditure and investment, whilst $\beta_*^- < 0$ is consistent with the nature of managerial R&D expenditure and investment as substitutes. We find that the substitution effect will be stronger than the complementary effect in the long run.

Next, from the short-run dynamic estimation results reported in Table 10, we find no evidence of residual autocorrelation up to order 4, with the p-value of the Breusch-Godfrey Lagrange multiplier (LM) test being 0.39. But, the Breusch-Pagan LM test rejects the conditional homoskedasticity with a p-value of 0.035. Thus, we report the robust standard errors obtained using the HAC covariance matrix estimator. We observe

[7] We observe that the time trend coefficient is significantly different from zero for i_t, but not for r_t.

[8] Due to the reparamerization the Wald test of $H_0 : \beta_*^+ = \beta_*^-$ versus $H_1 : \beta_*^+ \neq \beta_*^-$ is equivalent to a t-test of $H_0 : \lambda_* = 0$ versus $H_1 : \lambda_* \neq 0$, which returns a p-value almost identical to zero.

[9] The average of U.S. R&D intensity over our sample period is 2.69% of GDP with a standard deviation of 0.2%. Hence, a shock equivalent to 1% of GDP is relatively large by historical standards.

that disequilibrium errors are corrected significantly at 6.8% per quarter, but do not find any evidence of short-run asymmetry.[10]

— Insert Tables 9 and 10 Here —

In Figure 1, we report the cumulative dynamic multipliers associated with an increase in R&D intensity equal to 1% of GDP in each regime (i.e. when R&D grows faster (slower) than GDP). We also display the difference between these two dynamic multipliers as a measure of asymmetry at each horizon with an empirical 95% confidence interval obtained from 5,000 iterations of a moving block bootstrap procedure with a block length of $T^{1/3}$. In Figure 1(a), when R&D growth exceeds GDP growth (i.e. innovative R&D predominates), we find that a 1% increase in R&D intensity initially reduces real investment with a peak reduction of 6.7% after one quarter. From the perspective of creative destruction, this initial reduction may reflect that large innovative R&D expenditures focus on new product development, creating a degree of obsolescence in existing technologies and promoting an incentive to reduce investment in those technologies. The dynamic multiplier rises steadily and becomes positive after 8 quarters, as newly developed technologies begin to mature and scale. In the long run, the impact of innovative R&D expenditure on real physical investment reaches the long-run multiplier at 2.7%. Figure 1(b) shows that when managerial R&D predominates, a 1% increase in R&D intensity leads to an immediate reduction of -3.6% in the real investment, reflecting short-term substitution. The dynamic multiplier effect is then indistinguishable from zero until horizon 11, after which it converges to a long-run multiplier at -6.4%. Overall, an economic environment that favors managerial R&D expenditure is conducive to decreased real investment in the long run, as the efficiency gains derived from managerial R&D raise the return on each dollar invested.

In Figure 1(c), we characterize the asymmetry between the cumulative dynamic multipliers associated with innovative and managerial R&D expenditures by constructing the difference between the cumulative dynamic multiplier reported in panels (a) and (b) with 95% bootstrap confidence intervals, that can be used to test for asymmetry at any horizon. In the short run, we observe substantial negative asymmetry that is significant at the 10% level, suggesting that real investment is more responsive to innovative than managerial R&D in the short run. In the long run, however, we observe positive asymmetry as the substitution effect associated with managerial R&D becomes stronger than the complementary effect of innovative R&D. This pattern is generally in line with the product life cycle, where large innovative R&D occurs early often exerting a disruptive influence on existing products. Once the new product becomes established, managerial

[10] The Wald test for the of impact symmetry, $H_0 : \pi^+_{0*} = \pi^-_{0*}$ vs. $H_1 : \pi^+_{0*} \neq \pi^-_{0*}$, returns a p-value of 0.677. Moreover, the null hypothesis of additive short-run symmetry, $H_0 : \pi^+_{0*} + \pi^+_{1*} = \pi^-_{0*} + \pi^-_{1*}$, is not rejected against $H_1 : \pi^+_{0*} + \pi^+_{1*} \neq \pi^-_{0*} + \pi^-_{1*}$, with a p-value of 0.146.

R&D focuses on scaling-up production and delivering efficiency gains. Collectively, these results have important implications for the endogenous growth literature, where linear functional forms are routinely imposed to characterize the relationship between the stock of knowledge and R&D intensity (e.g. Romer, 1990). Our main findings suggest that the imposition of a linear functional form may produce misleading results.

— Insert Figure 1 Here —

Next, we present the additional estimation results obtained using the single-step OLS estimation procedure popularized by SYG, which are summarized in Figure 2. This exercise sheds light on the performance of the single-step estimation of SYG relative to our two-step counterpart. In general, we find that both procedures yield similar estimation and testing results. This indicates that they may be used interchangeably in practice. However, the two-step framework yields greater precision in the estimation of the long-run parameters, as it is not subject to the influence of nuisance parameters. This may improve one's ability to detect long-run asymmetry, particularly in small samples. This represents an important practical benefit of our two-step estimation framework, given that NARDL models are often used in macroeconomic applications, where a low sampling frequency and relatively short time period necessitate the use of small samples.

— Insert Figure 2 Here —

7 Concluding Remarks

We have analyzed the potentially asymmetric relationship between R&D intensity and physical investment using the quarterly data in the U.S. over the period, 1960q1–2019q4. We have developed a theoretical model that exploits documented differences in innovative and managerial R&D characteristics, establishing that there exists an asymmetric relationship between R&D intensity and investment. We have also developed the testable hypothesis that innovative (managerial) R&D expenditure is a complement to (a substitute for) physical investment.

We have proposed a corresponding empirical NARDL specification in which real investment is regressed on the positive and negative partial sums of R&D intensity. While the NARDL model has been widely applied to the analysis of asymmetric relationships (see Cho et al., 2023b), the asymptotic theory for the single-step NARDL estimator has yet to be fully developed due to asymptotic singularity issues. In the first step, we estimate the parameters of a reparameterized long-run relationship using the FM estimator that accounts for serial correlation and potential endogeneity of the regressors and that facilitates standard inference. In the second step, the short-run dynamic parameters are estimated by OLS, treating the error-correction term as given. We derive the asymptotic distributions of the two-step NARDL estimators and develop Wald tests for inference on the short- and long-run parameters. A suite of Monte Carlo simulations demonstrates that our asymptotic results offer good approximations in finite samples.

Employing the U.S. quarterly data covering the period from 1960q1 to 2019q4, we find comprehensive empirical evidence in favor of the asymmetric relationship between R&D intensity and investment. In the long run, investment responds positively to R&D expenditures when their growth rate exceeds the growth rate of GDP and negatively when they grow more slowly than GDP. This supports theoretical predictions that the innovative (managerial) R&D expenditure is a complement to (substitute for) physical investment. Furthermore, we find that investment is more sensitive to changes in R&D intensity when the growth rate of R&D expenditure is lower than GDP growth.

Our work opens several avenues for continuing research. On the methodological side, there is scope to generalize our approach to accommodate trending regressors or to estimate an unknown threshold parameter in the construction of the partial sum processes. On the empirical side, our results motivate the study of potential asymmetries in other areas of the innovation literature, such as in the knowledge production function that is routinely estimated in linear form in the endogenous growth literature.

References

AGARWAL, R. AND D. B. AUDRETSCH (2001): "Does Entry Size Matter? The Impact of the Life Cycle and Technology on Firm Survival," *Journal of Industrial Economics*, 49, 21–43.

AGHION, P., R. BLUNDELL, R. GRIFFTH, P. HOWITT, AND S. PRANTL (2009): "The Effects of Entry on Incumbent Innovation and Productivity," *Review of Economics and Statistics*, 91, 20–32.

AUDRETSCH, D. B. (1987): "An Empirical Test of the Industry Life Cycle," *Weltwirtschaftliches Archiv*, 123, 297–308.

BARATI, M. AND H. FARIDITAVANA (2020): "Asymmetric Effect of Income on the US Healthcare Expenditure: Evidence from the Nonlinear Autoregressive Distributed Lag (ARDL) Approach," *Empirical Economics*, 58, 1979–2008.

BAUSSOLA, M. (2000): "The Causality Between R&D and Investment," *Economics of Innovation and New Technology*, 9, 385–399.

Box, M., K. Gratzer, and X. Lin (2019): "The Asymmetric Effect of Bankruptcy Fraud in Sweden: A Long-Term Perspective," *Journal of Quantitative Criminology*, 35, 287–312.

Brun-Aguerre, R. X., A.-M. Fuertes, and M. J. Greenwood-Nimmo (2017): "Heads I Win; Tails You Lose: Asymmetry in Exchange Rate Pass-Through into Import Prices," *Journal of the Royal Statistical Society: Series A (Statistics in Society)*, 180, 587–612.

Chiao, C. (2001): "The Relationship between R&D and Physical Investment of Firms in Science-Based Industries," *Applied Economics*, 33, 23–35.

Cho, J., M. Greenwood-Nimmo, and Y. Shin (2023a): "Nonlinear Autoregressive Distributed Lag Model Estimation Using Data with Drifts," Working paper, School of Economics, Yonsei University, Seoul.

——— (2023b): "Recent Developments of the Autoregressive Distributed Lag Modelling Framework," *Journal of Economic Surveys*, 37, 7–32.

Chung, D. and D. Shin (2020): "When do Firms Invest in R&D? Two Types of Performance Feedback and Organizational Search in the Korean Shipbuilding Industry," *Asian Business & Management*, 20, 583–617.

Comin, D. and T. Philippon (2005): "The Rise in Firm-level Volatility: Causes and Consequences," *NBER/Macroeconomics Annual*, 20, 167–201.

Eberhardt, M. and A. F. Presbitero (2015): "Public Debt and Growth: Heterogeneity and Non-Linearity," *Journal of International Economics*, 97, 45–58.

Engle, R. F. and C. W. Granger (1987): "Co-integration and Error Correction: Representation, Estimation and Testing," *Econometrica*, 55, 251–276.

Ferris, J. S., S. L. Winer, and D. E. Olmstead (2020): "A Dynamic Model of Political Party Equilibrium: The Evolution of ENP in Canada, 1870 – 2015," Working Paper 8387, CESifo, Munich.

Fraumeni, B. M. and S. Okubo (2005): "R&D in the National Income and Product Accounts: A First Look at Its Effect on GDP," in *Measuring Capital in the New Economy*, ed. by J. H. C. Corrado and D. Sichel, Chicago (IL): The University of Chicago Press, 275–322.

Fudenberg, D., R. Gilbert, J. Stiglitz, and J. Tirole (1983): "Preemption, Leapfrogging and Competition in Patent Races," *European Economic Review*, 22, 3–31.

GORT, M. AND R. A. WALL (1986): "The Evolution of Technologies and Investment in Innovations," *Economic Journal*, 96, 741–757.

GREENWOOD-NIMMO, M. J. AND Y. SHIN (2013): "Taxation and the Asymmetric Adjustment of Selected Retail Energy Prices in the UK," *Economics Letters*, 121, 411–416.

GROSSMAN, G. M. AND C. SHAPIRO (1987): "Dynamic R&D Competition," *Economic Journal*, 97, 372–387.

HAMMOUDEH, S., A. LAHIANI, D. K. NGUYEN, AND R. M. SOUSA (2015): "An Empirical Analysis of Energy Cost Pass-Through to CO2 Emission Prices," *Energy Economics*, 49, 149–156.

HARRIS, C. J. AND J. S. VICKERS (1987): "Racing with Uncertainty," *Review of Economic Studies*, 54, 1–21.

HE, Z. AND F. ZHOU (2018): "Time-Varying and Asymmetric Eeffects of the Oil-Specific Demand Shock on Investor Sentiment," *PLOS ONE*, 13, e0200734.

KAMIEN, M. I. AND N. L. SCHWARTZ (1972): "Timing of Innovations under Rivalry," *Econometrica*, 40, 43–60.

KLEPPER, S. (1996): "Entry, Exit, Growth, and Innovation over the Product Life Cycle," *American Economic Review*, 86, 562–583.

——— (1997): "Industry Life Cycles," *Industrial and Corporate Change*, 6, 145–182.

LACH, S. AND R. ROB (1996): "R&D Investment and Industry Dynamics," *Journal of Economics and Management Strategy*, 5, 217–249.

LACH, S. AND M. SCHANKERMAN (1989): "Dynamics of R&D and Physical Investment in the Scientific Sector," *Journal of Political Economy*, 97, 880–904.

NEWEY, W. K. AND K. D. WEST (1987): "A Simple, Positive Semi-Definite, Heteroskedasticity and Autocorrelation Consistent Covariance Matrix," *Econometrica*, 55, 703–708.

PESARAN, M. H. AND Y. SHIN (1998): "An Autoregressive Distributed Lag Modelling Approach to Cointegration Analysis," in *Econometrics and Economic Theory: The Ragnar Frisch Centennial Symposium*, ed. by S. Strom, Cambridge: Cambridge University Press, Econometric Society Monographs, 371–413.

PESARAN, M. H., Y. SHIN, AND R. J. SMITH (2001): "Bounds Testing Approaches to the Analysis of Level Relationships," *Journal of Applied Econometrics*, 16, 289–326.

PHILLIPS, P. AND P. PERRON (1988): "Testing for a Unit Root in Time Series Regression," *Biometrika*, 75, 335–346.

PHILLIPS, P. C. AND B. E. HANSEN (1990): "Statistical Inference in Instrumental Variable Regression with I(1) Processes," *Review of Economic Studies*, 57, 99–125.

REINGANUM, J. F. (1982): "A Dynamic Game of R&D: Patent Protection and Competitive Behavior," *Econometrica*, 50, 671–688.

ROMER, P. M. (1990): "Endogenous Technological Change," *Journal of Political Economy*, 98, 71–102.

SCHMOOKLER, J. (1966): *Innovation and Economic Growth*, Cambridge (MA): Harvard University Press.

SCHUMPETER, J. A. (1942): *Capitalism, Socialism, and Democracy*, New York (NY): Harper & Row.

SHIN, Y., B. YU, AND M. J. GREENWOOD-NIMMO (2014): "Modelling Asymmetric Cointegration and Dynamic Multipliers in a Nonlinear ARDL Framework," in *Festschrift in Honor of Peter Schmidt: Econometric Methods and Applications*, ed. by W. Horrace and R. Sickles, New York (NY): Springer Science & Business Media, 281–314.

UTTERBACK, J. AND W. Y. ABERNATHY (1975): "A Dynamic Model of Process and Product Innovation," *Omega*, 3, 639–659.

ZIF, J. AND D. J. MCCARTHY (1997): "The R&D Cycle: The Influence of Product and Process R&D on Short-Term ROI," *IEEE Transactions on Engineering Management*, 44, 114–123.

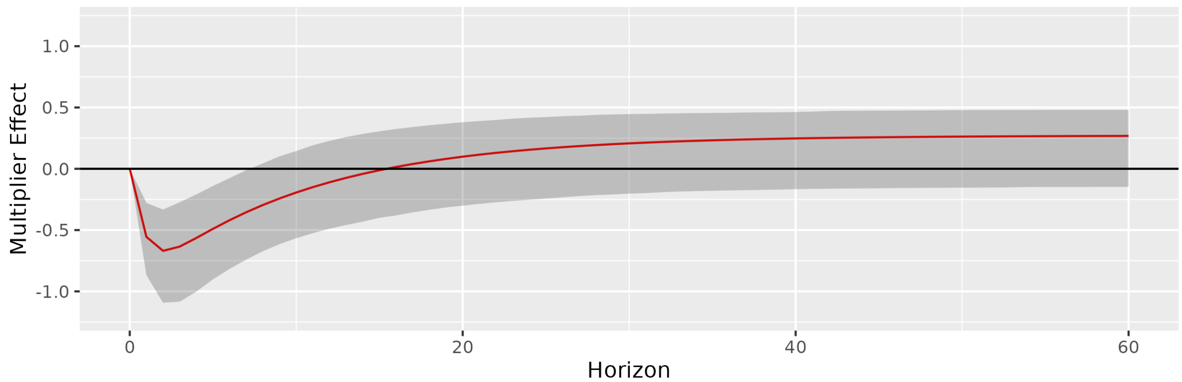

(a) Cumulative response of i_{t+h} to a +1 unit shock to r_t^+ in period 1

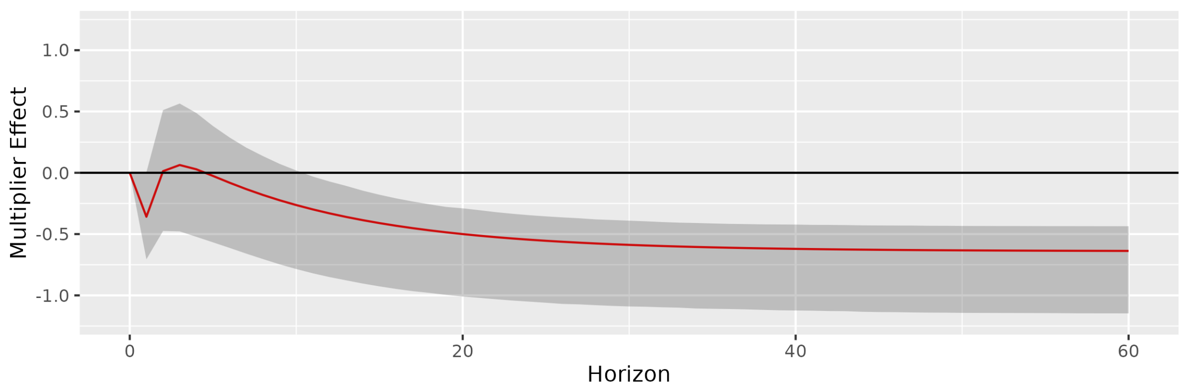

(b) Cumulative response of i_{t+h} to a +1 unit shock to r_t^- in period 1

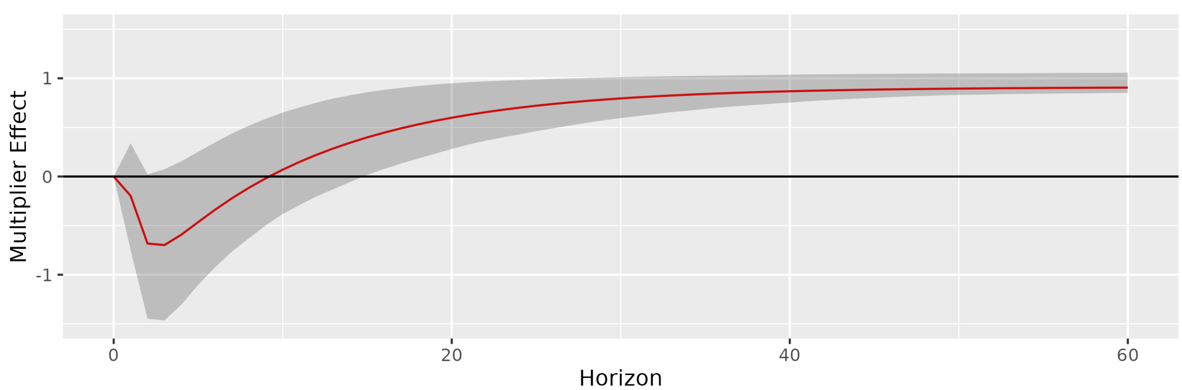

(c) Asymmetry across horizons

Figure 1: CUMULATIVE DYNAMIC MULTIPLIERS BASED ON THE TWO-STEP ESTIMATOR. Panels (a) and (b) present the cumulative dynamic multipliers with respect to unit shocks to r_t^+ and r_t^-, respectively. Panel (c) shows the asymmetry at each horizon, i.e., the difference between the cumulative dynamic multipliers in panel (a) and those in panel (b). We also report empirical 95% confidence intervals that are obtained using a moving block bootstrap procedure with 5,000 replications.

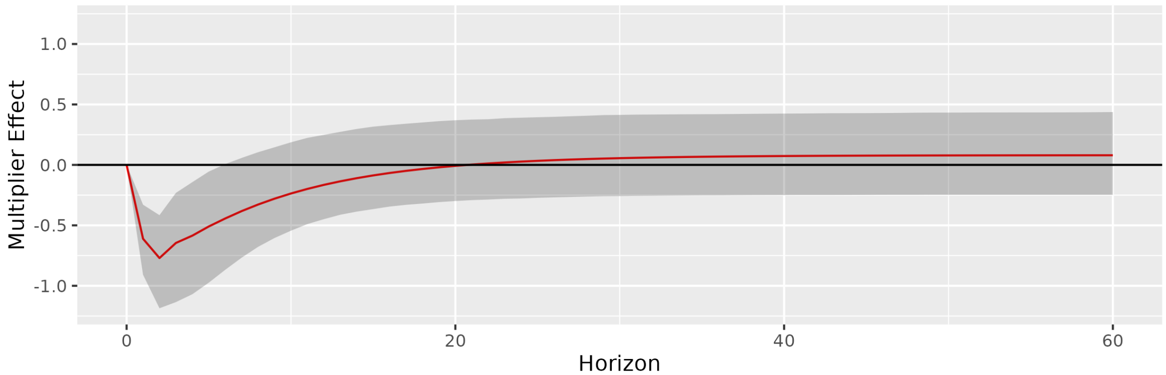

(a) Cumulative response of i_{t+h} to a +1 unit shock to r_t^+ in period 1

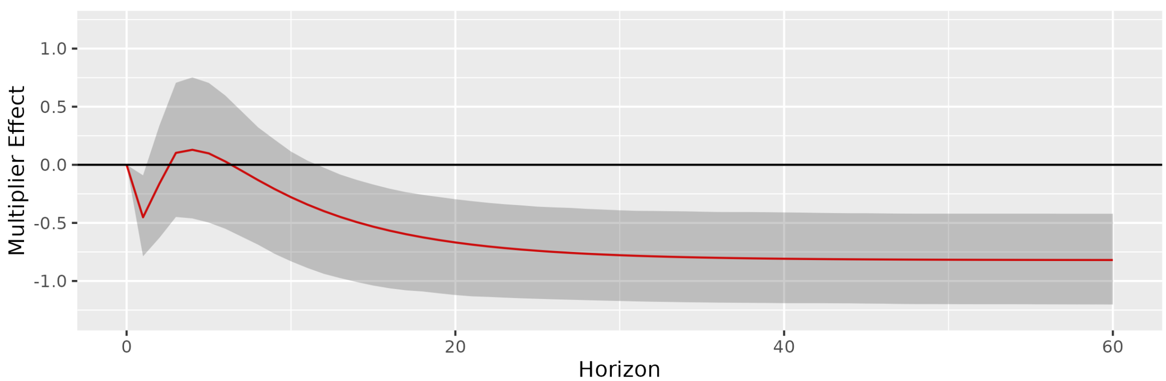

(b) Cumulative response of i_{t+h} to a +1 unit shock to r_t^- in period 1

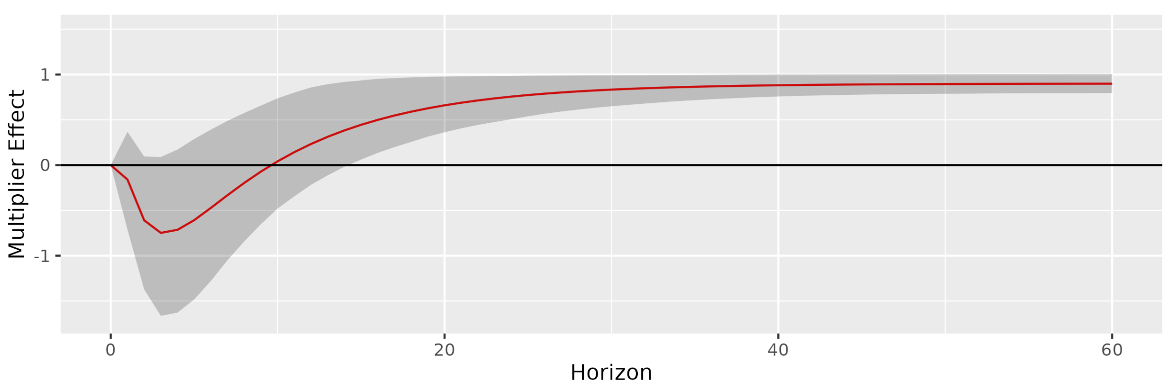

(c) Asymmetry across horizons

Figure 2: CUMULATIVE DYNAMIC MULTIPLIERS BASED ON THE ONE-STEP ESTIMATOR. Panels (a) and (b) present the cumulative dynamic multiplier effects with respect to unit shocks to r_t^+ and r_t^-, respectively, occurring in period 1. Panel (c) shows the asymmetry at each horizon, i.e., the difference between the cumulative dynamic multipliers in panel (a) and those in panel (b). We also report empirical 95% confidence intervals that are obtained using a moving block bootstrap procedure with 5,000 replications.

φ_*	sample size	100	250	500	750	1,000
-0.50	1%	12.40	5.06	2.38	1.82	1.44
	5%	23.34	12.88	7.96	7.70	5.90
	10%	31.50	21.04	14.08	13.22	11.46
-0.25	1%	8.74	3.80	2.54	1.74	1.18
	5%	19.06	11.10	8.44	6.62	5.48
	10%	27.22	18.36	14.96	11.68	10.48
0.00	1%	4.96	2.92	1.84	1.72	1.42
	5%	13.86	9.76	7.20	6.60	6.12
	10%	21.40	16.28	13.02	12.20	11.34
0.25	1%	3.32	1.62	1.34	1.22	1.06
	5%	10.38	6.24	5.56	5.66	5.60
	10%	17.28	11.42	10.96	11.22	10.70
0.50	1%	1.70	0.86	0.78	0.66	0.72
	5%	5.82	4.06	4.60	4.30	4.22
	10%	10.74	8.20	9.88	9.08	9.12

Table 1: EMPIRICAL LEVELS OF THE WALD TEST FOR LONG-RUN SYMMETRY. This table reports the empirical level (in %) of the Wald test for the symmetry of the long-run parameters estimated by FM in the first step. The data is generated by $\Delta y_t = -(2/3)u_{t-1} + \varphi_* \Delta y_{t-1} + (1/3)\Delta x_t^+ + (1/2)\Delta x_t^- + e_t$, where $u_t := y_t - x_t^+ - x_t^-$, $\Delta x_t = 0.5\Delta x_{t-1} + \sqrt{1-0.5^2}v_t$, and $(e_t, v_t)' \sim \text{IID}N(\mathbf{0}_2, \mathbf{I}_2)$. $H_0^{(\ell)} : \beta_*^+ - \beta_*^- = 0$ vs. $H_1^{(\ell)} : \beta_*^+ - \beta_*^- \neq 0$.

φ_*	sample size	100	250	500	750	1,000
-0.50	1%	9.80	20.76	83.66	97.34	99.76
	5%	20.00	35.78	89.36	98.54	99.96
	10%	27.66	44.70	91.98	98.92	99.96
-0.25	1%	7.90	26.04	88.16	98.44	99.82
	5%	17.98	41.74	92.88	99.32	99.92
	10%	25.08	51.30	94.58	99.60	99.94
0.00	1%	5.74	32.24	91.22	99.20	99.86
	5%	14.72	49.46	95.12	99.68	99.96
	10%	22.40	58.54	96.66	99.80	99.98
0.25	1%	4.4	34.46	92.36	99.38	99.96
	5%	12.08	52.82	96.04	99.70	100.0
	10%	19.2	61.96	97.22	99.82	100.0
0.50	1%	2.92	25.40	90.96	99.16	99.98
	5%	9.44	47.06	95.40	99.70	100.0
	10%	16.08	58.68	96.98	99.82	100.0

Table 2: EMPIRICAL POWER OF THE WALD TEST FOR LONG-RUN SYMMETRY. This table shows the empirical power (in %) of the Wald test for the symmetry of the long-run parameters estimated by FM in the first step. The data is generated by $\Delta y_t = -(2/3)u_{t-1} + \varphi_* \Delta y_{t-1} + (1/3)\Delta x_t^+ + (1/2)\Delta x_t^- + e_t$, where $u_t := y_t - 1.01x_t^+ - x_t^-$, $\Delta x_t = 0.5\Delta x_{t-1} + \sqrt{1-0.5^2}v_t$, and $(e_t, v_t)' \sim \text{IID}N(\mathbf{0}_2, \mathbf{I}_2)$. $H_0^{(\ell)} : \beta_*^+ - \beta_*^- = 0$ vs. $H_1^{(\ell)} : \beta_*^+ - \beta_*^- \neq 0$.

φ_*	sample size	100	250	500	750	1,000
-0.50	1%	2.44	1.60	0.98	1.18	1.12
	5%	8.06	6.06	5.42	5.46	6.02
	10%	13.82	11.00	10.90	10.36	10.94
-0.25	1%	2.38	1.74	1.46	1.30	1.14
	5%	7.38	6.44	6.02	5.36	5.30
	10%	12.90	11.38	11.28	10.54	10.48
0.00	1%	2.12	1.18	1.22	1.26	0.98
	5%	7.30	5.86	5.76	6.00	5.20
	10%	13.40	11.26	10.94	11.16	10.22
0.25	1%	2.28	1.42	1.36	0.96	0.82
	5%	7.32	6.14	5.84	5.12	4.68
	10%	13.42	11.40	10.96	9.76	9.50
0.50	1%	2.02	1.80	0.98	1.10	1.22
	5%	6.64	6.44	5.44	5.52	5.54
	10%	11.84	11.54	10.62	10.60	10.74

Table 3: EMPIRICAL LEVELS OF THE WALD TEST FOR SHORT-RUN SYMMETRY. This table reports the empirical levels (in %) of the Wald test for the symmetry of the short-run parameters, where FM is used in the first step and OLS used in the second step. The data is generated as $\Delta y_t = -(2/3)u_{t-1} + \varphi_* \Delta y_{t-1} + (1/2)\Delta x_t^+ + (1/2)\Delta x_t^- + e_t$, where $u_t := y_t - 2x_t^+ - x_t^-$, $\Delta x_t = 0.5\Delta x_{t-1} + \sqrt{1-0.5^2}v_t$, and $(e_t, v_t)' \sim$ IID$N(\mathbf{0}_2, \mathbf{I}_2)$. $H_0^{(s)} : \pi_*^+ - \pi_*^- = 0$ vs. $H_1^{(s)} : H_0 : \pi_*^+ - \pi_*^- \neq 0$.

φ_*	sample size	100	250	500	750	1,000
-0.50	1%	17.86	44.00	78.48	93.50	98.40
	5%	35.38	66.66	91.82	98.44	99.76
	10%	45.56	76.70	95.76	99.34	99.92
-0.25	1%	17.58	44.84	79.40	93.70	98.32
	5%	34.96	66.66	91.90	98.26	99.72
	10%	46.04	76.64	95.96	99.14	99.86
0.00	1%	17.26	43.16	78.56	93.28	98.60
	5%	35.66	66.68	92.38	98.14	99.72
	10%	46.62	76.14	96.06	99.18	99.90
0.25	1%	17.90	43.02	78.76	93.34	98.72
	5%	35.02	66.14	92.12	98.32	99.68
	10%	45.80	76.24	95.48	99.34	99.98
0.50	1%	17.50	42.82	77.82	92.94	98.54
	5%	34.20	65.78	91.32	98.28	99.78
	10%	44.90	76.06	94.90	99.26	99.92

Table 4: EMPIRICAL POWER OF THE WALD TEST FOR SHORT-RUN SYMMETRY. This table reports the empirical rejection rates (in %) of the Wald test for the symmetry of the short-run parameters, where FM is used in the first step and OLS is used in the second step. The data is generated as follows: $\Delta y_t = -(2/3)u_{t-1} + \varphi_* \Delta y_{t-1} + \Delta x_t^+ + (1/2)\Delta x_t^- + e_t$, where $u_t := y_t - 2x_t^+ - x_t^-$, $\Delta x_t = 0.5\Delta x_{t-1} + \sqrt{1-0.5^2}v_t$, and $(e_t, v_t)' \sim$ IID$N(\mathbf{0}_2, \mathbf{I}_2)$. $H_0^{(s)} : \pi_*^+ - \pi_*^- = 0$ vs. $H_1^{(s)} : H_0 : \pi_*^+ - \pi_*^- \neq 0$.

φ_*	sample size	100	250	500	1,000	3,000	5,000
-0.30	1%	45.20	17.06	7.46	2.62	1.10	1.32
	5%	58.92	30.68	17.62	9.50	5.64	5.86
	10%	65.82	40.08	25.76	16.40	11.72	10.62
-0.10	1%	42.96	18.12	8.12	3.32	1.48	1.24
	5%	57.82	31.10	19.04	10.76	6.02	5.48
	10%	65.34	39.20	26.66	17.48	11.64	10.34
0.00	1%	42.50	16.78	8.44	4.30	1.42	1.28
	5%	56.38	29.90	19.20	11.62	5.80	5.60
	10%	64.06	38.70	28.20	18.74	11.36	10.76
0.10	1%	41.24	16.18	8.56	4.02	1.68	1.18
	5%	56.14	30.00	19.30	11.32	6.68	5.56
	10%	63.30	38.78	27.12	19.24	12.50	11.26
0.30	1%	40.10	15.72	6.94	3.92	2.16	1.84
	5%	54.52	28.24	17.16	12.52	8.00	7.34
	10%	63.44	36.76	24.94	19.10	14.24	12.88

Table 5: EMPIRICAL LEVELS OF THE WALD TEST FOR LONG-RUN SYMMETRY. This table reports the empirical level (in %) of the Wald test for the symmetry of the long-run parameters estimated by the TFM estimator in the first step. The data is generated by $\Delta y_t = -u_{t-1} + \varphi_* \Delta y_{t-1} + \boldsymbol{\pi}_{0*}^{+\prime} \Delta \boldsymbol{x}_t^+ + \boldsymbol{\pi}_{0*}^{-\prime} \Delta \boldsymbol{x}_t^- + e_t$, where $u_t := y_t - \boldsymbol{\beta}_*^{+\prime} \boldsymbol{x}_t^+ - \boldsymbol{\beta}_*^{-\prime} \boldsymbol{x}_t^-$, $\Delta \boldsymbol{x}_t = 0.5 \Delta \boldsymbol{x}_{t-1} + \sqrt{1 - 0.5^2} \boldsymbol{v}_t$, and $(e_t, \boldsymbol{v}_t')' \sim \text{IID}N(\mathbf{0}_3, \mathbf{I}_3)$. $\dot{H}_0^{(\ell)} : \boldsymbol{\iota}_2' \boldsymbol{\beta}_*^+ = -0.5$ and $\boldsymbol{\iota}_2' \boldsymbol{\beta}_*^- = -0.75$ vs. $\dot{H}_1^{(\ell)} : \boldsymbol{\iota}_2' \boldsymbol{\beta}_*^+ \neq -0.5$ or $\boldsymbol{\iota}_2' \boldsymbol{\beta}_*^- \neq -0.75$.

φ_*	sample size	100	200	300	400	500
-0.30	1%	47.46	70.16	90.44	98.10	99.74
	5%	62.40	80.76	94.26	99.00	99.88
	10%	70.16	85.42	96.18	99.32	99.92
-0.10	1%	48.98	71.36	91.30	98.24	99.70
	5%	63.08	81.32	95.26	99.10	99.88
	10%	70.12	86.22	96.76	99.36	99.94
0.00	1%	47.32	70.54	90.56	98.20	99.78
	5%	61.72	81.70	94.02	99.12	99.94
	10%	69.78	86.56	95.44	99.46	99.94
0.10	1%	46.36	69.20	90.22	98.06	99.86
	5%	60.26	79.82	94.00	98.98	99.96
	10%	67.16	84.56	95.86	99.36	99.98
0.30	1%	43.10	63.52	88.70	97.58	99.44
	5%	56.98	75.22	93.74	98.88	99.78
	10%	65.50	80.66	95.68	99.18	99.88

Table 6: EMPIRICAL POWER OF THE WALD TEST FOR LONG-RUN SYMMETRY This table shows the empirical power (in %) of the Wald test for the symmetry of the long-run parameter estimated by the TFM estimator in the first step. The data is generated by $\Delta y_t = -u_{t-1} + \varphi_* \Delta y_{t-1} + \boldsymbol{\pi}_{0*}^{+\prime} \Delta \boldsymbol{x}_t^+ + \boldsymbol{\pi}_{0*}^{-\prime} \Delta \boldsymbol{x}_t^- + e_t$, where $u_t := y_t - \boldsymbol{\beta}_*^{+\prime} \boldsymbol{x}_t^+ - \boldsymbol{\beta}_*^{-\prime} \boldsymbol{x}_t^-$, $\Delta \boldsymbol{x}_t = 0.5 \Delta \boldsymbol{x}_{t-1} + \sqrt{1 - 0.5^2} \boldsymbol{v}_t$, and $(e_t, \boldsymbol{v}_t')' \sim \text{IID}N(\mathbf{0}_3, \mathbf{I}_3)$. $\ddot{H}_0^{(\ell)} : \boldsymbol{\iota}_2' \boldsymbol{\beta}_*^+ = -0.4$ and $\boldsymbol{\iota}_2' \boldsymbol{\beta}_*^- = -0.65$ vs. $\ddot{H}_1^{(\ell)} : \boldsymbol{\iota}_2' \boldsymbol{\beta}_*^+ \neq -0.4$ or $\boldsymbol{\iota}_2' \boldsymbol{\beta}_*^- \neq -0.65$.

φ_*	sample size	100	200	400	600	800	1,000
-0.30	1%	10.62	4.16	1.58	1.66	1.28	1.56
	5%	23.24	11.90	7.28	6.78	5.88	5.74
	10%	31.96	18.88	13.34	12.26	11.34	10.80
-0.10	1%	10.58	3.72	2.02	1.34	1.20	1.22
	5%	22.50	11.12	7.56	6.36	6.06	5.84
	10%	32.18	18.66	13.38	12.28	11.38	10.94
0.00	1%	10.90	3.92	2.00	1.54	1.48	1.28
	5%	23.34	11.80	7.90	6.36	6.64	5.50
	10%	31.46	19.30	13.96	11.36	12.46	10.50
0.10	1%	10.80	3.98	2.00	1.36	1.44	1.26
	5%	22.60	11.96	7.36	6.54	6.46	5.40
	10%	30.78	18.68	12.74	12.38	12.16	10.82
0.30	1%	11.04	4.14	1.84	1.72	1.38	1.10
	5%	22.68	11.56	7.60	7.20	6.74	5.14
	10%	32.22	18.98	13.06	12.56	12.34	10.62

Table 7: EMPIRICAL LEVELS OF THE WALD TEST FOR SHORT-RUN SYMMETRY. This table reports the empirical levels (in %) of the Wald test for the symmetry of the short-run parameters, where the TFM estimator is used in the first step and OLS in the second step. The data is generated as $\Delta y_t = -u_{t-1} + \varphi_* \Delta y_{t-1} + \boldsymbol{\pi}_{0*}^{+\prime} \Delta \boldsymbol{x}_t^+ + \boldsymbol{\pi}_{0*}^{-\prime} \Delta \boldsymbol{x}_t^- + e_t$, where $u_t := y_t - \boldsymbol{\beta}_*^{+\prime} \boldsymbol{x}_t^+ - \boldsymbol{\beta}_*^{-\prime} \boldsymbol{x}_t^-$, $\Delta \boldsymbol{x}_t = 0.5 \Delta \boldsymbol{x}_{t-1} + \sqrt{1 - 0.5^2} \boldsymbol{v}_t$, and $(e_t, \boldsymbol{v}_t')' \sim \text{IID}N(\mathbf{0}_3, \mathbf{I}_3)$. $\dot{H}_0^{(s)} : \boldsymbol{\pi}_{0*}^+ - \boldsymbol{\pi}_{0*}^- = \mathbf{0}_2$ vs. $\dot{H}_1^{(s)} : \boldsymbol{\pi}_{0*}^+ - \boldsymbol{\pi}_{0*}^- \neq \mathbf{0}_2$.

φ_*	sample size	100	200	400	600	800	1,000
-0.30	1%	20.96	21.94	39.98	60.80	77.26	86.48
	5%	36.20	39.78	62.62	80.76	91.16	95.32
	10%	45.90	51.10	73.52	87.68	94.76	97.76
-0.10	1%	21.56	22.94	41.36	61.54	76.68	86.96
	5%	37.70	41.56	63.86	80.14	91.18	95.40
	10%	46.98	52.92	74.76	87.70	95.16	97.72
0.00	1%	21.04	23.38	42.32	61.96	76.86	86.66
	5%	36.70	42.28	64.08	81.12	90.50	95.58
	10%	46.52	53.74	74.38	88.60	94.46	97.34
0.10	1%	20.04	24.42	40.92	61.14	76.30	86.52
	5%	35.20	42.46	63.34	80.60	90.32	95.54
	10%	45.34	53.40	73.86	87.96	94.84	97.78
0.30	1%	20.48	23.32	42.08	62.02	76.58	86.82
	5%	36.56	42.84	63.60	80.88	90.20	95.28
	10%	46.76	53.20	73.78	87.98	94.48	97.42

Table 8: EMPIRICAL POWER OF THE WALD TEST FOR SHORT-RUN SYMMETRY. This table reports the empirical rejection rates (in %) of the Wald test for the symmetry of the short-run parameters, where the TFM estimator is used in the first step and OLS in the second step. The data is generated as follows: $\Delta y_t = -u_{t-1} + \varphi_* \Delta y_{t-1} + \boldsymbol{\pi}_{0*}^{+\prime} \Delta \boldsymbol{x}_t^+ + \boldsymbol{\pi}_{0*}^{-\prime} \Delta \boldsymbol{x}_t^- + e_t$, where $u_t := y_t - \boldsymbol{\beta}_*^{+\prime} \boldsymbol{x}_t^+ - \boldsymbol{\beta}_*^{-\prime} \boldsymbol{x}_t^-$, $\Delta \boldsymbol{x}_t = 0.5 \Delta \boldsymbol{x}_{t-1} + \sqrt{1 - 0.5^2} \boldsymbol{v}_t$, and $(e_t, \boldsymbol{v}_t')' \sim \text{IID}N(\mathbf{0}_3, \mathbf{I}_3)$. $\ddot{H}_0^{(s)} : \boldsymbol{\pi}_{0*}^+ - \boldsymbol{\pi}_{0*}^- = 0.3\boldsymbol{\iota}_2$ vs. $\ddot{H}_1^{(s)} : \boldsymbol{\pi}_{0*}^+ - \boldsymbol{\pi}_{0*}^- \neq 0.3\boldsymbol{\iota}_2$.

	Estimate	S.E.
Intercept	7.453	0.381
β_*^+	0.271	0.133
β_*^-	-0.640	0.154

Table 9: THE LONG-RUN PARAMETER ESTIMATES. This table reports the long-run parameter estimates obtained by our two-step estimation procedure applied to quarterly observations from 1960q1 to 2019q4, where FM is used in the first step.

	Estimate	S.E.
γ_*	0.015	0.005
ρ_*	-0.068	0.016
φ_*	0.255	0.066
π_{0*}^+	-0.555	0.179
π_{1*}^+	-0.029	0.150
π_{0*}^-	-0.359	0.344
π_{1*}^-	0.482	0.176
Adjusted R^2	0.199	
$\mathcal{X}^2_{\text{S.Corr.}}$	0.385	
$\mathcal{X}^2_{\text{Hetero.}}$	0.035	

Table 10: THE SHORT-RUN DYNAMIC PARAMETER ESTIMATES. This table reports parameter estimates for the NARDL(2,2) ECM model obtained using the two-step procedure applied to quarterly observations from 1960q1 to 2019q4, where FM is used in the first step and OLS in the second step. The lag order is selected by AIC. The standard errors are evaluated using HAC covariance matrix estimation. $\mathcal{X}^2_{\text{S.Corr.}}$ and $\mathcal{X}^2_{\text{Hetero.}}$ denote the Breusch–Godfrey LM test for serial correlation (up to order four) and the Breusch–Pagan–Godfrey LM test for residual heteroskedasticity, respectively. We report asymptotic p-values for these two tests.

Online Supplement for

"Two-Step Nonlinear ARDL Estimation: Theory and Application"

by Jin Seo Cho, Matthew Greenwood-Nimmo and Yongcheol Shin

This Online Supplement consists of six sections. In Sections A and B we provide the proofs of the main claims of the manuscript. Section C explores further singularity issues associated with the one-step NARDL estimator. Section D presents additional simulation and estimation results. In Section E we develop the theory relating early-stage innovative and later-stage managerial R&D expenditures to physical investment and conduct a comparative static analysis to confirm the theoretical predictions. Section F reports additional estimation results.

A Preliminary Equations

We provide some equations for an efficient exposition of our proofs. As they are already explained, we provide them without reiterating their motivation and derivations.

$$\boldsymbol{x}_t^+ = \boldsymbol{\mu}_*^+ t + \sum_{j=1}^{t} \boldsymbol{s}_j^+ \quad \text{and} \quad \boldsymbol{x}_t^- = \boldsymbol{\mu}_*^- t + \sum_{j=1}^{t} \boldsymbol{s}_j^-; \tag{A.1}$$

$$y_t = \delta_* t + \sum_{j=1}^{t} d_j; \tag{A.2}$$

$$\begin{aligned}\Delta y_t = {} & \rho_* y_{t-1} + (\theta_*^+ - \theta_*^-) x_{t-1}^+ + \theta_*^- x_{t-1} \\ & + \gamma_* + \sum_{j=1}^{p-1} \varphi_{j*} \Delta y_{t-j} + \sum_{j=0}^{q-1} \left(\pi_{j*}^+ \Delta x_{t-j}^+ + \pi_{j*}^- \Delta x_{t-j}^- \right) + e_t;\end{aligned} \tag{A.3}$$

$$y_t = \alpha_* + \lambda_* x_t^+ + \eta_* x_t + u_t; \tag{A.4}$$

$$u_{t-1} := y_{t-1} - \beta_*^+ x_{t-1}^+ - \beta_*^- x_{t-1}^-; \tag{A.5}$$

$$\Delta y_t = \rho_* u_{t-1} + \gamma_* + \sum_{j=1}^{p-1} \varphi_{j*} \Delta y_{t-j} + \sum_{j=0}^{q-1} \left(\boldsymbol{\pi}_{j*}^{+\prime} \Delta \boldsymbol{x}_{t-j}^+ + \boldsymbol{\pi}_{j*}^{-\prime} \Delta \boldsymbol{x}_{t-j}^- \right) + e_t; \tag{A.6}$$

$$\widehat{\boldsymbol{\varrho}}_T = \boldsymbol{\varrho}_* + \left(\sum_{t=1}^{T} \boldsymbol{q}_t \boldsymbol{q}_t' \right)^{-1} \left(\sum_{t=1}^{T} \boldsymbol{q}_t u_t \right); \tag{A.7}$$

$$\widehat{\boldsymbol{\zeta}}_T := \left(\sum_{t=1}^{T} \boldsymbol{h}_t \boldsymbol{h}_t'\right)^{-1} \left(\sum_{t=1}^{T} \boldsymbol{h}_t \Delta y_t\right) = \boldsymbol{\zeta}_* + \left(\sum_{t=1}^{T} \boldsymbol{h}_t \boldsymbol{h}_t'\right)^{-1} \left(\sum_{t=1}^{T} \boldsymbol{h}_t e_t\right). \tag{A.8}$$

B Proofs

Proof of Lemma 1. (*i*) By (A.1) and (A.2), we obtain the following results:

- $T^{-3} \sum_{t=1}^{T} y_{t-1}^2 = \frac{1}{3}\delta_*^2 + o_{\mathbb{P}}(1)$;
- $T^{-3} \sum_{t=1}^{T} y_{t-1} \boldsymbol{x}_t^{+\prime} = \frac{1}{3}\delta_* \boldsymbol{\mu}_*^{+\prime} + o_{\mathbb{P}}(1)$;
- $T^{-3} \sum_{t=1}^{T} y_{t-1} \boldsymbol{x}_t^{-\prime} = \frac{1}{3}\delta_* \boldsymbol{\mu}_*^{-\prime} + o_{\mathbb{P}}(1)$;
- $T^{-3} \sum_{t=1}^{T} \boldsymbol{x}_t^{+} \boldsymbol{x}_t^{+\prime} = \frac{1}{3}\boldsymbol{\mu}_*^{+} \boldsymbol{\mu}_*^{+\prime} + o_{\mathbb{P}}(1)$;
- $T^{-3} \sum_{t=1}^{T} \boldsymbol{x}_t^{+} \boldsymbol{x}_t^{-\prime} = \frac{1}{3}\boldsymbol{\mu}_*^{+} \boldsymbol{\mu}_*^{-\prime} + o_{\mathbb{P}}(1)$; and
- $T^{-3} \sum_{t=1}^{T} \boldsymbol{x}_t^{-} \boldsymbol{x}_t^{-\prime} = \frac{1}{3}\boldsymbol{\mu}_*^{-} \boldsymbol{\mu}_*^{-\prime} + o_{\mathbb{P}}(1)$.

These limits imply that $T^{-3} \sum_{t=1}^{T} \boldsymbol{z}_{1t} \boldsymbol{z}_{1t}' = \mathbf{M}_{11} + o_{\mathbb{P}}(1)$.

(*ii*) By (A.1) and (A.2), we note that:

- $T^{-2} \sum_{t=1}^{T} y_{t-1} = \frac{1}{2}\delta_* + o_{\mathbb{P}}(1)$;
- $T^{-2} \sum_{t=1}^{T} y_{t-1} \boldsymbol{w}_{1t}' = T^{-2} \sum_{t=1}^{T} [\delta_*^2 t, \delta_*^2 t, \ldots, \delta_*^2 t] + o_{\mathbb{P}}(1) = \frac{1}{2}\delta_*^2 \boldsymbol{\iota}_{p-1}' + o_{\mathbb{P}}(1)$;
- $T^{-2} \sum_{t=1}^{T} y_{t-1} \boldsymbol{w}_{2t}' = T^{-2} \sum_{t=1}^{T} [\delta_* \boldsymbol{\mu}_*^{+\prime} t, \delta_* \boldsymbol{\mu}_*^{+\prime} t, \ldots, \delta_* \boldsymbol{\mu}_*^{+\prime} t] + o_{\mathbb{P}}(1) = \frac{1}{2}\delta_* \boldsymbol{\iota}_q' \otimes \boldsymbol{\mu}_*^{+\prime} + o_{\mathbb{P}}(1)$;
- $T^{-2} \sum_{t=1}^{T} y_{t-1} \boldsymbol{w}_{3t}' = T^{-2} \sum_{t=1}^{T} [\delta_* \boldsymbol{\mu}_*^{-\prime} t, \delta_* \boldsymbol{\mu}_*^{-\prime} t, \ldots, \delta_* \boldsymbol{\mu}_*^{-\prime} t] + o_{\mathbb{P}}(1) = \frac{1}{2}\delta_* \boldsymbol{\iota}_q' \otimes \boldsymbol{\mu}_*^{-\prime} + o_{\mathbb{P}}(1)$;
- $T^{-2} \sum_{t=1}^{T} \boldsymbol{x}_{t-1}^{+} = \frac{1}{2}\boldsymbol{\mu}_*^{+} + o_{\mathbb{P}}(1)$;
- $T^{-2} \sum_{t=1}^{T} \boldsymbol{x}_{t-1}^{+} \boldsymbol{w}_{1t}' = T^{-2} \sum_{t=1}^{T} [\delta_* \boldsymbol{\mu}_*^{+} t, \delta_* \boldsymbol{\mu}_*^{+} t, \ldots, \delta_* \boldsymbol{\mu}_*^{+} t] + o_{\mathbb{P}}(1) = \frac{1}{2}\delta_* \boldsymbol{\mu}_*^{+} \boldsymbol{\iota}_{p-1}' + o_{\mathbb{P}}(1)$;
- $T^{-2} \sum_{t=1}^{T} \boldsymbol{x}_{t-1}^{+} \boldsymbol{w}_{2t}' = T^{-2} \sum_{t=1}^{T} [\boldsymbol{\mu}_*^{+} \boldsymbol{\mu}_*^{+\prime} t, \boldsymbol{\mu}_*^{+} \boldsymbol{\mu}_*^{+\prime} t, \ldots, \boldsymbol{\mu}_*^{+} \boldsymbol{\mu}_*^{+\prime} t] + o_{\mathbb{P}}(1) = \frac{1}{2}\boldsymbol{\iota}_q' \otimes \boldsymbol{\mu}_*^{+} \boldsymbol{\mu}_*^{+\prime} + o_{\mathbb{P}}(1)$;
- $T^{-2} \sum_{t=1}^{T} \boldsymbol{x}_{t-1}^{+} \boldsymbol{w}_{3t}' = T^{-2} \sum_{t=1}^{T} [\boldsymbol{\mu}_*^{+} \boldsymbol{\mu}_*^{-\prime} t, \boldsymbol{\mu}_*^{+} \boldsymbol{\mu}_*^{-\prime} t, \ldots, \boldsymbol{\mu}_*^{+} \boldsymbol{\mu}_*^{-\prime} t] + o_{\mathbb{P}}(1) = \frac{1}{2}\boldsymbol{\iota}_q' \otimes \boldsymbol{\mu}_*^{+} \boldsymbol{\mu}_*^{-\prime} + o_{\mathbb{P}}(1)$;
- $T^{-2} \sum_{t=1}^{T} \boldsymbol{x}_{t-1}^{-} = -\frac{1}{2}\boldsymbol{\mu}_*^{+} + o_{\mathbb{P}}(1)$;
- $T^{-2} \sum_{t=1}^{T} \boldsymbol{x}_{t-1}^{-} \boldsymbol{w}_{1t}' = T^{-2} \sum_{t=1}^{T} [\delta_* \boldsymbol{\mu}_*^{-} t, \delta_* \boldsymbol{\mu}_*^{-} t, \ldots, \delta_* \boldsymbol{\mu}_*^{-} t] + o_{\mathbb{P}}(1) = \frac{1}{2}\delta_* \boldsymbol{\mu}_*^{-} \boldsymbol{\iota}_{p-1}' + o_{\mathbb{P}}(1)$;
- $T^{-2} \sum_{t=1}^{T} \boldsymbol{x}_{t-1}^{-} \boldsymbol{w}_{2t}' = T^{-2} \sum_{t=1}^{T} [\boldsymbol{\mu}_*^{-} \boldsymbol{\mu}_*^{+\prime} t, \boldsymbol{\mu}_*^{-} \boldsymbol{\mu}_*^{+\prime} t, \ldots, \boldsymbol{\mu}_*^{-} \boldsymbol{\mu}_*^{+\prime} t] + o_{\mathbb{P}}(1) = \frac{1}{2}\boldsymbol{\iota}_q' \otimes \boldsymbol{\mu}_*^{-} \boldsymbol{\mu}_*^{+\prime} + o_{\mathbb{P}}(1)$;
- $T^{-2} \sum_{t=1}^{T} \boldsymbol{x}_{t-1}^{-} \boldsymbol{w}_{3t}' = T^{-2} \sum_{t=1}^{T} [\boldsymbol{\mu}_*^{-} \boldsymbol{\mu}_*^{-\prime} t, \boldsymbol{\mu}_*^{-} \boldsymbol{\mu}_*^{-\prime} t, \ldots, \boldsymbol{\mu}_*^{-} \boldsymbol{\mu}_*^{-\prime} t] + o_{\mathbb{P}}(1) = \frac{1}{2}\boldsymbol{\iota}_q' \otimes \boldsymbol{\mu}_*^{-} \boldsymbol{\mu}_*^{-\prime} + o_{\mathbb{P}}(1)$.

These limit results imply that $T^{-1} \sum_{t=1}^{T} \boldsymbol{z}_{1t} \boldsymbol{z}_{2t}' = \mathbf{M}_{12} + o_{\mathbb{P}}(1)$.

(*iii*) We note that:

- $T^{-1} \sum_{t=1}^{T} \boldsymbol{w}_{1t}' = \mathbb{E}[\Delta \boldsymbol{y}_{t-1}]' + o_{\mathbb{P}}(1) = \delta_* \boldsymbol{\iota}_{p-1}' + o_{\mathbb{P}}$;
- $T^{-1} \sum_{t=1}^{T} \boldsymbol{w}_{2t}' = [\mathbb{E}[\Delta \boldsymbol{x}_t^{+\prime}], \mathbb{E}[\Delta \boldsymbol{x}_{t-1}^{+\prime}], \ldots, \mathbb{E}[\Delta \boldsymbol{x}_{t-q+1}^{+\prime}]] + o_{\mathbb{P}}(1) = [\boldsymbol{\mu}_*^{+\prime}, \ldots, \boldsymbol{\mu}_*^{+\prime}] + o_{\mathbb{P}}(1) = \boldsymbol{\iota}_q' \otimes \boldsymbol{\mu}_*^{+} + o_{\mathbb{P}}(1)$;
- $T^{-1} \sum_{t=1}^{T} \boldsymbol{w}_{3t}' = [\mathbb{E}[\Delta \boldsymbol{x}_t^{-\prime}], \mathbb{E}[\Delta \boldsymbol{x}_{t-1}^{-\prime}], \ldots, \mathbb{E}[\Delta \boldsymbol{x}_{t-q+1}^{-\prime}]] + o_{\mathbb{P}}(1) = [\boldsymbol{\mu}_*^{-\prime}, \ldots, \boldsymbol{\mu}_*^{-\prime}] + o_{\mathbb{P}}(1) = \boldsymbol{\iota}_q' \otimes \boldsymbol{\mu}_*^{-} + o_{\mathbb{P}}(1)$; and

- $T^{-1}\sum_{t=1}^{T}\boldsymbol{w}_t\boldsymbol{w}_t' = \mathbb{E}[\boldsymbol{w}_t\boldsymbol{w}_t'] + o_{\mathbb{P}}(1)$.

These limits imply that $T^{-1}\sum_{t=1}^{T}\boldsymbol{z}_{2t}\boldsymbol{z}_{2t}' = \mathbf{M}_{22} + o_{\mathbb{P}}(1)$, as desired. ■

Proof of Lemma 2. (*i*) We note that:

- $T^{-2}\sum_{t=1}^{T}x_t^+ = T^{-1}\sum_{t=1}^{T}\mu_*^+(t/T) + o_{\mathbb{P}}(1) \stackrel{\mathbb{P}}{\to} \frac{1}{2}\mu_*^+$;
- $T^{-3/2}\sum_{t=1}^{T}x_t = T^{-1}\sum_{t=1}^{T}(T^{-1/2}\sum_{i=1}^{t}\Delta x_i) \Rightarrow \int \mathcal{B}_x$ using that $T^{-1/2}\sum_{i=1}^{[T(\cdot)]}\Delta x_i \Rightarrow \int_0^{(\cdot)} d\mathcal{B}_x$;
- $T^{-3}\sum_{t=1}^{T}x_t^+x_t^+ = T^{-1}\sum_{t=1}^{T}\mu_*^+\mu_*^+(t/T)^2 + o_{\mathbb{P}}(1) \stackrel{\mathbb{P}}{\to} \frac{1}{3}\mu_*^+\mu_*^+$;
- $T^{-5/2}\sum_{t=1}^{T}x_t^+x_t = T^{-1}\sum_{t=1}^{T}\mu_*^+(t/T)(T^{-1/2}\sum_{i=1}^{t}\Delta x_t) + o_{\mathbb{P}}(1) \Rightarrow \mu_*^+\int r\mathcal{B}_x$; and
- $T^{-2}\sum_{t=1}^{T}x_tx_t = T^{-1}\sum_{t=1}^{T}(T^{-1/2}\sum_{i=1}^{t}\Delta x_t)(T^{-1/2}\sum_{i=1}^{t}\Delta x_t) \Rightarrow \int \mathcal{B}_x^2$.

Thus, $\widehat{\mathbf{Q}}_T \Rightarrow \boldsymbol{\mathcal{Q}}$, as desired.

(*ii*) We note that:

- $T^{-1/2}\sum_{t=1}^{T}u_t \Rightarrow \int d\mathcal{B}_u$ using that $T^{-1/2}\sum_{t=1}^{[T(\cdot)]}u_t \Rightarrow \int_0^{(\cdot)} d\mathcal{B}_u$;
- $T^{-3/2}\sum_{t=1}^{T}x_t^+u_t = T^{-1/2}\sum_{t=1}^{T}\mu_*^+(t/T)u_t + o_{\mathbb{P}}(1) \Rightarrow \mu_*^+\int r d\mathcal{B}_u$; and
- $T^{-1}\sum_{t=1}^{T}x_tu_t = T^{-1/2}\sum_{t=1}^{T}(T^{-1/2}\sum_{i=1}^{t}\Delta x_i)u_t \Rightarrow \int \mathcal{B}_x d\mathcal{B}_u + \upsilon_*$ using the fact that $\upsilon_* := \lim_{T\to\infty} T^{-1}\sum_{t=1}^{T}\sum_{i=1}^{t}\mathbb{E}[\Delta x_i u_t]$ is finite.

Therefore, $\widehat{\mathbf{U}}_T \Rightarrow \boldsymbol{\mathcal{U}}$. ■

Proof of Corollary 1. Given (A.7), the desired result follows from Lemma 4. ■

Proof of Theorem 1. Using the definition of $\widehat{\lambda}_T$, we have: $T\{(\widehat{\beta}_T^+ - \widehat{\beta}_T^-) - (\beta_*^+ - \beta_*^-)\} = O_{\mathbb{P}}(T^{-1/2})$, implying that the weak limit of $T(\widehat{\beta}_T^+ - \beta_*^+)$ is equivalent to that of $T(\widehat{\beta}_T^- - \beta_*^-)$. Furthermore, by Corollary 1, we obtain the desired result, $T(\widehat{\beta}_T^- - \beta_*^-) \Rightarrow \mathbf{S}\boldsymbol{\mathcal{Q}}^{-1}\boldsymbol{\mathcal{U}}$. ■

Proof of Lemma 3. Under Assumption 2, we have: $\widetilde{\upsilon}_T \stackrel{\mathbb{P}}{\to} \upsilon_*$ and $(\widetilde{\sigma}_T^{(1,1)})^{-1}\widetilde{\sigma}_T^{(1,2)} \stackrel{\mathbb{P}}{\to} \boldsymbol{\nu}_* := (\sigma_*^{(1,1)})^{-1}\sigma_*^{(1,2)}$. Next, let $\dot{u}_t := u_t - \Delta x_t\boldsymbol{\nu}_*$, $\widetilde{\mathbf{U}}_T = \widetilde{\mathbf{D}}_T^{-1}\sum_{t=1}^{T}\{\boldsymbol{q}_t\dot{u}_t - \mathbf{S}'\upsilon_*\} + o_{\mathbb{P}}(1)$, then $\widetilde{\mathbf{U}}_T \Rightarrow [\int d\mathcal{B}_{\dot{u}}, \mu_*^+\int r d\mathcal{B}_{\dot{u}}, \int \mathcal{B}_x\, d\mathcal{B}_{\dot{u}}]'$, where $\mathcal{B}_{\dot{u}}(\cdot) := \tau_*\mathcal{W}_u(\cdot)$. Therefore, $\widetilde{\mathbf{U}}_T \Rightarrow \widetilde{\boldsymbol{\mathcal{U}}}$. ■

Proof of Corollary 2. Given that $\widetilde{\mathbf{D}}_T(\widetilde{\boldsymbol{\varrho}}_T - \boldsymbol{\varrho}_*) = [\widetilde{\mathbf{D}}_T^{-1}(\sum_{t=1}^{T}\boldsymbol{q}_t\boldsymbol{q}_t')\widetilde{\mathbf{D}}_T^{-1}]^{-1}\widetilde{\mathbf{U}}_T$, the desired result follows from Lemmas 2(*i*) and 3. ■

Proof of Theorem 2. Given that $(\widetilde{\beta}_T^+ - \beta_*^+) - (\widetilde{\beta}_T^- - \beta_*^-) = \widetilde{\lambda}_T - \lambda_* = O_{\mathbb{P}}(T^{-3/2})$ and $(\widetilde{\beta}_T^- - \beta_*^-) = O_{\mathbb{P}}(T^{-1})$, it follows that $(\widetilde{\beta}_T^+ - \beta_*^+) = O_{\mathbb{P}}(T^{-1})$, implying that the weak limit of $T(\widetilde{\beta}_T^+ - \beta_*^+)$ is equivalent to that of $T(\widetilde{\beta}_T^- - \beta_*^-)$. By Corollary 1, we obtain the desired result, $T(\widetilde{\eta}_T^- - \eta_*^-) = T(\widetilde{\beta}_T^- - \beta_*^-) \Rightarrow \mathbf{S}\boldsymbol{\mathcal{Q}}^{-1}\widetilde{\boldsymbol{\mathcal{U}}}$.

■

Proof of Lemma 4. The result is established by the ergodic theorem and the multivariate central limit theorem. ■

Proof of Theorem 3. (*i*) Given (A.8), we can combine Lemmas 4 (*i* and *ii*) and obtain the desired result.

(*ii*) Further, if it holds that $\mathbb{E}[e_t^2|\boldsymbol{h}_t] = \sigma_*^2$, then we have: $\boldsymbol{\Omega}_* = \sigma_*^2\boldsymbol{\Gamma}_*$ by Lemma 4(*iii*). Thus, Theorem 3(*i*) implies that $\sqrt{T}(\widehat{\boldsymbol{\zeta}}_T - \boldsymbol{\zeta}_*) \overset{\text{A}}{\sim} N(\mathbf{0}, \sigma_*^2\boldsymbol{\Gamma}_*^{-1})$. ■

Proof of Lemma 5. (*i*) We note that:

- $T^{-2}\sum_{t=1}^T t = \frac{1}{2} + o(1)$;
- $T^{-3/2}\sum_{t=1}^T \widehat{\boldsymbol{m}}_t = T^{-3/2}\sum_{t=1}^T \boldsymbol{m}_t - (T^{-2}\sum_{t=1}^T t)(T^{-3}\sum_{t=1}^T t^2)^{-1}T^{-5/2}\sum_{t=1}^T t\boldsymbol{m}_t = T^{-1}\sum_{t=1}^T T^{-1/2}(\sum_{i=1}^t \Delta\boldsymbol{m}_i) - (T^{-2}\sum_{t=1}^T t)(T^{-3}\sum_{t=1}^T t^2)^{-1}(T^{-1}\sum_{t=1}^T (t/T)T^{-1/2}\sum_{i=1}^t \Delta\boldsymbol{m}_i) \Rightarrow \int \boldsymbol{\mathcal{B}}_m - \frac{3}{2}\int r\boldsymbol{\mathcal{B}}_m$ using the fact that $T^{-1/2}\sum_{i=1}^{[T(\cdot)]}\Delta\boldsymbol{m}_i \Rightarrow \int_0^{(\cdot)} d\boldsymbol{\mathcal{B}}_m$;
- $T^{-3/2}\sum_{t=1}^T \boldsymbol{x}_t = T^{-1}\sum_{t=1}^T (T^{-1/2}\sum_{i=1}^t \Delta\boldsymbol{x}_i) \Rightarrow \int \boldsymbol{\mathcal{B}}_x$ using the fact that $T^{-1/2}\sum_{i=1}^{[T(\cdot)]}\Delta\boldsymbol{x}_i \Rightarrow \int_0^{(\cdot)} d\boldsymbol{\mathcal{B}}_x$;
- $T^{-3}\sum_{t=1}^T t^2 = \frac{1}{3} + o(1)$;
- $T^{-5/2}\sum_{t=1}^T t\widehat{\boldsymbol{m}}_t = T^{-5/2}\sum_{t=1}^T t\boldsymbol{m}_t - T^{-5/2}(\sum_{t=1}^T t^2)(\sum_{t=1}^T t^2)^{-1}(\sum_{t=1}^T t\boldsymbol{m}_t) = \mathbf{0}$;
- $T^{-5/2}\sum_{t=1}^T t\boldsymbol{x}_t = T^{-1}\sum_{t=1}^T (t/T)(T^{-1/2}\sum_{i=1}^t \Delta\boldsymbol{x}_i) \Rightarrow \int r\boldsymbol{\mathcal{B}}_x$;
- $T^{-2}\sum_{t=1}^T \widehat{\boldsymbol{m}}_t\widehat{\boldsymbol{m}}_t' = T^{-2}\sum_{t=1}^T \boldsymbol{m}_t\boldsymbol{m}_t' - T^{-2}\sum_{t=1}^T t\,\boldsymbol{m}_t\,(\sum_{t=1}^T t^2)^{-1}\sum_{t=1}^T t\,\boldsymbol{m}_t' = T^{-1}\sum_{t=1}^T (T^{-1/2}\sum_{i=1}^t \Delta\boldsymbol{m}_i)(T^{-1/2}\sum_{i=1}^t \Delta\boldsymbol{m}_i)' - T^{-1}\sum_{t=1}^T ((t/T)\,T^{-1/2}\sum_{i=1}^t \Delta\boldsymbol{m}_i)(T^{-3}\sum_{t=1}^T t^2)^{-1} T^{-1}\sum_{t=1}^T ((t/T)T^{-1/2}\sum_{i=1}^t \Delta\boldsymbol{m}_i)' \Rightarrow \int \boldsymbol{\mathcal{B}}_m\boldsymbol{\mathcal{B}}_m' - 3\int r\boldsymbol{\mathcal{B}}_m\int r\boldsymbol{\mathcal{B}}_m'$;
- $T^{-2}\sum_{t=1}^T \boldsymbol{x}_t\widehat{\boldsymbol{m}}_t' = T^{-2}\sum_{t=1}^T \boldsymbol{x}_t\boldsymbol{m}_t' - T^{-2}\sum_{i=1}^t t\boldsymbol{x}_t(\sum_{i=1}^t t^2)^{-1}\sum_{t=1}^T t\boldsymbol{m}_t' = T^{-1}\sum_{t=1}^T (T^{-1/2}\sum_{i=1}^t \Delta\boldsymbol{x}_i)(T^{-1/2}\sum_{i=1}^t \Delta\boldsymbol{m}_i) - T^{-1}\sum_{t=1}^T ((t/T)T^{-1/2}\sum_{i=1}^t \Delta\boldsymbol{x}_i)(T^{-3}\sum_{t=1}^T t^2)^{-1}((t/T)T^{-1/2}\sum_{i=1}^t \Delta\boldsymbol{m}_i') \Rightarrow \int \boldsymbol{\mathcal{B}}_x\boldsymbol{\mathcal{B}}_m' - 3\int r\boldsymbol{\mathcal{B}}_x\int r\boldsymbol{\mathcal{B}}_m'$;
- $T^{-2}\sum_{t=1}^T \boldsymbol{x}_t\boldsymbol{x}_t' = T^{-1}\sum_{t=1}^T (T^{-1/2}\sum_{i=1}^t \Delta\boldsymbol{x}_t)(T^{-1/2}\sum_{i=1}^t \Delta\boldsymbol{x}_t) \Rightarrow \int \boldsymbol{\mathcal{B}}_x\boldsymbol{\mathcal{B}}_x'$.

Therefore, $\ddot{\mathbf{R}}_T \Rightarrow \boldsymbol{\mathcal{R}}$, as desired.

(*ii*) We note that:

- $T^{-1/2}\sum_{t=1}^T u_t \Rightarrow \int d\mathcal{B}_u$ using the fact that $T^{-1/2}\sum_{t=1}^{[T(\cdot)]} u_t \Rightarrow \int_0^{(\cdot)} d\mathcal{B}_u$;
- $T^{-3/2}\sum_{t=1}^T tu_t = T^{-1/2}\sum_{t=1}^T (t/T)u_t + o_{\mathbb{P}}(1) \Rightarrow \int rd\mathcal{B}_u$;
- $T^{-1}\sum_{t=1}^T \widehat{\boldsymbol{m}}_t u_t = T^{-1}\sum_{t=1}^T u_t(\boldsymbol{m}_t - t(\sum_{t=1}^T t^2)^{-1}\sum_{t=1}^T t\boldsymbol{m}_t) = T^{-1}\sum_{t=1}^T u_t\boldsymbol{m}_t - T^{-3/2}\sum_{t=1}^T u_t t(T^{-3}\sum_{t=1}^T t^2)^{-1}T^{-5/2}\sum_{t=1}^T t\boldsymbol{m}_t \Rightarrow \int \boldsymbol{\mathcal{B}}_m d\mathcal{B}_u + \boldsymbol{v}_{m*} - 3\int rd\mathcal{B}_u\int r\boldsymbol{\mathcal{B}}_m$ using the fact that $\boldsymbol{v}_{m*} := \lim_{T\to\infty} T^{-1}\sum_{t=1}^T\sum_{i=1}^t \mathbb{E}[\Delta\boldsymbol{m}_i u_t]$ is finite.
- $T^{-1}\sum_{t=1}^T \boldsymbol{x}_t u_t = T^{-1/2}\sum_{t=1}^T (T^{-1/2}\sum_{i=1}^t \Delta\boldsymbol{x}_i)u_t \Rightarrow \int \boldsymbol{\mathcal{B}}_x d\mathcal{B}_u + \boldsymbol{v}_{x*}$ using the fact that $\boldsymbol{v}_{x*} := \lim_{T\to\infty} T^{-1}\sum_{t=1}^T\sum_{i=1}^t \mathbb{E}[\Delta\boldsymbol{x}_i u_t]$ is finite.

Therefore, $\ddot{\mathbf{U}}_T \Rightarrow \ddot{\boldsymbol{\mathcal{U}}}$. ■

Proof of Corollary 3. As it is straightforward to show that the first claim follows from Lemma 5, we focus on the second claim. As $T^{3/2}(\widehat{\xi}_T - \xi_{*T}) = O_{\mathbb{P}}(1)$ and $\xi_{*T} = \boldsymbol{\lambda}_*'\boldsymbol{\mu}_*^+ + \boldsymbol{\lambda}_*'\sum t\boldsymbol{m}_t(\sum t^2)^{-1}$, $T^{3/2}(\widehat{\xi}_T - \boldsymbol{\lambda}_*'\boldsymbol{\mu}_*^+ - \boldsymbol{\lambda}_*'\sum t\boldsymbol{m}_t(\sum t^2)^{-1}) = O_{\mathbb{P}}(1)$, where $T^{1/2}\sum t\boldsymbol{m}_t(\sum t^2)^{-1} \Rightarrow \frac{1}{3}\int r\boldsymbol{\mathcal{B}}_m$. Thus, it follows that $T^{1/2}(\widehat{\xi}_T - \boldsymbol{\lambda}_*'\boldsymbol{\mu}_*^+) = T^{1/2}\boldsymbol{\lambda}_*'\sum t\boldsymbol{m}_t\,(\sum t^2)^{-1}) + O_{\mathbb{P}}(T^{-1}) \Rightarrow 3\boldsymbol{\lambda}_*'\int r\boldsymbol{\mathcal{B}}_m$. ■

Proof of Theorem 4. This result is easily obtained from Corollary 3. ■

Proof of Lemma 6. Under Assumption 3, notice that $\bar{\boldsymbol{v}}_T \overset{\mathbb{P}}{\to} \ddot{\boldsymbol{v}}_* := [\boldsymbol{v}_{m*}', \boldsymbol{v}_{x*}']'$ and $(\bar{\boldsymbol{\Sigma}}_T^{(1,1)})^{-1}\bar{\boldsymbol{\sigma}}_T^{(1,2)} \overset{\mathbb{P}}{\to} \ddot{\boldsymbol{\nu}}_* := (\boldsymbol{\Sigma}_*^{(1,1)})^{-1}\boldsymbol{\sigma}_*^{(1,2)}$. Let $\mathring{u}_t := u_t - \boldsymbol{\ell}_t'\ddot{\boldsymbol{\nu}}_*$, $\bar{\mathbf{U}}_T = \ddot{\mathbf{D}}_T^{-1}\sum_{t=1}^T\{\boldsymbol{r}_t\mathring{u}_t - \bar{\mathbf{S}}'\ddot{\boldsymbol{v}}_*\} + o_{\mathbb{P}}(1)$, then $\bar{\mathbf{U}}_T \Rightarrow [\int d\mathcal{B}_{\mathring{u}}, \int rd\mathcal{B}_{\mathring{u}}, \int \boldsymbol{\mathcal{B}}_m'd\mathcal{B}_{\mathring{u}} - 3\int rd\mathcal{B}_{\mathring{u}}\int r\boldsymbol{\mathcal{B}}_m', \int \boldsymbol{\mathcal{B}}_x'd\mathcal{B}_{\mathring{u}}]'$, where $\mathcal{B}_{\mathring{u}}(\cdot) := \ddot{\tau}\mathcal{W}_u(\cdot)$. Therefore, $\bar{\mathbf{U}}_T \Rightarrow \bar{\boldsymbol{\mathcal{U}}}$. ■

Proof of Theorem 5. Given that $\ddot{\mathbf{D}}_T(\bar{\boldsymbol{\varpi}}_T - \bar{\boldsymbol{\varpi}}_{*T}) = (\ddot{\mathbf{D}}_T^{-1}(\sum_{t=1}^T \boldsymbol{r}_t\boldsymbol{r}_t')\ddot{\mathbf{D}}_T^{-1})^{-1}\bar{\mathbf{U}}_T$, Lemma 6 establishes the first claim. Second, $T[(\bar{\boldsymbol{\beta}}_T^+ - \boldsymbol{\beta}_*^+)', (\bar{\boldsymbol{\beta}}_T^- - \boldsymbol{\beta}_*^-)']' = \ddot{\mathbf{S}}\ddot{\mathbf{D}}_T(\bar{\boldsymbol{\varpi}}_T - \bar{\boldsymbol{\varpi}}_{*T}) \Rightarrow \ddot{\mathbf{S}}\boldsymbol{\mathcal{R}}^{-1}\bar{\boldsymbol{\mathcal{U}}}$, as desired. ■

Proof of Theorem 6. By Corollary 2 we have: $T^{3/2}(\widetilde{\boldsymbol{\lambda}}_T - r) \Rightarrow \mathbf{S}\boldsymbol{\mathcal{Q}}^{-1}\widetilde{\boldsymbol{\mathcal{U}}}$ under H_0''. By Lemma 2(*i*) we have: $\widehat{\mathbf{Q}}_T := \widetilde{\mathbf{D}}_T^{-1}(\sum_{t=1}^T \boldsymbol{q}_t\,\boldsymbol{q}_t')\widetilde{\mathbf{D}}_T^{-1} \Rightarrow \boldsymbol{\mathcal{Q}}$. Further, under Assumption 2(*i*), we have: $\widetilde{\tau}_T^2 = \tau_*^2 + o_{\mathbb{P}}(1)$. Given the mixed normal distribution of the FM estimator of the long-run parameter in Corollary 2, it follows that $\mathcal{W}_T^{(\ell)} \overset{\text{A}}{\sim} \mathcal{X}_1^2$ under $\mathcal{H}_0''$.

Next, we note that $\widetilde{\mathcal{W}}_T^{(\ell)} = (\widetilde{\mathbf{R}}\widetilde{\boldsymbol{\varrho}}_T - \mathbf{r})'\widetilde{\mathbf{D}}_T(\widetilde{\tau}_T^2\widetilde{\mathbf{R}}\widehat{\mathbf{Q}}_T^{-1}\widetilde{\mathbf{R}}')^{-1}\widetilde{\mathbf{D}}_T(\widetilde{\mathbf{R}}\widetilde{\boldsymbol{\varrho}}_T - \mathbf{r})$. By Theorem 2 we have: $\widetilde{\mathbf{D}}_T(\widetilde{\mathbf{R}}\widetilde{\boldsymbol{\varrho}}_T - \mathbf{r}) \overset{\text{A}}{\sim} N(\mathbf{0}, \tau_*^2\widetilde{\mathbf{R}}\boldsymbol{\mathcal{Q}}^{-1}\widetilde{\mathbf{R}}')$ conditional on $\sigma\{\mathcal{B}_x(r) : r \in (0,1]\}$ under H_0'''. Given that $\widehat{\mathbf{Q}}_T \Rightarrow \boldsymbol{\mathcal{Q}}$ and $\widetilde{\tau}_T^2 \overset{\mathbb{P}}{\to} \tau_*^2$, it follows that $\widetilde{\mathcal{W}}_T^{(\ell)} \overset{\text{A}}{\sim} \mathcal{X}_2^2$ under H_0'''.

Given that $(\widetilde{\boldsymbol{\lambda}}_T - \boldsymbol{\lambda}_*) = O_{\mathbb{P}}(T^{-3/2})$, we have: $\mathcal{W}_T^{(\ell)} = O_{\mathbb{P}}(T^3)$ under H_1'' such that $\mathbb{P}(\mathcal{W}_T^{(\ell)} > c_T) \to 1$ for any $c_T = o(T^3)$. Further, $(\widetilde{\beta}_T - \beta_*) = O_{\mathbb{P}}(T^{-1})$, implying that $\widetilde{\mathcal{W}}_T^{(\ell)} = O_{\mathbb{P}}(T^2)$ under H_1'''. Therefore, $\mathbb{P}(\widetilde{\mathcal{W}}_T^{(\ell)} > \widetilde{c}_T) \to 1$ for any $\widetilde{c}_T = o(T^2)$. This completes the proof. ■

Proof of Theorem 7. Due to its similarity to the standard case, we omit the proof. ■

Proof of Theorem 8. Due to its similarity to the standard case, we omit the proof. ■

C Further Singularity Issues Associated with Single-Step NARDL Estimation

The re-parameterization of the long-run relationship to resolve the singularity issue under 2-step estimation in (A.4) is insufficient to resolve the singularity issue involved in single-step NARDL estimation. In fact, the estimation of the short-run and the long-run parameters in a single step by combining (A.5) with (A.6) will encounter a further singularity problem. Using $\lambda_* := \beta_*^+ - \beta_*^-$ and $\eta_* := \beta_*^-$, it follows that $u_{t-1} = y_{t-1} - \lambda_* x_{t-1}^+ - \beta_* x_{t-1}$. Then,

$$\Delta y_t = \rho_* y_{t-1} + (\theta_*^+ - \theta_*^-) x_{t-1}^+ + \theta_*^- x_{t-1} + \gamma_* + \sum_{j=1}^{p-1} \varphi_{j*} \Delta y_{t-j} + \sum_{j=0}^{q-1} \left(\pi_{j*}^+ \Delta x_{t-j}^+ + \pi_{j*}^- \Delta x_{t-j}^- \right) + e_t,$$

where $\boldsymbol{\beta}_*^+ := -\theta_*^+/\rho_*$ and $\boldsymbol{\beta}_*^- := -\theta_*^-/\rho_*$. Let:

$$\boldsymbol{\xi}_* := \left[\ \boldsymbol{\xi}_{1*}' \ \vdots\ \boldsymbol{\xi}_{2*}'\ \right]' := \left[\ \rho_* \quad \theta_* \quad \theta_*^- \ \vdots\ \boldsymbol{\alpha}_{2*}'\ \right]', \quad \boldsymbol{p}_t := \left[\ \boldsymbol{p}_{1t}' \ \vdots\ \boldsymbol{p}_{2t}'\ \right]' := \left[\ y_{t-1} \quad x_{t-1}^+ \quad x_{t-1} \ \vdots\ \boldsymbol{z}_{2t}'\ \right]'.$$

Note that $\boldsymbol{\xi}_{2*}$ and $\boldsymbol{p}_{2t}$ are identical to $\boldsymbol{\alpha}_{2*}$ and $\boldsymbol{z}_{2t}$, respectively, where $\theta_* := \theta_*^+ - \theta_*^-$. If we attempt to estimate $\boldsymbol{\xi}_*$ in (A.3) by OLS, we obtain:

$$\widehat{\boldsymbol{\xi}}_T := \left(\sum_{t=1}^{T} \boldsymbol{p}_t \boldsymbol{p}_t' \right)^{-1} \left(\sum_{t=1}^{T} \boldsymbol{p}_t \Delta y_t \right).$$

Lemma 1 shows that the inverse matrix in $\widehat{\boldsymbol{\xi}}_T$ is asymptotically singular.

Lemma A.1. *Under Assumption 1,*

(i) $\ddot{\mathbf{D}}_{1,T}^{-1} \left(\sum_{t=1}^{T} \boldsymbol{p}_{1t} \boldsymbol{p}_{1t}' \right) \ddot{\mathbf{D}}_{1,T}^{-1} \Rightarrow \boldsymbol{\mathcal{P}}_{11}$, *where* $\ddot{\mathbf{D}}_{1,T} := diag[T^{3/2}\mathbf{I}_2, T]$ *and:*

$$\boldsymbol{\mathcal{P}}_{11} := \begin{bmatrix} \frac{1}{3}\delta_*^2 & \frac{1}{3}\delta_*\mu_*^+ & \delta_* \int r\mathcal{B}_x \\ \frac{1}{3}\delta_*\mu_*^+ & \frac{1}{3}\mu_*^+\mu_*^+ & \mu_*^+ \int r\mathcal{B}_x \\ \delta_* \int r\mathcal{B}_x & \int r\mathcal{B}_x \mu_*^+ & \int \mathcal{B}_x^2 \end{bmatrix};$$

(ii) $\ddot{\mathbf{D}}_{1,T}^{-1}\left(\sum_{t=1}^{T}\boldsymbol{p}_{1t}\boldsymbol{p}_{2t}'\right)\ddot{\mathbf{D}}_{2,T}^{-1}\Rightarrow\boldsymbol{\mathcal{P}}_{12}$, *where* $\ddot{\mathbf{D}}_{2,T}:=$ *diag*$[T^{1/2}\mathbf{I}_{1+p+2q}]$ *and:*

$$\boldsymbol{\mathcal{P}}_{12}:=\begin{bmatrix}\frac{1}{2}\delta_* & \frac{1}{2}\delta_*^2\boldsymbol{\iota}_{p-1}' & \frac{1}{2}\delta_*\boldsymbol{\iota}_q'\otimes\mu_*^+ & \frac{1}{2}\delta_*\boldsymbol{\iota}_q'\otimes\mu_*^- \\ \frac{1}{2}\mu_*^+ & \frac{1}{2}\delta_*\mu_*^+\boldsymbol{\iota}_{p-1}' & \frac{1}{2}\boldsymbol{\iota}_q'\otimes\mu_*^+\mu_*^+ & \frac{1}{2}\boldsymbol{\iota}_q'\otimes\mu_*^+\mu_*^- \\ \int\mathcal{B}_x & \delta_*\int\mathcal{B}_x\boldsymbol{\iota}_{p-1}' & \boldsymbol{\iota}_q'\otimes\int\mathcal{B}_x\mu_*^+ & \boldsymbol{\iota}_q'\otimes\int\mathcal{B}_x\mu_*^-\end{bmatrix};\quad and$$

(iii) $\ddot{\mathbf{D}}_{2,T}^{-1}\left(\sum_{t=1}^{T}\boldsymbol{p}_{2t}\boldsymbol{p}_{2t}'\right)\ddot{\mathbf{D}}_{2,T}^{-1}\overset{\mathbb{P}}{\to}\mathbf{P}_{22}:=\mathbf{M}_{22}$. □

The proof of Lemma A.1 is omitted as it is easily derived from the proof of Lemma 1.

Let $\ddot{\mathbf{D}}_T:=\text{diag}[T^{3/2}\mathbf{I}_2,T,T^{1/2}\mathbf{I}_{1+p+2q}]$, then,

$$\ddot{\mathbf{D}}_T^{-1}\left(\sum_{t=1}^{T}\boldsymbol{p}_t\boldsymbol{p}_t'\right)\ddot{\mathbf{D}}_T^{-1}\Rightarrow\boldsymbol{\mathcal{P}}:=\begin{bmatrix}\boldsymbol{\mathcal{P}}_{11} & \boldsymbol{\mathcal{P}}_{12}\\ \boldsymbol{\mathcal{P}}_{21} & \mathbf{P}_{22}\end{bmatrix},$$

where $\boldsymbol{\mathcal{P}}_{21}:=\boldsymbol{\mathcal{P}}_{12}'$. Since $\boldsymbol{\mathcal{P}}$ is singular, it is difficult to obtain the limit distribution of $\widehat{\boldsymbol{\xi}}_T$ even after re-parameterizing the long-run level relationship in (A.4).

D Additional Monte Carlo Simulations

We investigate the finite sample bias and mean squared error (MSE) of the two-step estimators, where the long-run parameters are estimated by OLS or FM for $k=1$; or by TOLS or TFM for $k=2$, while the short-run parameters are estimated by OLS.

D.1 Simulation results for $k=1$

We generate the same NARDL(1,0) DGP empoyed in Section 5.1:

$$\Delta y_t=\gamma_*+\rho_*u_{t-1}+\varphi_*\Delta y_{t-1}+\pi_*^+\Delta x_t^++\pi_*^-\Delta x_t^-+e_t,$$

where $u_{t-1}:=y_{t-1}-\alpha_*-\beta_*^+x_{t-1}^+-\beta_*^-x_{t-1}^-$, $\Delta x_t:=\kappa_*\Delta x_{t-1}+\sqrt{1-\kappa_*^2}v_t$, and $(e_t,v_t)'\sim$ IID$N(\mathbf{0}_2,\mathbf{I}_2)$. We set $(\alpha_*,\beta_*^+,\beta_*^-,\gamma_*,\rho_*,\varphi_*,\pi_*^+,\pi_*^-,\kappa_*)=(0,2,1,0,-2/3,\varphi_*,1,1/2,1/2)$ and we allow the sample size T and the parameter φ_* to vary. Note that Δx_t is generated by an AR(1) process with normally distributed disturbances and that u_t is both serially correlated and contemporaneously correlated with Δx_t.

Next, we consider the following specifications for the long-run and short-run models:

$$y_t = \alpha + \lambda x_t^+ + \eta x_t + u_t \quad \text{and} \quad \Delta y_t = \gamma + \rho \widehat{u}_{t-1} + \varphi_1 \Delta y_{t-1} + \pi_0^+ \Delta x_t^+ + \pi_0^- \Delta x_t^- + e_t,$$

where $\widehat{u}_t := y_t - \widehat{\alpha}_T - \widehat{\lambda}_T x_t^+ - \widehat{\eta}_T x_t$. In the first step, we estimate the parameters of the long-run relationship using OLS or FM. In the second step, we estimate the short-run parameters by OLS. We evaluate the performance of the estimators in terms of their finite sample bias and MSE. We evaluate the bias as

$$\text{Bias}_T(\beta_*^+) := R^{-1} \sum_{j=1}^{R} (\widehat{\beta}_{T,j}^+ - \beta_*^+) \quad \text{and} \quad \text{Bias}_T(\varphi_*) := R^{-1} \sum_{j=1}^{R} (\widehat{\varphi}_{T,j} - \varphi_*),$$

where R is the number of replications, $\widehat{\beta}_T^+$ is the first step OLS or FM estimator and $\widehat{\varphi}_T$ is the second-step OLS estimator. Next, we calculate the finite sample MSE of $\widehat{\beta}_T^+$ and $\widehat{\varphi}_T$ as:

$$\text{MSE}_T(\beta_*^+) := R^{-1} \sum_{j=1}^{R} (\widehat{\beta}_{T,j}^+ - \beta_*^+)^2 \quad \text{and} \quad \text{MSE}_T(\varphi_*) := R^{-1} \sum_{j=1}^{R} (\widehat{\varphi}_{T,j} - \varphi_*)^2.$$

The finite sample bias and MSE of the estimated parameters with $R = 5,000$ replications are reported in Tables A.1 and A.2, respectively.[1]

— Insert Tables A.1 and A.2 Here —

First, consider the long-run parameter estimators obtained in the first step. The finite sample bias of the FM estimator is substantially smaller than that of the OLS estimator. We find that the finite sample bias of the FM estimator is mostly close to zero, because $T(\widetilde{\beta}_T^+ - \beta_*^+)$ and $T(\widetilde{\beta}_T^- - \beta_*^-)$ are asymptotically mixed-normally distributed around zero. By contrast, as the OLS estimator is not asymptotically distributed around zero, it exhibits non-negligible bias. We also find that the FM estimator tends to be more efficient than OLS, thus producing a smaller MSE with the sample size. The efficiency gain is more apparent for small and/or negative values of φ_*. Overall, these results strongly advocate the use of FM in the first step.

Next, consider the short-run parameter estimators obtained by OLS in the second step. The finite sample biases of the second step OLS estimators of the dynamic parameters become mostly negligible (even in $T = 50$), irrespective of whether we use OLS or FM in the first step, though the smallest biases are mostly obtained when we emply the FM estimator. The MSEs of the second step OLS estimators are similar,

[1]To conserve space, we do not report the finite sample bias or MSE for the intercepts, α and γ, but these results are available upon request.

irrespective of whether we use OLS or FM in the first step. This evidence is encouraging since many applications of the NARDL model rely upon the use of small samples, mainly due the low sampling frequency and limited history of macroeconomic database.

D.2 Simulation results for $k = 2$

We considewr the same NARDL(1,0) DGP employed in Section 5.2:

$$\Delta y_t = \gamma_* + \rho_* u_{t-1} + \varphi_* \Delta y_{t-1} + \boldsymbol{\pi}_{0*}^{+\prime} \Delta \boldsymbol{x}_t^+ + \pi_{0*}^{-\prime} \Delta \boldsymbol{x}_t^- + e_t,$$

where $u_{t-1} := y_{t-1} - \alpha_* - \boldsymbol{\beta}_*^{+\prime} \boldsymbol{x}_{t-1}^+ - \boldsymbol{\beta}_*^{-\prime} \boldsymbol{x}_{t-1}^-$, $\Delta \boldsymbol{x}_t := \kappa_* \Delta \boldsymbol{x}_{t-1} + \sqrt{1 - \kappa_*^2} \boldsymbol{v}_t$, and $(e_t, \boldsymbol{v}_t)' \sim$ IID$N(\mathbf{0}_3, \mathbf{I}_3)$. We set $(\alpha_*, \gamma_*, \rho_*, \varphi_*, \kappa_*) = (0, 0, -1, \varphi_*, 0.5)$, $(\boldsymbol{\beta}_*^{+\prime}, \boldsymbol{\beta}_*^{-\prime})' = (-1, 0.5, 0.75, -1.5)'$, and $(\boldsymbol{\pi}_{0*}^{+\prime}, \boldsymbol{\pi}_{0*}^{-\prime})' = (0.5, -0.5, -1, 1)'$. As before, we allow φ_* to vary and examine the effects of serial correlations.

The long-run and short-run models are specified as: $y_t = \alpha + \boldsymbol{\lambda}' \boldsymbol{x}_t^+ + \boldsymbol{\eta} \boldsymbol{x}_t + u_t$ and $\Delta y_t = \gamma + \rho \widehat{u}_{t-1} + \varphi_1 \Delta y_{t-1} + \boldsymbol{\pi}_0^+ \Delta \boldsymbol{x}_t^+ + \boldsymbol{\pi}_0^- \Delta \boldsymbol{x}_t^- + e_t$, where $\widehat{u}_t$ is the regression residual obtained from the first step estimation. In the first step, we estimate the long-run parameters by TOLS or TFM, and then estimate the short-run parameters by OLS. We evaluate the finite-sample performance of the estimators in terms of bias and MSE, which are obtained using $R = 5,000$ replications. The simulation results are reported in Tables A.3 and A.4.

— Insert Tables A.3 and A.4 Here —

As T increases, the finite sample bias of the TFM estimator of the long-run parameters, $\boldsymbol{\beta}_*^+$ and $\boldsymbol{\beta}_*^-$, becomes smaller than that of TOLS. As the FM-OLS yields normally distributed estimators for the long-run parameters, the finite sample bias of TFM approaches zero much faster than TOLS. Further, the TFM estimator becomes more efficient than the TOLS estimator, with a smaller MSE in almost all sample sizes. Based on these results we advocate the use of the TFM estimator in the first step.

Next, we find that the finite sample biases of the OLS estimator of the short-run dynamic parameters become negligible as the sample size rises, irrespective of whether we use either TOLS or TFM. Again, the MSEs of the OLS estimator are more or less similar, irrespective of whether we use TOLS or TFM in the first step, especially for the large samples.

E The Asymmetric Relationship between R&D Intensity and Investment

We review the literature on the link between R&D expenditure and investment, and develop a theory that predicts an asymmetric relationship between R&D intensity and investment.

E.1 Literature Review

Following Schumpeter's seminal 1942 work on creative destruction, a large literature has emerged on R&D activities. Important contributions include Utterback and Abernathy (1975), who find that R&D activity is conducted differently across the different stages of product life, the product life-cycle theory developed by Gort and Wall (1986) and Audretsch (1987), and the game-theoretic approach to R&D activity associated with Kamien and Schwartz (1972), Reinganum (1982), Fudenberg et al. (1983), Grossman and Shapiro (1987) and Harris and Vickers (1987).

It is common to distinguish between two different stages of R&D activity. Early-stage (innovative) R&D expenditure focuses on the development of a new product or technology, leading to a subsequent large-scale investment. By contrast, later-stage (managerial) R&D expenditure focuses on improvements to production efficiency. Consequently, managerial R&D expenditure should not exceed the expected increase in output, which results in a smaller-scale investment than innovative R&D. Overall, R&D expenditure tends to increase sharply in the early stage before leveling off or decreasing at the later stage.

A number of theoretical studies distinguish between innovative and managerial R&D activities and their effects on other economic variables, including Klepper (1996, 1997) and Agarwal and Audretsch (2001). Comin and Philippon (2005) and Aghion et al. (2009) empirically examine the relationship between the entry and/or exit rate of firms and innovative R&D expenditure. Similar theories have been developed in other fields including engineering and management—for example, Zif and McCarthy (1997), who classify R&D activity into multiple stages following the product life-cycle theory (see also Chung and Shin, 2020).

However, one area in which the distinction between innovative and managerial R&D activity is yet to be fully investigated is the relationship between R&D expenditure and investment. Early studies (e.g. Schmookler, 1966) focus on the causal relationship between R&D expenditure and investment. Applying vector autoregressions (VARs) to firm- and industry-level data, Lach and Schankerman (1989) and Lach and Rob (1996) find that R&D expenditure Granger causes investment but not *vice versa*. However, using longer time series, Chiao (2001) documents a two-way causal relationship between the growth rates of the R&D expenditure and investment. Employing a vector error-correction (VEC) model, Baussola (2000) documents evidence in favor of unidirectional Granger causality from R&D expenditure to investment. These results should be treated with care because the failure to distinguish between innovative and managerial R&D activity undermines efforts to accurately capture the potentially asymmetric relationship between R&D expenditure and investment.

E.2 Theoretical Predictions

We propose a theoretical model relating innovative and managerial R&D expenditures to investment. Innovative R&D determines the scope of production, as it describes a research activity that creates a new product or technology through the discovery of a novel production function. The more innovative R&D activity, the larger the scale of production, suggesting that the limit of production activity is determined by the amount of innovative R&D activity. By contrast, managerial R&D does not create a new product, but instead produces an existing product more efficiently, implying that less physical capital is required per unit of output.

Let k and y be the levels of physical capital and output, while we let c and s be the capital levels converted from innovative and managerial R&D expenditures, respectively. We assume that c is complementary to production activity conducted using physical capital while s is a substitute. Consider a production function embodying this mechanism as:

$$y = \min[c, k + s]. \tag{A.9}$$

The complementary relationship with c limits production activity, as output cannot be produced in excess of the level of innovative R&D activity. On the other hand, managerial R&D activity can produce capital s that substitutes for k.

We use a dynamic optimization approach and apply the q-theory of investment to examine how physical investment responds to external shocks to R&D expenditure. First, physical capital k_t is formed by accumulating physical investment i_t through $\dot{k}_t = i_t - \delta k_t$, where δ is the depreciation rate of the physical capital. Similarly, c_t and s_t are accumulated through $\dot{c}_t = r_t - \tau c_t$ and $\dot{s}_t = d_t - \gamma s_t$, where τ and γ denote depreciation rates of c_t and s_t, respectively. Next, consider the cost functions associated with converting R&D expenditures and physical investment into capital. Let $\kappa(r_t)$, $\xi(d_t)$ and $\phi(i_t)$ be the cost levels from innovative and managerial R&D expenditure and physical investment, respectively. We assume that the cost functions are convex with respect to R&D expenditures and physical investment, such that $\kappa'(\cdot) > 0$, $\xi'(\cdot) > 0$, $\phi'(\cdot) > 0$, $\kappa''(\cdot) > 0$, $\xi''(\cdot) > 0$, and $\phi''(\cdot) > 0$.[2]

To generalize the production function (A.9) into a differentiable function, we assume that output is

[2] For example, incidental and/or additional costs may be incurred to convert R&D expenditures into capital for production. These include patent fees, monetary or non-monetary incentives for researchers, safety management fees, training costs, and so on. These costs and fees are assumed to form the convex functions.

given by $y_t = f(c_t, k_t + s_t)$, where $f(\cdot,\cdot)$ is a differentiable function with $f_c(c,a) > 0$, $f_a(c,a) > 0$, $f_{cc}(c,a) < 0$, $f_{aa}(c,a) < 0$, and $f_{ca}(c,a) > 0$ uniformly on the space of (c,a). Notice that k_t and s_t are strictly substitutes, while c_t and $a_t := k_t + s_t$ are weakly complements.[3]

The representative firm determines the optimal path of capital, investment, and R&D expenditures by maximizing discounted aggregate profit:

$$\max_{\{c_t,k_t,s_t,r_t,i_t,d_t\}} \int_0^\infty \{f(c_t, k_t + s_t) - \kappa(r_t) - \phi(i_t) - \xi(d_t)\} e^{-\rho t} dt$$
$$\text{subject to } \dot{c}_t = r_t - \tau c_t, \quad \dot{k}_t = i_t - \delta k_t \quad \text{and} \quad \dot{s}_t = d_t - \gamma s_t,$$

where ρ is the discount rate. This extends the standard q-theory of investment by considering the role of capital converted from R&D expenditures as well as physical capital, with the three different accumulation rules as constraints.[4]

To analyze the long-run relationship between physical investment and R&D expenditures, we set up the dynamic optimization problem. Let $(c_*, k_*, s_*, r_*, i_*, d_*)$ be the steady-state equilibrium, which must satisfy the steady-state conditions given by $f_a(c_*, k_* + s_*) = (\delta + \rho)\phi'(i_*)$, $f_a(c_*, k_* + s_*) = (\gamma + \rho)\xi'(d_*)$, $f_c(c_*, k_* + s_*) = (\tau + \rho)\kappa'(r_*)$, $i_* = \delta k_*$, $d_* = \gamma s_*$, and $r_* = \tau c_*$. To display the steady-state equilibrium, we plot a set of phase diagrams and marginal cost functions in Figure A.1. The panels on the left show the phase diagrams of (r_t, c_t), (i_t, k_t), and (d_t, s_t), while those on the right display the marginal cost functions of innovative R&D expenditure, physical investment, and managerial R&D expenditure, respectively. The phase diagrams also indicate the steady-state equilibrium levels of the variables along with the stable arms denoted by the dotted lines, such that the steady-state equilibrium can be reached by moving toward the equilibrium following the arms. The equilibrium cannot be reached unless the initial levels of (r_0, c_0), (i_0, k_0), and (d_0, s_0) are on the stable arms, simultaneously, as it would violate the transversality conditions.

— Insert Figure A.1 Here —

To examine how the steady-state equilibrium responds to external shocks, we conduct two experiments by changing the marginal cost functions of each type of R&D expenditure. In the first experiment, we let

[3] It is possible to define alternative production functions that exhibit a weakly substitutionary relationship between s_t and k_t. Suppose that the production function (A.9) can be generalized by the constant elasticity of substitution (CES) function, $\ell(x, y; \beta) := (x^{\frac{\beta-1}{\beta}} + y^{\frac{\beta-1}{\beta}})^{\frac{\beta}{\beta-1}}$. Then, we can derive the generalized twofold CES production function: $f(c_t, k_t, s_t; \beta, \sigma) := \ell(c_t, \ell(k_t, s_t; \sigma); \beta)$, from which it follows that $\lim_{\sigma\to\infty} \lim_{\beta\to 0} f(c_t, k_t, s_t; \beta, \sigma) = \min[c_t, k_t + s_t]$. Provided that σ, $\beta > 0$, we can apply optimization theory as the production function is differentiable.

[4] The representative firm is assumed to choose the optimal time paths of r_t and d_t simultaneously, ignoring the fact that innovative R&D activity is conducted earlier than managerial R&D activity. This is not restrictive, as the firm represents a multitude of firms in the economy, where innovative and managerial R&D activities are conducted simultaneously.

the marginal cost function of innovative R&D expenditure decrease from $\kappa_0'(\cdot)$ to $\kappa_1'(\cdot)$. Denote (c_*, k_*, s_*, r_*, i_*, d_*) and (c_{**}, k_{**}, s_{**}, r_{**}, i_{**}, d_{**}) as the initial and new steady-state equilibria. The adjustment processes are displayed in the left panel of Figure A.2. This decline in the marginal cost function shifts the locus of $\dot{c}_t = 0$ to the locus of $\dot{c}_t' = 0$, denoted by the dashed line in the first phase diagram. The steady-state equilibrium (r_{**}, c_{**}) is reached at a level greater than (r_*, c_*). To attain the new steady-state equilibrium, r_* jumps to the new stable arm, denoted by the dotted line. By contrast, c_t is a stock, so it cannot jump to the new stable arm. Thus, (r_t, c_t) gradually tends to (r_{**}, c_{**}). Then, the loci of $\dot{i}_t = 0$ and $\dot{d}_t = 0$ move to $\dot{i}_t' = 0$ and $\dot{d}_t' = 0$, which are denoted by the dashed lines in the second and third diagrams. The steady-state equilibrium is determined at (i_{**}, k_{**}) and (d_{**}, s_{**}), which are greater than (i_*, k_*) and (d_*, s_*). Both i_t and d_t jump to the new stable arms denoted by the dotted lines, and (i_t, k_t) and (d_t, s_t) tend to the new steady-state equilibrium. This reveals that physical investment and innovative R&D expenditure move in the same direction following the change in the cost function of innovative R&D expenditure, implying that they are complements. The economic intuition is straightforward—as innovative R&D activities become relatively cheaper, the firm tends to accumulate more capital from innovative R&D activities, enhancing productivity. This allows the firm to invest more, thereby accumulating more physical capital.

— Insert Figure A.2 Here —

In the second experiment, the marginal cost function of managerial R&D expenditure decreases from $\xi_0'(\cdot)$ to $\xi_1'(\cdot)$. The right panel in Figure A.2 displays the adjustment process to the new equilibrium. The decrease in the marginal cost function shifts the locus of $\dot{d}_t = 0$ to the locus of $\dot{d}_t' = 0$, denoted by the dashed line in the third phase diagram. The new steady-state equilibrium (d_{**}, s_{**}) is reached at a level greater than (d_*, s_*). To attain the new steady-state equilibrium, d_* jumps to the new stable arm, denoted by the dotted line. However, s_t, as a stock, cannot jump to the new stable arm. Consequently, (d_t, s_t) tends to (d_{**}, s_{**}) gradually and the locus of $\dot{i}_t = 0$ shifts to the locus of $\dot{i}_t' = 0$. The steady-state equilibrium level is determined at (i_{**}, k_{**}), where k_t, as a stock, cannot jump to a new level while i_t jumps to the stable arm denoted as the dotted line in the second phase diagram. Overall, following the decrease in the marginal cost of managerial R&D expenditure, d_* rises to d_{**} but i_* falls to i_{**}, revealing a substitutionary relationship between i_t and d_t. This implies that physical capital decreases from k_* to k_{**}, while s increases to s_* from s_{**}.

As s_t and k_t move in opposite directions, $a_{**} := k_{**} + s_{**}$ can be greater or less than $a_* := k_* + s_*$. The sign of the change depends upon the functional shapes of $f_a(\cdot, \cdot)$, $\xi'(\cdot)$, $\phi'(\cdot)$, and the depreciation rates δ and γ. In Figure A.2 under the assumption that $a_{**} > a_*$, the locus of $\dot{c}_t = 0$ is shifted to $\dot{c}_t' = 0$, and a new equilibrium is achieved at (r_{**}, c_{**}), as indicated in the first phase diagram. Then, r_t jumps to the new stable arm denoted as the dotted line, and (r_t, c_t) approaches (r_{**}, c_{**}) gradually. In this case, $r_{**} > r_*$ and $c_{**} > c_*$, which is achieved mainly by virtue of the complementary relationship between c_t and a_t. On the other hand, consider the case with a_{**} less than a_* in which case the locus of $\dot{c}'_t = 0$ is shifted to the left of $\dot{c}_t = 0$. Then, we obtain $r_{**} < r_*$ and $c_{**} < c_*$. The economic intuition of the substitutionary relationship between i_t and d_t is also straightforward. As managerial R&D activity becomes relatively cheaper, the firm tends to accumulate capital by converting managerial R&D expenditures, thereby substituting physical investment, implying that both physical investment and capital will decrease.

These experiments yield important testable implications—the relationship between physical investment and innovative R&D expenditure is expected to be positive by virtue of their complementarity, while the relationship between managerial R&D expenditure and investment is more likely to be negative due to their nature as substitutes.

E.3 The NARDL Specification

Our empirical specification is grounded in two stylized features of R&D expenditure highlighted in Section E.1 and the theory developed in Section E.2. First, as innovative R&D expenditures tend to focus on product innovation, their scale is often large relative to output. This suggests that R&D expenditure is expected to grow faster than output in the early stage, where start-up costs are large and the scale of production typically small. Second, as managerial R&D expenditures focus on enhancing production efficiency, their scale is typically smaller than output.

Let r_t denote aggregate R&D intensity in the t-th period, defined as a ratio of aggregate R&D expenditure to GDP. Noting that aggregate R&D expenditure incorporates the spectrum of R&D activities conducted throughout the economy, the sign of Δr_t determines the relative prevalence of innovative and managerial R&D activities. If $\Delta r_t \geq 0$, then R&D expenditure grows as fast as output, indicating a prevalence of innovative R&D activity. By contrast, if $\Delta r_t < 0$, then output grows faster than R&D expenditure, indicating a prevalence of managerial R&D activity. Given the different characteristics of innovative and managerial R&D, it is reasonable to expect that the relationship between R&D intensity and physical investment may be asymmetric.

To analyze the potential asymmetric impacts of r_t on the log of investment (i_t) in the short-run and the long-run, we consider the following asymmetric error-correction model:

$$\Delta i_t = \gamma_* + \rho_* u_{t-1} + \sum_{j=1}^{p-1} \varphi_{j*} \Delta i_{t-j} + \sum_{j=0}^{q-1} \pi_{j*}^{+} \Delta r_{t-j}^{+} + \sum_{j=0}^{q-1} \pi_{j*}^{-} \Delta r_{t-j}^{-} + e_t, \tag{A.10}$$

where $u_{t-1} = i_{t-1} - \beta_*^{+} r_{t-1}^{+} - \beta_*^{-} r_{t-1}^{-}$ is the asymmetric error correction term and e_t is a serially uncorrelated error term, given sufficiently large lag orders, p and q. Here, $\Delta r_t^{+} := \Delta r_t \mathbb{1}_{\{\Delta r_t \geq 0\}}$ and $\Delta r_t^{-} := \Delta r_t \mathbb{1}_{\{\Delta r_t < 0\}}$, where $\mathbb{1}_{\{\cdot\}}$ is an indicator function taking unity if the condition in brace is satisfied, and zero otherwise.

The process in (A.10) is equivalent to the NARDL(p, q) process advanced by SYG,

$$i_t = \gamma_* + \sum_{j=1}^{p} \phi_{j*} i_{t-j} + \sum_{j=0}^{q} (\theta_{j*}^{+\prime} r_{t-j}^{+} + \theta_{j*}^{-\prime} r_{t-j}^{-}) + e_t.$$

The NARDL process allows for both the long-run parameters, β_*^{+} and β_*^{-}, and the short-run parameters, π_{j*}^{+} and π_{j*}^{-}, to differ, enabling us to jointly analyze long- and short-run asymmetric relationships between R&D intensity and investment. Furthermore, it is important to notice that the NARDL process can accommodate a cointegrating relationship between integrated time series with mismatched time drifts. As $\Delta r_t^{+} \geq 0$ and $\Delta r_t^{-} \leq 0$ with probability one even if $E(\Delta r_t) = 0$, the partial sum processes, r_t^{+} and r_t^{-}, will be integrated series with positive and negative time drifts, respectively. Thus, if there exists an asymmetric cointegrating relationship between i_t and r_t, then the dependent variable, i_t should be an integrated series with a drift. This has the important implication that the NARDL model can analyze an asymmetric cointegrating relationship between two integrated variables with different drifts without the need to include a deterministic time trend in the model. In Section F, we find that r_t is a unit-root process without a drift while i_t is a unit-root process with a drift, and establish that there exists a cointegrating relationship between them without including a deterministic time trend.

F Additional Empirical Results

Table A.5 reports the descriptive statistics of both the R&D ratio to GDP and the log of GPDI, revealing that the R&D intensity growth looks more standard than the GPDI growth in the sense that the first has the characteristics of a normal distribution centered at zero, whereas the latter is centered at a non-zero value and more widely distributed with a negative skew and excess kurtosis. These different characteristics may imply that their interrelationship cannot be explained by a simple linear model.

— Insert Table A.5 Here —

We apply Phillips and Perron (1988) unit root test to both series. We test the unit root hypothesis both including and excluding the time trend. The results reported in Table A.6 show that the unit-root hypothesis cannot be rejected irrespective of the presence of the time trend, implying that both series are unit-root nonstationary. Furthermore, the time trend coefficient in the univarite regression is statistically significant for the log of GPDI, but insignificant for the R&D intensity, implying that the log of GPDI is a unit root process with a time drift, while the R&D ratio to GDP is a unit root process without a time drift, viz., $\mathbb{E}[\Delta r_t] = 0$ but $\mathbb{E}[\Delta i_t] > 0$.

— Insert Table A.6 Here —

	Sample Size	50		100		150		200		250	
	First Step	OLS	FM-OLS	OLS	FM-OLS	OLS	FM-OLS	OLS	FM-OLS	OLS	FM-OLS
φ_*	Second Step	OLS	OLS	OLS	OLS	OLS	OLS	OLS	OLS	OLS	OLS
-0.50	β_*^+	-0.263	-0.130	-0.140	-0.038	-0.095	-0.017	-0.072	-0.010	-0.058	-0.006
	β_*^-	-0.269	-0.038	-0.140	-0.009	-0.095	-0.004	-0.071	-0.002	-0.058	-0.001
	ρ_*	-0.101	-0.083	-0.036	-0.029	-0.022	-0.017	-0.015	-0.012	-0.012	-0.009
	φ_*	0.112	0.074	0.055	0.028	0.036	0.016	0.028	0.012	0.023	0.009
	π_*^+	-0.062	-0.022	-0.026	0.004	-0.018	0.007	-0.012	0.005	-0.010	0.006
	π_*^-	-0.107	-0.038	-0.044	-0.008	-0.032	-0.008	-0.024	-0.006	-0.020	-0.005
-0.25	β_*^+	-0.185	-0.073	-0.098	-0.020	-0.066	-0.007	-0.050	-0.002	-0.040	-0.001
	β_*^-	-0.192	0.004	-0.099	0.002	-0.066	0.003	-0.050	0.004	-0.041	0.003
	ρ_*	-0.084	-0.070	-0.030	-0.026	-0.018	-0.017	-0.012	-0.012	-0.011	-0.010
	φ_*	0.088	0.044	0.048	0.016	0.033	0.008	0.025	0.006	0.020	0.004
	π_*^+	-0.042	-0.002	-0.024	0.002	-0.017	0.003	-0.010	0.005	-0.009	0.005
	π_*^-	-0.069	-0.011	-0.032	-0.005	-0.026	-0.007	-0.019	-0.004	-0.015	-0.003
0.00	β_*^+	-0.112	-0.033	-0.057	-0.010	-0.037	-0.001	-0.027	0.000	-0.022	0.002
	β_*^-	-0.117	0.023	-0.057	0.004	-0.037	0.005	-0.027	0.005	-0.022	0.004
	ρ_*	-0.081	-0.069	-0.035	-0.034	-0.024	-0.023	-0.017	-0.016	-0.013	-0.012
	φ_*	0.051	0.016	0.028	0.007	0.019	0.003	0.015	0.001	0.011	0.000
	π_*^+	-0.035	-0.010	-0.018	-0.006	-0.009	0.001	-0.008	0.000	-0.006	0.002
	π_*^-	-0.047	-0.007	-0.026	-0.011	-0.017	-0.007	-0.015	-0.007	-0.009	-0.003
0.25	β_*^+	-0.024	0.000	-0.009	-0.006	-0.006	-0.003	-0.004	-0.001	-0.004	-0.001
	β_*^-	-0.027	0.024	-0.010	-0.003	-0.007	-0.001	-0.004	0.000	-0.004	-0.001
	ρ_*	-0.072	-0.068	-0.035	-0.036	-0.022	-0.023	-0.017	-0.018	-0.014	-0.014
	φ_*	0.015	0.001	0.006	0.002	0.005	0.001	0.003	0.000	0.003	0.000
	π_*^+	-0.001	-0.004	-0.004	-0.011	0.001	-0.004	-0.003	-0.007	-0.001	-0.005
	π_*^-	-0.024	-0.022	-0.007	-0.015	-0.007	-0.012	-0.004	-0.008	-0.005	-0.008
0.50	β_*^+	0.065	0.015	0.034	-0.023	0.024	-0.016	0.018	-0.013	0.014	-0.011
	β_*^-	0.062	-0.004	0.034	-0.035	0.024	-0.021	0.017	-0.016	0.014	-0.012
	ρ_*	-0.046	-0.046	-0.022	-0.019	-0.015	-0.013	-0.011	-0.010	-0.008	-0.007
	φ_*	-0.016	-0.008	-0.009	0.002	-0.005	0.003	-0.004	0.002	-0.003	0.002
	π_*^+	0.023	-0.017	0.011	-0.021	0.010	-0.012	0.006	-0.012	0.005	-0.009
	π_*^-	0.026	-0.019	0.013	-0.021	0.007	-0.017	0.005	-0.012	0.004	-0.010

Table A.1: FINITE SAMPLE BIAS OF THE TWO-STEP ESTIMATORS FOR $k = 1$. This table reports the finite sample biases when OLS/FM is used in the first step and OLS is used in the second step. The data is generated as $\Delta y_t = -(2/3)u_{t-1} + \varphi_*\Delta y_{t-1} + \Delta x_t^+ + (1/2)\Delta x_t^- + e_t$, where $u_t := y_t - 2x_t^+ - x_t^-$, $\Delta x_t = 0.5\Delta x_{t-1} + \sqrt{1 - 0.5^2}v_t$, and $(e_t, v_t)' \sim \text{IID}N(\mathbf{0}_2, \mathbf{I}_2)$.

	Sample Size	50		100		150		200		250	
	First Step	OLS	FM-OLS	OLS	FM-OLS	OLS	FM-OLS	OLS	FM-OLS	OLS	FM-OLS
φ_*	Second Step	OLS	OLS	OLS	OLS	OLS	OLS	OLS	OLS	OLS	OLS
-0.50	β_*^+	0.104	0.057	0.029	0.009	0.013	0.003	0.007	0.001	0.005	0.001
	β_*^-	0.120	0.129	0.029	0.010	0.014	0.003	0.007	0.001	0.005	0.001
	ρ_*	0.026	0.024	0.006	0.006	0.003	0.003	0.002	0.002	0.002	0.002
	φ_*	0.020	0.013	0.006	0.004	0.003	0.002	0.002	0.001	0.002	0.001
	π_*^+	0.153	0.134	0.062	0.053	0.037	0.032	0.025	0.022	0.019	0.017
	π_*^-	0.180	0.152	0.062	0.053	0.038	0.032	0.026	0.022	0.020	0.017
-0.25	β_*^+	0.060	0.034	0.016	0.006	0.007	0.002	0.004	0.001	0.003	0.001
	β_*^-	0.068	0.096	0.016	0.007	0.007	0.002	0.004	0.001	0.003	0.001
	ρ_*	0.023	0.022	0.007	0.007	0.004	0.004	0.003	0.003	0.002	0.002
	φ_*	0.016	0.011	0.007	0.004	0.004	0.003	0.003	0.002	0.002	0.002
	π_*^+	0.136	0.125	0.055	0.051	0.034	0.031	0.023	0.021	0.018	0.017
	π_*^-	0.140	0.130	0.056	0.050	0.033	0.030	0.023	0.021	0.018	0.017
0.00	β_*^+	0.032	0.023	0.007	0.004	0.003	0.001	0.002	0.001	0.001	0.000
	β_*^-	0.036	0.045	0.007	0.005	0.003	0.001	0.002	0.001	0.001	0.000
	ρ_*	0.022	0.021	0.008	0.008	0.005	0.005	0.003	0.003	0.003	0.003
	φ_*	0.011	0.010	0.005	0.004	0.003	0.003	0.002	0.002	0.002	0.002
	π_*^+	0.126	0.121	0.050	0.048	0.031	0.030	0.022	0.022	0.018	0.017
	π_*^-	0.128	0.126	0.050	0.048	0.030	0.029	0.023	0.022	0.018	0.017
0.25	β_*^+	0.015	0.018	0.002	0.003	0.001	0.001	0.001	0.001	0.000	0.000
	β_*^-	0.015	0.034	0.003	0.004	0.001	0.001	0.001	0.001	0.000	0.000
	ρ_*	0.019	0.019	0.007	0.007	0.004	0.004	0.003	0.003	0.002	0.002
	φ_*	0.007	0.009	0.004	0.004	0.002	0.002	0.002	0.002	0.001	0.001
	π_*^+	0.116	0.117	0.047	0.046	0.030	0.029	0.021	0.021	0.017	0.017
	π_*^-	0.112	0.114	0.047	0.047	0.030	0.030	0.022	0.022	0.017	0.017
0.50	β_*^+	0.022	0.020	0.004	0.004	0.002	0.002	0.001	0.001	0.001	0.001
	β_*^-	0.022	0.033	0.004	0.007	0.002	0.002	0.001	0.001	0.001	0.001
	ρ_*	0.011	0.011	0.005	0.004	0.003	0.003	0.002	0.002	0.002	0.002
	φ_*	0.007	0.007	0.003	0.003	0.002	0.002	0.001	0.001	0.001	0.001
	π_*^+	0.116	0.115	0.045	0.046	0.030	0.030	0.021	0.021	0.017	0.017
	π_*^-	0.113	0.111	0.046	0.047	0.029	0.029	0.021	0.021	0.017	0.017

Table A.2: FINITE SAMPLE MEAN SQUARED ERROR (MSE) OF THE TWO-STEP ESTIMATORS FOR $k = 1$. This table reports the finite sample MSEs when OLS/FM is used in the first step and OLS is used in the second step. The data is generated as $\Delta y_t = -(2/3)u_{t-1} + \varphi_* \Delta y_{t-1} + \Delta x_t^+ + (1/2)\Delta x_t^- + e_t$, where $u_t := y_t - 2x_t^+ - x_t^-$, $\Delta x_t = 0.5\Delta x_{t-1} + \sqrt{1-0.5^2}v_t$, and $(e_t, v_t)' \sim \text{IID}N(\mathbf{0}_2, \mathbf{I}_2)$.

	Sample Size	50		100		200		300		400		500	
	First Step	TOLS	FM-TOLS	TOLS	FM-TOLS	TOLS	FM-TOLS	TOLS	FM-TOLS	TOLS	FM-TOLS	TOLS	FM-TOLS
φ_*	Second Step	OLS	OLS	OLS	OLS	OLS	OLS	OLS	OLS	OLS	OLS	OLS	OLS
-0.30	β_{1*}^+	0.416	0.723	0.208	0.246	0.102	0.061	0.067	0.035	0.051	0.019	0.040	0.011
	β_{2*}^+	-0.334	-0.737	-0.168	-0.242	-0.082	-0.064	-0.057	-0.039	-0.039	-0.024	-0.033	-0.013
	β_{1*}^-	-0.431	-0.816	-0.212	-0.289	-0.107	-0.071	-0.069	-0.043	-0.053	-0.023	-0.042	-0.014
	β_{2*}^-	0.568	1.065	0.289	0.365	0.144	0.095	0.097	0.057	0.071	0.032	0.057	0.018
	ρ_*	-0.190	0.024	-0.076	-0.031	-0.032	-0.032	-0.021	-0.020	-0.015	-0.016	-0.011	-0.011
	φ_*	0.137	0.036	0.067	0.043	0.033	0.023	0.022	0.016	0.016	0.010	0.013	0.007
	π_{1*}^+	0.091	0.226	0.023	0.083	0.004	0.015	0.003	0.012	0.004	0.007	0.000	0.003
	π_{2*}^+	-0.120	-0.312	-0.057	-0.099	-0.030	-0.024	-0.021	-0.013	-0.008	-0.008	-0.012	-0.004
	π_{1*}^-	-0.047	-0.222	0.002	-0.076	0.003	-0.014	0.008	-0.008	0.003	-0.002	0.005	-0.001
	π_{2*}^-	-0.011	0.219	-0.027	0.066	-0.022	0.017	-0.017	0.012	-0.017	0.006	-0.014	0.004
-0.10	β_{1*}^+	0.390	0.694	0.190	0.259	0.090	0.075	0.059	0.040	0.044	0.021	0.034	0.015
	β_{2*}^+	-0.318	-0.683	-0.153	-0.265	-0.074	-0.078	-0.048	-0.043	-0.037	-0.024	-0.029	-0.016
	β_{1*}^-	-0.414	-0.779	-0.198	-0.293	-0.098	-0.086	-0.062	-0.047	-0.047	-0.025	-0.037	-0.018
	β_{2*}^-	0.522	0.999	0.252	0.384	0.121	0.111	0.080	0.062	0.059	0.034	0.047	0.022
	ρ_*	-0.158	0.019	-0.063	-0.016	-0.026	-0.026	-0.016	-0.017	-0.012	-0.013	-0.009	-0.011
	φ_*	0.124	0.050	0.068	0.042	0.034	0.024	0.024	0.015	0.017	0.010	0.013	0.007
	π_{1*}^+	0.073	0.227	0.017	0.079	0.003	0.024	0.001	0.013	0.003	0.008	-0.001	0.006
	π_{2*}^+	-0.109	-0.280	-0.048	-0.111	-0.021	-0.031	-0.010	-0.012	-0.010	-0.009	-0.008	-0.003
	π_{1*}^-	-0.030	-0.222	0.005	-0.071	0.004	-0.022	0.010	-0.009	0.004	-0.008	0.007	-0.005
	π_{2*}^-	-0.017	0.233	-0.036	0.088	-0.032	0.033	-0.026	0.016	-0.018	0.011	-0.015	0.008
0.00	β_{1*}^+	0.379	0.698	0.173	0.264	0.083	0.078	0.053	0.042	0.040	0.026	0.031	0.016
	β_{2*}^+	-0.317	-0.686	-0.146	-0.267	-0.071	-0.081	-0.047	-0.045	-0.034	-0.026	-0.028	-0.017
	β_{1*}^-	-0.409	-0.811	-0.186	-0.310	-0.092	-0.090	-0.058	-0.049	-0.044	-0.030	-0.034	-0.019
	β_{2*}^-	0.501	1.014	0.232	0.391	0.111	0.116	0.075	0.065	0.055	0.038	0.044	0.025
	ρ_*	-0.141	0.033	-0.057	-0.007	-0.025	-0.021	-0.014	-0.015	-0.011	-0.013	-0.008	-0.010
	φ_*	0.112	0.044	0.061	0.040	0.032	0.023	0.021	0.015	0.017	0.010	0.013	0.007
	π_{1*}^+	0.084	0.237	0.015	0.089	0.003	0.027	0.002	0.016	0.001	0.011	-0.002	0.006
	π_{2*}^+	-0.106	-0.287	-0.043	-0.118	-0.023	-0.029	-0.014	-0.014	-0.009	-0.012	-0.007	-0.007
	π_{1*}^-	-0.041	-0.239	0.011	-0.086	0.008	-0.025	0.010	-0.013	0.007	-0.009	0.007	-0.008
	π_{2*}^-	-0.027	0.226	-0.045	0.094	-0.033	0.037	-0.023	0.019	-0.019	0.016	-0.015	0.009
0.10	β_{1*}^+	0.345	0.729	0.169	0.272	0.077	0.083	0.049	0.048	0.036	0.030	0.029	0.019
	β_{2*}^+	-0.306	-0.706	-0.148	-0.291	-0.067	-0.085	-0.042	-0.049	-0.032	-0.030	-0.026	-0.020
	β_{1*}^-	-0.389	-0.829	-0.182	-0.311	-0.086	-0.095	-0.053	-0.054	-0.040	-0.034	-0.033	-0.022
	β_{2*}^-	0.476	1.059	0.223	0.411	0.101	0.122	0.066	0.071	0.049	0.043	0.039	0.029
	ρ_*	-0.125	0.051	-0.050	0.005	-0.020	-0.018	-0.014	-0.012	-0.010	-0.011	-0.007	-0.009
	φ_*	0.101	0.035	0.055	0.038	0.029	0.022	0.021	0.013	0.015	0.010	0.012	0.007
	π_{1*}^+	0.056	0.258	0.018	0.092	0.004	0.036	0.001	0.019	-0.001	0.014	-0.001	0.008
	π_{2*}^+	-0.105	-0.294	-0.042	-0.129	-0.019	-0.035	-0.008	-0.020	-0.009	-0.014	-0.007	-0.007
	π_{1*}^-	-0.022	-0.239	0.013	-0.081	0.010	-0.029	0.012	-0.014	0.009	-0.015	0.006	-0.008
	π_{2*}^-	-0.027	0.265	-0.041	0.100	-0.033	0.042	-0.022	0.026	-0.019	0.018	-0.014	0.011
0.30	β_{1*}^+	0.306	0.774	0.140	0.303	0.063	0.103	0.040	0.054	0.029	0.034	0.023	0.025
	β_{2*}^+	-0.308	-0.770	-0.128	-0.306	-0.062	-0.101	-0.040	-0.052	-0.028	-0.035	-0.023	-0.023
	β_{1*}^-	-0.369	-0.886	-0.160	-0.348	-0.071	-0.117	-0.047	-0.061	-0.034	-0.039	-0.027	-0.027
	β_{2*}^-	0.438	1.137	0.181	0.437	0.082	0.148	0.052	0.077	0.038	0.052	0.030	0.036
	ρ_*	-0.093	0.086	-0.039	0.022	-0.017	-0.007	-0.010	-0.009	-0.008	-0.008	-0.006	-0.006
	φ_*	0.069	0.012	0.041	0.028	0.022	0.019	0.015	0.012	0.011	0.008	0.009	0.006
	π_{1*}^+	0.044	0.269	0.013	0.114	0.001	0.046	-0.001	0.024	0.000	0.018	-0.002	0.012
	π_{2*}^+	-0.105	-0.323	-0.039	-0.133	-0.019	-0.040	-0.011	-0.023	-0.006	-0.013	-0.006	-0.011
	π_{1*}^-	-0.013	-0.268	0.018	-0.104	0.016	-0.045	0.014	-0.023	0.010	-0.016	0.009	-0.013
	π_{2*}^-	-0.032	0.304	-0.042	0.122	-0.034	0.050	-0.022	0.027	-0.021	0.021	-0.016	0.019

Table A.3: FINITE SAMPLE BIAS OF THE TWO-STEP ESTIMATORS FOR $k = 2$. This table reports the finite sample biases when OLS/FM is used in the first step and OLS is used in the second step. The data is generated as $\Delta y_t = -u_{t-1} + \varphi_* \Delta y_{t-1} + \boldsymbol{\pi}_{0*}^{+\prime} \Delta \boldsymbol{x}_t^+ + \boldsymbol{\pi}_{0*}^{-\prime} \Delta \boldsymbol{x}_t^- + e_t$, where $u_t := y_t - \boldsymbol{\beta}_*^{+\prime} \boldsymbol{x}_t^+ - \boldsymbol{\beta}_*^{-\prime} \boldsymbol{x}_t^-$, $\Delta \boldsymbol{x}_t = 0.5 \Delta \boldsymbol{x}_{t-1} + \sqrt{1 - 0.5^2} \boldsymbol{v}_t$, and $(e_t, \boldsymbol{v}_t')' \sim \text{IID}N(\mathbf{0}_3, \mathbf{I}_3)$.

	Sample Size	50		100		200		300		400		500	
	First Step	TOLS	FM-TOLS	TOLS	FM-TOLS	TOLS	FM-TOLS	TOLS	FM-TOLS	TOLS	FM-TOLS	TOLS	FM-TOLS
φ_*	Second Step	OLS	OLS	OLS	OLS	OLS	OLS	OLS	OLS	OLS	OLS	OLS	OLS
-0.30	β_{1*}^+	0.461	1.373	0.113	0.183	0.027	0.017	0.012	0.007	0.007	0.002	0.004	0.001
	β_{2*}^+	0.406	1.443	0.096	0.188	0.024	0.019	0.011	0.007	0.006	0.003	0.004	0.001
	β_{1*}^-	0.472	1.573	0.111	0.221	0.028	0.020	0.012	0.008	0.007	0.003	0.004	0.001
	β_{2*}^-	0.543	2.052	0.139	0.279	0.035	0.025	0.016	0.009	0.008	0.003	0.006	0.001
	ρ_*	0.059	0.060	0.012	0.012	0.003	0.003	0.002	0.002	0.001	0.001	0.001	0.001
	φ_*	0.027	0.020	0.007	0.006	0.002	0.002	0.001	0.001	0.001	0.001	0.001	0.000
	π_{1*}^+	0.423	0.586	0.117	0.132	0.040	0.031	0.021	0.018	0.015	0.011	0.011	0.009
	π_{2*}^+	0.412	0.673	0.115	0.142	0.039	0.031	0.023	0.017	0.015	0.011	0.011	0.009
	π_{1*}^-	0.408	0.595	0.117	0.132	0.039	0.032	0.022	0.018	0.015	0.012	0.011	0.008
	π_{2*}^-	0.345	0.505	0.112	0.124	0.040	0.032	0.023	0.018	0.016	0.012	0.012	0.009
-0.10	β_{1*}^+	0.445	1.257	0.098	0.192	0.023	0.019	0.010	0.006	0.005	0.002	0.003	0.001
	β_{2*}^+	0.378	1.234	0.087	0.192	0.020	0.019	0.008	0.007	0.005	0.002	0.003	0.001
	β_{1*}^-	0.438	1.438	0.098	0.224	0.024	0.022	0.010	0.008	0.006	0.003	0.003	0.001
	β_{2*}^-	0.509	1.812	0.114	0.289	0.027	0.028	0.011	0.010	0.006	0.003	0.004	0.002
	ρ_*	0.043	0.041	0.010	0.010	0.003	0.003	0.002	0.002	0.001	0.001	0.001	0.001
	φ_*	0.024	0.018	0.008	0.006	0.003	0.002	0.001	0.001	0.001	0.001	0.001	0.001
	π_{1*}^+	0.382	0.549	0.102	0.130	0.036	0.031	0.020	0.017	0.014	0.011	0.010	0.009
	π_{2*}^+	0.378	0.569	0.111	0.133	0.035	0.032	0.020	0.017	0.014	0.011	0.010	0.009
	π_{1*}^-	0.355	0.565	0.102	0.126	0.034	0.031	0.020	0.017	0.013	0.011	0.010	0.009
	π_{2*}^-	0.341	0.507	0.105	0.126	0.037	0.032	0.021	0.018	0.014	0.012	0.011	0.009
0.00	β_{1*}^+	0.429	1.254	0.088	0.190	0.020	0.020	0.008	0.006	0.005	0.003	0.003	0.001
	β_{2*}^+	0.371	1.350	0.077	0.196	0.019	0.020	0.008	0.007	0.004	0.003	0.003	0.001
	β_{1*}^-	0.440	1.516	0.093	0.235	0.021	0.024	0.009	0.008	0.005	0.003	0.003	0.001
	β_{2*}^-	0.476	1.933	0.099	0.305	0.023	0.030	0.010	0.010	0.006	0.004	0.004	0.002
	ρ_*	0.037	0.042	0.009	0.009	0.003	0.003	0.001	0.002	0.001	0.001	0.001	0.001
	φ_*	0.021	0.018	0.007	0.006	0.002	0.002	0.001	0.001	0.001	0.001	0.001	0.001
	π_{1*}^+	0.365	0.549	0.099	0.127	0.034	0.030	0.019	0.017	0.013	0.012	0.010	0.009
	π_{2*}^+	0.352	0.609	0.096	0.132	0.033	0.031	0.019	0.017	0.013	0.012	0.009	0.009
	π_{1*}^-	0.343	0.559	0.102	0.124	0.033	0.030	0.020	0.017	0.013	0.012	0.010	0.009
	π_{2*}^-	0.332	0.505	0.098	0.122	0.035	0.031	0.020	0.017	0.014	0.012	0.010	0.009
0.10	β_{1*}^+	0.397	1.286	0.084	0.209	0.017	0.021	0.007	0.007	0.004	0.003	0.003	0.001
	β_{2*}^+	0.372	1.294	0.078	0.219	0.017	0.022	0.007	0.007	0.004	0.003	0.002	0.001
	β_{1*}^-	0.416	1.551	0.087	0.238	0.019	0.026	0.008	0.008	0.004	0.003	0.003	0.002
	β_{2*}^-	0.461	2.088	0.097	0.323	0.020	0.032	0.009	0.011	0.005	0.004	0.003	0.002
	ρ_*	0.030	0.041	0.007	0.009	0.002	0.002	0.001	0.001	0.001	0.001	0.001	0.001
	φ_*	0.018	0.016	0.006	0.006	0.002	0.002	0.001	0.001	0.001	0.001	0.001	0.001
	π_{1*}^+	0.340	0.539	0.095	0.131	0.032	0.031	0.018	0.017	0.013	0.012	0.010	0.009
	π_{2*}^+	0.336	0.567	0.091	0.143	0.032	0.031	0.018	0.017	0.013	0.012	0.010	0.009
	π_{1*}^-	0.317	0.553	0.091	0.126	0.032	0.032	0.020	0.018	0.013	0.011	0.010	0.009
	π_{2*}^-	0.318	0.532	0.095	0.126	0.032	0.032	0.020	0.018	0.014	0.012	0.011	0.009
0.30	β_{1*}^+	0.360	1.553	0.071	0.225	0.014	0.027	0.006	0.008	0.003	0.003	0.002	0.002
	β_{2*}^+	0.391	1.511	0.066	0.232	0.014	0.026	0.006	0.008	0.003	0.003	0.002	0.002
	β_{1*}^-	0.413	1.866	0.074	0.276	0.015	0.032	0.006	0.009	0.003	0.004	0.002	0.002
	β_{2*}^-	0.436	2.386	0.076	0.357	0.016	0.043	0.006	0.012	0.003	0.005	0.002	0.002
	ρ_*	0.021	0.041	0.006	0.009	0.002	0.002	0.001	0.001	0.001	0.001	0.001	0.001
	φ_*	0.012	0.015	0.005	0.005	0.002	0.002	0.001	0.001	0.001	0.001	0.001	0.001
	π_{1*}^+	0.305	0.567	0.084	0.134	0.029	0.034	0.018	0.017	0.012	0.012	0.009	0.009
	π_{2*}^+	0.320	0.611	0.083	0.140	0.029	0.034	0.017	0.018	0.012	0.011	0.009	0.009
	π_{1*}^-	0.313	0.603	0.081	0.131	0.029	0.034	0.017	0.017	0.012	0.012	0.009	0.009
	π_{2*}^-	0.282	0.573	0.089	0.130	0.031	0.035	0.019	0.018	0.013	0.012	0.010	0.009

Table A.4: FINITE SAMPLE MEAN SQUARED ERROR (MSE) OF THE TWO-STEP ESTIMATORS FOR $k = 2$. This table reports the finite sample MSEs when OLS/FM is used in the first step and OLS is used in the second step. The data is generated as $\Delta y_t = -u_{t-1} + \varphi_* \Delta y_{t-1} + \boldsymbol{\pi}_{0*}^{+\prime} \Delta \boldsymbol{x}_t^+ + \boldsymbol{\pi}_{0*}^{-\prime} \Delta \boldsymbol{x}_t^- + e_t$, where $u_t := y_t - \boldsymbol{\beta}_*^{+\prime} \boldsymbol{x}_t^+ - \boldsymbol{\beta}_*^{-\prime} \boldsymbol{x}_t^-$, $\Delta \boldsymbol{x}_t = 0.5 \Delta \boldsymbol{x}_{t-1} + \sqrt{1 - 0.5^2} \boldsymbol{v}_t$, and $(e_t, \boldsymbol{v}_t')' \sim \text{IID} N(\mathbf{0}_3, \mathbf{I}_3)$.

	$\Delta \log$ GPDI	Δ(R&D/GDP)
Mean	0.009	0.004
Median	0.009	0.001
Maximum	0.110	0.082
Minimum	-0.176	-0.082
Standard Deviation	0.039	0.028
Skewness	-0.752	0.190
Excess Kurtosis	2.701	0.256
Sample Size	240	240

Table A.5: DESCRIPTIVE STATISTICS. Descriptive statistics are computed over 240 quarters from 1960q1 to 2019q4. GPDI is measured in US Dollars at 2012 prices and seasonally adjusted. R&D and GDP are seasonally adjusted nominal values.

PP test	$\log$ GPDI	R&D/GDP
PP test w/o trend	-1.138	-1.946
p-value	0.701	0.311
PP test w/ trend	-3.198	-2.255
p-value	0.087	0.457

Table A.6: PHILLIPS AND PERRON'S (1988) UNIT-ROOT TEST STATISTICS. Two Phillips and Perron tests are computed, one including and the other excluding a time trend. When the time trend is included, it is statistically significant for the log of GPDI but not for R&D intensity. The lag lengths of the ADF regressions are selected by the SIC.

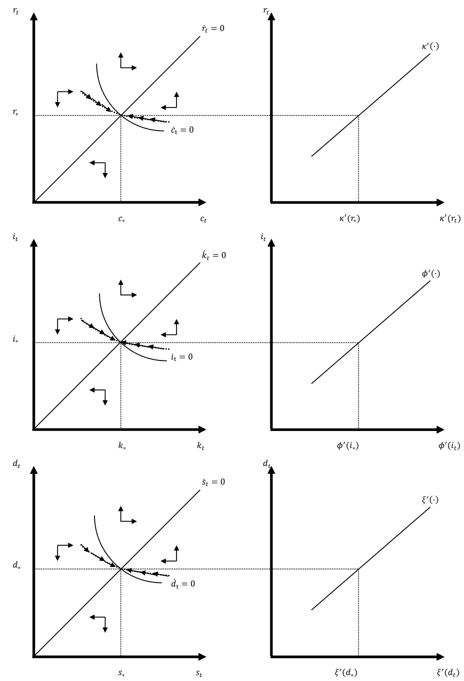

Figure A.1: PHASE DIAGRAMS AND STEADY STATE. This figure shows the phase diagrams of (r_t, c_t), (i_t, k_t), and (d_t, k_t) and their relationships with the marginal cost functions.

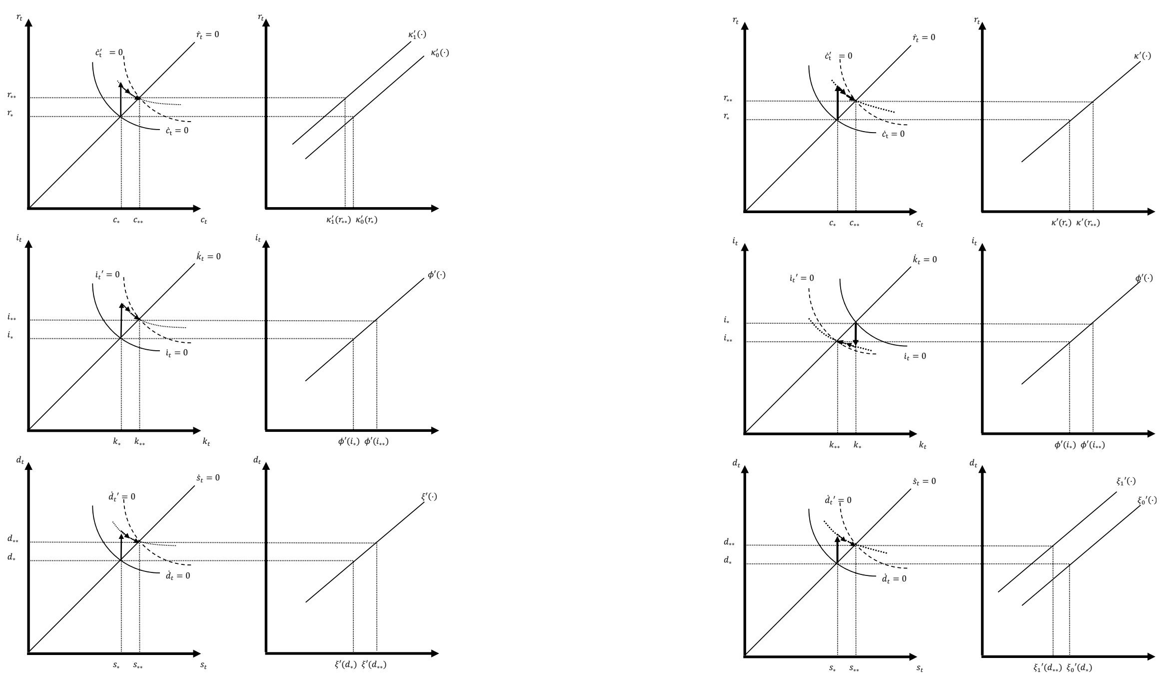

Figure A.2: PHASE DIAGRAMS AND STEADY STATE. The left figure demonstrates how the steady-state levels are adjusted as the marginal cost function $\kappa'(\cdot)$ of innovative R&D expenditure decreases from $\kappa_0'(\cdot)$ to $\kappa_1'(\cdot)$. The right figure demonstrates how the steady-state levels are adjusted as the marginal cost function of managerial R&D expenditure decreases from $\xi_0'(\cdot)$ to $\xi_1'(\cdot)$.